Functional analysis of the ABC protein ABCE1 from the archaeon *Sulfolobus solfataricus*

Dissertation

zur Erlangung des Doktorgrades
der Naturwissenschaften

Vorgelegt beim Fachbereich Biochemie, Chemie und Pharmazie
der Johann Wolfgang Goethe-Universität
in Frankfurt am Main

von
Stephanie Dinkelaker geb. Becker
aus Frankfurt am Main

Frankfurt am Main, 2007
(D30)

Vom Fachbereich Biochemie, Chemie und Pharmazie der

Johann Wolfgang Goethe-Universität als Dissertation angenommen.

Dekan:	Prof. Dr. Harald Schwalbe
Gutachter:	1. Prof. Dr. Robert Tampé
	2. Prof. Dr. Bernd Ludwig
Datum der Promotion:	02. November 2007

Index

Zusammenfassung

Das ABCE1-Protein ist eines der hochkonserviertesten Proteine in der Evolution. Orthologe ABCE1 Sequenzen kommen bis auf Bakterien in allen untersuchten Organismen vor. Dabei sind die ABCE1 Sequenzen von Archaeen und Eukaryoten zu mehr als 48% identisch. Unter den Eukaryoten ist die Identität sogar noch größer und liegt beispielsweise bei 68% im Vergleich zwischen der Bäckerhefe und dem Menschen. Da es sich hierbei um eine ungewöhnlich hohe Sequenzidentität handelt, ist es nahe liegend, dass ABCE1 eine Schlüsselrolle in der eukaryotischen und archaealen Zellphysiologie spielt. Verschiedene Studien in Eukaryoten haben gezeigt, dass ABCE1 essentiell für das Überleben der Zellen ist. Wenn die Expression von ABCE1 durch RNA-Interferenz stark herunterreguliert wird, kommt es zum Wachstumsstillstand oder zum Absterben des Organismus im embryonalen Zustand. Allerdings ist die genaue Funktion von ABCE1 bislang nicht bekannt. Zuerst wurde ABCE1 als RNase L Inhibitor beschrieben. Die RNase L ist ein Enzym, das zum körpereigenen Abwehrsystem gegenüber Viren gehört und durch Interferone aktiviert wird. ABCE1 verhindert hierbei die Bindung von 2’-5’-Oligoadenylat an die RNase L, welches zur Aktivierung von RNase L notwendig ist. Daneben zeigte sich, dass ABCE1 eine entscheidende Rolle bei der HIV-Infektion spielt. Die Kapside der HI-Viren können nur durch die Mithilfe des ABCE1-Proteins in der Zelle zusammengebaut werden, wobei ABCE1 ausschließlich an unvollständig assemblierte Virenhüllen bindet, nicht aber an gereifte Viruspartikel. Weiterhin wurde gezeigt, dass ABCE1 eine Funktion bei der Translationsinitiation und der Ribosomenbiogenese spielt. Der zugrunde liegende molekulare Mechanismus von ABCE1 in diesen verschiedenen Prozessen ist jedoch weitgehend unbekannt.

ABCE1 gehört zur Superfamilie der ABC-Proteine. Alle ABC-Proteine enthalten zwei Nukleotidbindedomänen (NBDs), die charakteristische Sequenzmotive enthalten. Die größte Klasse der ABC-Proteine stellen die ABC-Transporter dar, welche üblicherweise aus zwei NBDs und zwei Transmembrandomänen bestehen und eine Vielzahl von Molekülen über Membranen transportieren. Das lösliche ABCE1-Protein (68 kDa) ist, verglichen mit anderen Vertretern der ABC-Familie, einzigartig, da ABCE1 außer den beiden durch eine Linkerregion miteinander verbundenen NBDs zwei Eisen-Schwefel (Fe-S) Cluster enthält. Fe-S-Cluster,

wie sie in ABCE1 vorkommen, stellen einen wichtigen Cofaktor in Proteinen verschiedenster Organismen dar und erfüllen ganz unterschiedliche Funktionen. Sie dienen als Elektronen-*carrier* in Redoxreaktionen oder als Sensoren für Eisen, außerdem spielen Fe-S-Cluster eine Rolle bei der Modulation der Proteinstabilität, sowie bei der Interaktion mit Nukleinsäuren. Welche Aufgabe die Fe-S-Cluster in ABCE1 erfüllen, ist bislang nicht bekannt. Die Kristallstruktur von ABCE1 wurde ohne die Fe-S-Domäne gelöst, welche zeigt, dass die beiden NBDs in ABCE1 in einer Kopf-an-Schwanz-Orientierung „V-förmig“ angeordnet sind.

In dieser Arbeit wurde die Funktion von ABCE1 und der molekulare Mechanismus der einzelnen Domänen im archaealen, thermoacidophilen Organismus *Sulfolobus solfataricus* (*S. solfataricus*) als Modellsystem untersucht. Da die Funktion von ABCE1 in Archaeen bisher unbekannt ist, wurde in dieser Arbeit die Fragestellung adressiert, ob eine mögliche universelle Rolle von ABCE1 bei der Translation der Grund für die evolutionär hohe Konservierung ist. Dazu wurde ABCE1 aus *S. solfataricus* heterolog in *Escherichia coli* (*E. coli)* und homolog in *S. solfataricus* exprimiert. Für die homologe Expression von ABCE1 in *S. solfataricus* wurde ein neues Expressionssystem etabliert. Dabei ist ABCE1 eines der ersten Beispiele für rekombinante Proteinexpression in *S. solfataricus*. Während viele Systeme für die Expression von rekombinanten Proteinen in Bakterien und eukaryotischen Modellorganismen existieren, wurden bis jetzt nur sehr wenige Transformationssysteme in Archaeen entwickelt. Ein derartiges homologes Expressionssystem ist wahrscheinlich besonders für die Assemblierung der Fe-S-Cluster in ABCE1 bei hohen Temperaturen und in Gegenwart nativer Cofaktoren von großem Vorteil. Für die Expression in *S. solfataricus* wurde ein *shuttle vector* entwickelt, in dem die gesamte DNA des *Sulfolobus shibatae*-Virus 1 mit pUC18 für die Replikation und Selektion in *E. coli* kombiniert wurde. Dieser Vektor integriert an spezifischen Stellen in das Genom von *S. solfataricus* und enthält einen Arabinose-induzierbaren Promotor. Für die Expression von ABCE1-Mutanten wurde das genetisch leichter zugängliche Expressionssystem in *E. coli* genutzt. ABCE1 wurde über einen C-terminalen *affinity tag* (His_8-*tag* oder StrepII-*tag*) im homologen Expressionssystem und einen C-terminalen His_6-*tag* im heterologen Expressionssystem isoliert. In beiden Systemen wurde die Isolation optimiert, um möglichst reines ABCE1-Protein (95%) zu erhalten, dabei wurden 0,5-0,75 mg isoliertes ABCE1-Protein pro Liter Kultur erhalten. Dies ist die erste Studie, die auf Experimenten mit isoliertem *full-length* ABCE1-Protein basiert.

In ABC-Transportern binden und hydrolysieren die NBDs ATP, um den Transport von Substraten über Membranen zu energetisieren. Da ABCE1 keine Transmembrandomänen enthält, stellt sich die Frage nach der Funktion der NBDs. In dieser Doktorarbeit wurde erstmals die ATPase-Aktivität von ABCE1 analysiert. Wildtyp ABCE1 hydrolysierte ATP mit einem K_M-Wert von 0,7 mM und einer Wechselzahl von 10 ATP/min bei 80°C, wobei kein kooperatives Verhalten beobachtet (Hill-Koeffizient = 1) wurde. Wie für ein Protein aus einem hyperthermophilen Organismus zu erwarten ist, war die ATPase-Aktivität von ABCE1 temperaturabhängig mit einem Maximum bei 80°C. Eine verkürzte ABCE1-Mutante ohne die Fe-S-Cluster zeigte dieselbe ATPase-Aktivität wie Wildtyp-ABCE1. Das heißt, dass die ATPase-Aktivität nicht durch die aminoterminalen Fe-S-Cluster von ABCE1 beeinflusst wird. Um die funktionale Rolle jeder der beiden NBDs in ABCE1 zu untersuchen, wurden konservierte Aminosäuren in den NBDs mutiert. Überraschenderweise stellte sich heraus, dass die beiden NBDs funktional nicht äquivalent sind. Wurden konservierte Aminosäurereste gleichzeitig in beiden NBDs mutiert, war ABCE1 wie erwartet ATPase-inaktiv. Wurde allerdings nur die zweite NBD durch Punktmutationen an einzelnen Resten mutiert, kam es zu einem 15-fachen Anstieg der ATPase-Aktivität, während die entsprechende Mutation in der ersten NBD zu einer leicht reduzierten ATPase-Aktivität gegenüber Wildtyp-ABCE1 führte. In ABC-Transportern dimerisieren die NBDs nach ATP-Bindung innerhalb eines Transportzyklus. Da ABCE1 zwei NBDs enthält, ist eine intramolekulare Dimerisierung oder eine intermolekulare Assoziation beider ABCE1-Moleküle denkbar. Daher wurde untersucht, ob die ATPase-Aktivität abhängig von der Proteinkonzentration ist. In einem dynamischen Gleichgewicht von ABCE1-Monomeren, die mit anderen Monomeren interagieren, würde man eine nicht-lineare Abhängigkeit von der Proteinkonzentration erwarten. Dies wurde jedoch nicht beobachtet, dagegen zeigte sich beim Wildtyp und bei den hyperaktiven ABCE1-Mutanten eine lineare Beziehung zwischen der Proteinkonzentration und der ATPase-Aktivität. Basierend auf diesen Ergebnissen ist ein Mechanismus denkbar, bei dem die beiden NBDs eines ABCE1-Moleküls nach ATP-Bindung intramolekular dimerisieren und nach ATP-Hydrolyse wieder dissoziieren. Durch die Mutation in der zweiten NBD wird ABCE1 möglicherweise in einer aktiven Konformation gehalten, was zu einer stark erhöhten ATPase-Aktivität in der ersten NBD führt. Die Nukleotidbindungseigenschaften der beiden NBDs von ABCE1 wurden durch *Photocrosslinking* mit 8-Azido-ATP, welches durch unmarkierte Nukleotide verdrängt wurde, untersucht. Im Gegensatz zu anderen bekannten ABC-

Transportern wurde nicht nur eine ATP-Bindung, sondern auch eine AMP-Bindung von ABCE1 festgestellt. Die verkürzte ABCE1-Mutante ohne die Fe-S-Cluster zeigte dieselben Bindungseigenschaften wie Wildtyp-ABCE1, wodurch ausgeschlossen werden kann, dass die gemessene Nukleotidbindung auf Bindung an die Fe-S-Cluster zurückzuführen ist.

Zusätzlich zu den ABC ATPase-Domänen wurden die strukturelle Organisation, die Funktion und der Typ der Fe-S-Cluster in der vorliegenden Arbeit untersucht. Die N-terminale Region von ABCE1 enthält 8 Cysteine innerhalb der Konsensus-Sequenz $CX_4CX_3CX_3CPX_nCX_2CX_2CX_3CP$. Isoliertes Wildtyp-ABCE1 zeichnete sich durch eine braune Farbe und Absorption bei 410 nm aus, welche typisch für Fe-S-Cluster ist. Ein [4Fe-4S]-Zentrum ist aus 4 organischen Schwefelatomen, die durch 4 Cysteine gebildet werden, und 4 anorganischen Schwefelatomen aufgebaut. Während 8 Eisenatome bei zwei [4Fe-4S]-Clustern zu erwarten wären, konnten jedoch bestenfalls nur 6,5 Eisenatome durch totale Röntgenfluoreszenzmessung in ABCE1 detektiert werden. Die fehlenden 1,5 Eisenatome für die beiden putativen [4Fe-4S]-Cluster lassen sich jedoch durch Messungenauigkeiten erklären. Der Typ der Fe-S-Cluster in ABCE1 sollte durch *electron paramagnetic resonance* (EPR) untersucht werden. ABCE1 war allerdings EPR-inaktiv, was darauf hindeutet, dass ABCE1 zwei diamagnetische $[4Fe\text{-}4S]^{2+}$-Cluster enthält. Nur nach partieller aerober Degradation konnte substöchiometrisch ein $[3Fe\text{-}4S]^{+}$-Zentrum detektiert werden, was zeigte, dass ABCE1 empfindlich gegenüber Sauerstoff ist. Ausschließlich 7 der 8 konservierten Cysteine sind essentielle Liganden der beiden [4Fe-4S]-Cluster und unbedingt notwendig für die Funktion von ABCE1, da in Hefe eine Mutation der jeweiligen Cysteine zu Alanin letal war. Aus diesen Ergebnissen und zusätzlichen Homologievergleichen kann gefolgert werden, dass ABCE1 einen Ferredoxin-ähnlichen $[4Fe\text{-}4S]^{2+}$-Cluster, der durch die Cysteine an den Positionen 4/5/6/7 gebildet wird, und einen ABCE1-spezifischen $[4Fe\text{-}4S]^{2+}$-Cluster enthält, der durch die Cysteine an den Positionen 1/2/3/8 koordiniert wird.

Während keine ATP-abhängige Dimerisierung von ABCE1-Molekülen beobachtet wurde, zeigte sich nach Isolation über den His_8-*Tag* des homolog in *S. solfataricus* exprimierten ABCE1-Proteins zusätzlich zum Monomer ein oligomerer Komplex. Dieser Komplex entspricht einem ABCE1-Hexamer, welcher RNase-sensitiv war. Daraus kann man schließen, dass der oligomere Anteil von ABCE1 mit RNA assoziiert vorliegt. Möglicherweise induziert eine Bindung von RNA an ABCE1 die beobachtete Oligomerisierung. Eine hexamere

Anordnung findet man auch in anderen Proteinen mit einer RecA-ähnlichen Faltung. Zum Beispiel beim Terminator der Transkription, Rho, führt die Bindung von RNA zu einer hexameren Anordnung. In vielen Proteinen beeinflusst diese Oligomerisierung die Aktivität und Proteinfunktion. Ein Einfluss der Fe-S-Cluster auf die Oligomerisierung von ABCE1 konnte jedoch ausgeschlossen werden, obwohl Redoxprozesse eine Rolle bei der Oligomerisierung spielten. Auch die ATPase-Aktivität des oligomeren ABCE1 war nicht nennenswert höher als im monomeren Anteil von ABCE1. Die physiologische Bedeutung des beobachteten Oligomers von ABCE1 bleibt somit unklar.

Da alle bekannten Funktionen von ABCE1 mit einer Bindung von RNA in Verbindung gebracht werden könnten und auch der ABCE1-Oligomer RNase-sensitiv war, wurde untersucht, ob endogenes, aus *S. solfataricus* aufgereinigtes ABCE1 an RNA gebunden vorliegt. Tatsächlich war im isolierten ABCE1-Protein RNA mit einer Größe von 20 bis 200 Nukleotiden vorhanden, wobei keine distinkten Banden, sondern eine Mischpopulation detektiert wurde. Außerdem wurde *in vitro* die RNA-Bindung von ABCE1 analysiert. Dabei konnte in Sucrosegradienten gezeigt werden, dass ABCE1 mit der 16S und 23S ribosomalen RNA aus *S. solfataricus* assoziierte. Die Fe-S-Cluster von ABCE1 sind nicht verantwortlich für diese RNA-Bindung, da auch verkürztes ABCE1 ohne die Fe-S-Cluster mit rRNA cosedimentierte. Die RNA-Bindung war jedoch nicht ATP-abhängig und verschiedene RNA-Moleküle hatten keinen Einfluss auf die ATPase-Aktivität von ABCE1. Möglicherweise wird ABCE1 ausschließlich durch ein spezifisches RNA-Molekül aktiviert. Da ABCE1 mit ribosomaler RNA interagierte, wurde untersucht, ob ABCE1 auch mit Ribosomen assembliert. Hierbei zeigte sich, dass sowohl endogenes als auch isoliertes ABCE1 mit Ribosomen wechselwirkt. Eine Bindung an Ribosomen war auch ohne die Fe-S-Cluster von ABCE1 möglich, was wiederum darauf hinweist, dass die Fe-S-Cluster in ABCE1 nicht für die Ribosomenbindung verantwortlich sind. Zugabe von ATP oder Punktmutationen in konservierten Aminosäureresten der ATP-Bindungstasche veränderte jedoch nicht die Ribosomenbindungseigenschaften von ABCE1.

Um die physiologische Funktion von ABCE1 in Archaeen zu untersuchen, wurde analysiert, ob ABCE1 in der Translation von *S. solfataricus* eine Rolle spielt. Hierbei zeigte sich in einem zellfreien, *in vitro*-System, dass die Translation in *S. solfataricus* auch nach der Depletion von ABCE1-Protein im Zellysat möglich ist. Ebenso konnte im *gel shift assay* mit

a/eIF2 gezeigt werden, dass ABCE1 nicht mit archaealen Initiationsfaktoren interagiert. Aus diesen Ergebnissen kann man schließen, dass ABCE1 bei der Translation in Archaeen keine entscheidende Rolle spielt. Vermutlich erfüllt ABCE1 jedoch eine andere, universelle Aufgabe in Archaeen und Eukaryoten, welche bis jetzt nicht bekannt ist und durch weitere Experimente aufgeklärt werden muss.

Abstract

The ABC protein ABCE1, also called HP68 or RNase L inhibitor (RLI), is one of the most conserved proteins in evolution. It is universally expressed in eukaryotes and archaea, where ABCE1 is essential for life. ABCE1 plays a crucial role in translation initiation and ribosome biogenesis, however, the molecular mechanism of ABCE1 remains unclear. In addition to two ABC ATPase domains, ABCE1 contains a unique N-terminal region with eight conserved cysteines predicted to coordinate iron-sulfur (Fe-S) clusters. To analyze the function of ABCE1, the hyperthermophilic crenarchaeote *Sulfolobus solfataricus* was chosen as a model system. *S. solfataricus* ABCE1 was overexpressed homologously in *S. solfataricus* and heterologously in *E. coli*. Noteworthy, for tagged-protein production in *S. solfataricus* a novel expression system based on a virus shuttle vector was established. This is the first example for a successful overexpression and purification of isolated full-length ABCE1. For the first time it was shown that ABCE1 indeed bears biochemical properties of an ABC protein even though it has unique features. Remarkably, the nucleotide binding domains (NBDs) of ABCE1 bound ATP and AMP, but were functionally non-equivalent in ATP hydrolysis. Mutations of conserved residues in the second NBD led to a hyperactive ATPase, which implies an intramolecular mechanism of dimer formation. Truncation of the Fe-S cluster domains did not influence ATPase activity. The Fe-S clusters of ABCE1 were analyzed by biophysical and biochemical methods. As presented in this study, ABCE1 harbors two essential diamagnetic $[4Fe\text{-}4S]^{2+}$ clusters, one ferredoxin-like cluster formed by cysteines at position 4/5/6/7 and one unique ABCE1 cluster formed by cysteines at position 1/2/3/8. ABCE1 was found to be associated with RNA after purification from *S. solfataricus* and bound ribosomal RNA *in vitro*. In addition, ABCE1 showed homo-oligomerization and appeared to form a hexameric complex of ~440 kDa, which was RNase sensitive. Archaeal ABCE1 associated with ribosomes, however, the unique Fe-S clusters of ABCE1 were not required for this interaction. Although archaeal ABCE1 assembled with ribosomes and ribosomal RNA, ABCE1 proved not to be essential for translation in *S. solfataricus* and did not interact with archaeal initiation factors. Nevertheless, the ABCE1 gene is one of the few genes conserved between archaea and eukaryotes and fulfills a universal task, which needs further characterization.

1 Introduction

1.1 Architecture and conservation of the ABC protein ABCE1

ABCE1, formerly called HP68 or RNase L inhibitor (RLI), is the most conserved ATP-binding cassette (ABC) enzyme in evolution. In general, ABCE1 is among the top five conserved proteins between any archaeon and yeast, as judged from the BLAST score (Tatusov *et al.*, 1997). Orthologous ABCE1 sequences are found in all organisms except bacteria and homologues with more than 48% identity are described from archaea to eukaryotes (Braz *et al.*, 2004; Chen *et al.*, 2006; Kispal *et al.*, 2005; Yarunin *et al.*, 2005; Zhao *et al.*, 2004). Among eukaryotes the identity is even higher with e.g. 68% between man and baker's yeast. This unusual high sequence conservation suggests that ABCE1 is a core enzyme in eukaryotic and archaeal cell physiology and various studies in eukaryotes demonstrated that ABCE1 is essential for cell viability. Down-modulation of ABCE1 by RNA interference (RNAi) in *Caenorhabditis elegans*, *Trypanosoma brucei*, and *Xenopus laevis* resulted either in embryonic lethality or in growth arrest (Chen *et al.*, 2006; Estevez *et al.*, 2004; Zhao *et al.*, 2004). A yeast knock-out strain was shown to be non-viable (Dong *et al.*, 2004). In the highly reduced genome of the enslaved algae nucleomorph of the cryptomonad *Guillardia theta* ABCE1 is actually the only ABC protein present (Douglas *et al.*, 2001), but the exact cellular function of ABCE1 remains unclear. Initially, ABCE1 was identified in humans as an inhibitor of ribonuclease L (RNase L). ABCE1 interferes with binding of 2'-5' oligoadenylate (2-5A) to RNase L, which is necessary for the activation of enzymatic activity of RNase L (Bisbal *et al.*, 1995). Further, it was shown that HIV capsid formation is dependent on the human homologue of ABCE1 (HP68) (Zimmerman *et al.*, 2002). In addition, ABCE1 was linked to ribosome biogenesis (Kispal *et al.*, 2005; Yarunin *et al.*, 2005) and the initiation of translation (Chen *et al.*, 2006; Dong *et al.*, 2004). All of the described roles of ABCE1 seem to be connected with binding and modulation of RNA and ribonucleoproteins. Nevertheless, the underlying molecular mechanism of ABCE1 in these processes remains unknown.

The structural organization of ABCE1 is unique compared with other proteins of the ABC superfamily. The soluble, 68 kDa ABC protein is composed of two nucleotide binding domains (NBDs) joined by a linker region and two N-terminal iron-sulfur (Fe-S) clusters. The

first Fe-S-Cluster is situated in the RLI domain, being responsible for the inhibition of RNase L in the 2-5A/RNase L pathway, while the second Fe-S domain represents a classical $[4Fe\text{-}4S]^{2+}$ cluster.

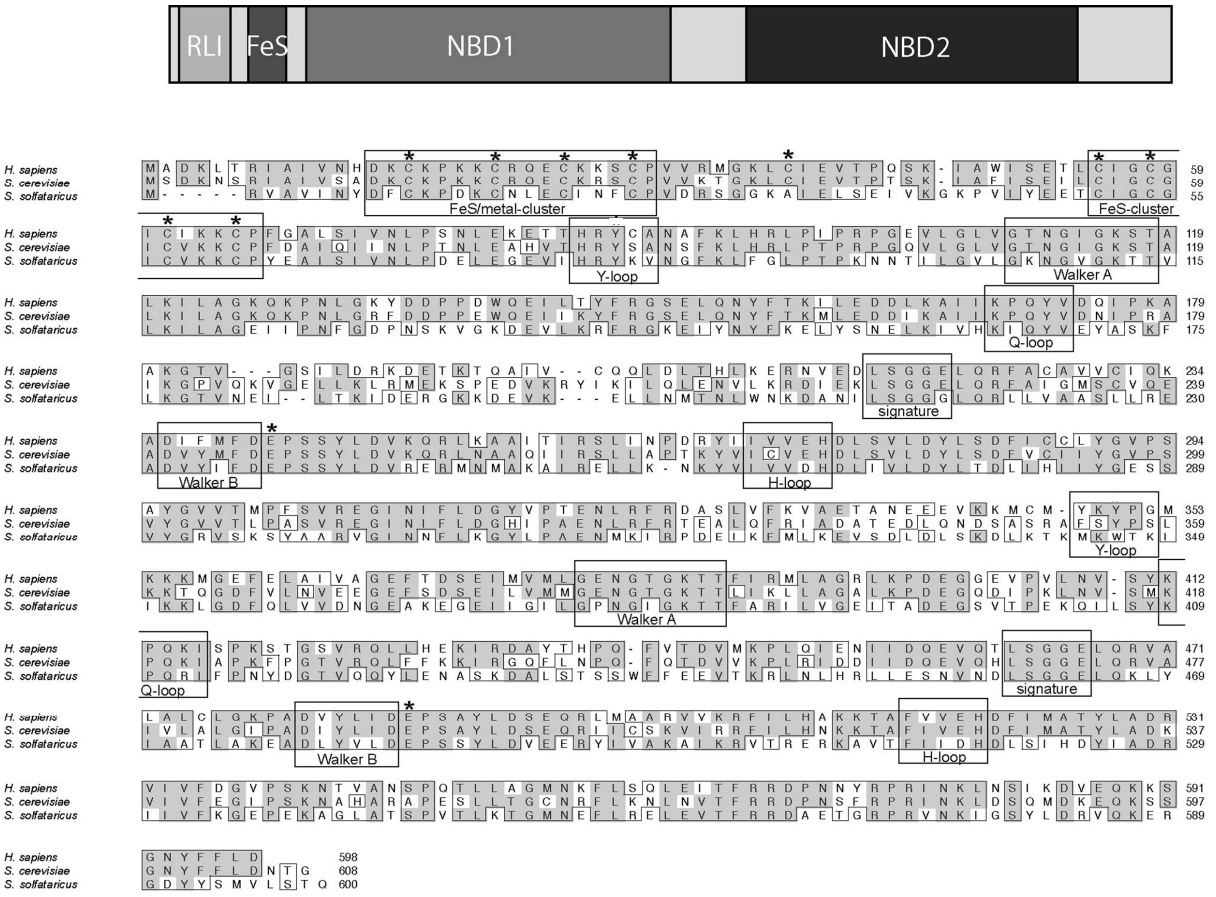

Figure 1: Alignment of ABCE1 from different species. The domain organization of ABCE1 is illustrated in the upper panel. An alignment of human, yeast (*S. cerevisiae*) and archaeal (*S. solfataricus*) ABCE1 sequences is shown in the lower panel. Conserved motifs are boxed and labeled, identical sequences are indicated in grey, whereas homologous sequences are shown in frames. Point mutations analyzed in this study are labeled with asterisks.

1.1.1 The ATP binding cassette (ABC) domain

All ABC proteins are characterized by the presence of the nucleotide binding domain (NBD), which contains a number of typical sequences. In addition to the Walker A and B motifs present in many families of ATPases, NBDs contain the ABC transporter signature motif (C-loop) (LSGGQ), a conserved aromatic amino acid-containing region (Y-loop), a conserved glutamine loop (Q-loop) and a conserved histidine loop (H-loop) (**Figure 1**). In eukaryotes,

seven sub-families of ABC proteins are known, ABCA to ABCG, five of which (ABCA, ABCB, ABCC, ABCD and ABCG) are responsible for membrane transport processes. The ABC transporter family is one of the largest groups of membrane proteins in most sequenced genomes. ABC transporters are involved in the transport of a wide variety of different compounds, such as sugars, ions, peptides and more complex organic molecules (Bauer *et al.*, 1999). For example, in humans, ABC transporters are responsible for antigen presentation and insulin secretion. Defective ABC transporters cause diseases such as cystic fibrosis, adrenoleukodystrophy (Dean *et al.*, 2001) and multidrug resistance of tumor cells (Callaghan and Riordan, 1993), while ABCE1 down-regulation has been correlated with chronic fatigue immune dysfunction syndrome (CFIDS) (Vojdani *et al.*, 1998). In ABC proteins associated with membrane transport, the NBDs bind and hydrolyze nucleotides and transmit conformational changes to membranes spanning domains (MSDs), which typically form a pathway for the transported substrate. The remaining two groups, ABCE and ABCF, contain a pair of linked NBDs, which are not fused to MSDs. Therefore, the functions of the ABCE and ABCF family are unlikely to be transport-related (Kerr, 2004). Noteworthy, no ABCF proteins exist in archaea in contrast to bacteria and eukaryotes. In eukaryotes three ABCF classes were identified, involved in the control of protein translation (Kerr, 2004; Tyzack *et al.*, 2000). Among eukaryotes, *Arabidopsis thaliana* is unique in containing two ABCE homologues, located on chromosome 3 and 4. Both ABCE-like genes show differential expression patterns (Braz *et al.*, 2004; Sarmiento *et al.*, 2006). Single NBD domains occur in a variety of non-transporter ABC proteins related to structural maintenance of chromosomes (SMC), like the DNA double-strand break repair enzyme Rad50 (Hopfner *et al.*, 2000), the DNA mismatch repair enzyme MutS (Obmolova *et al.*, 2000), the nucleotide excision repair enzyme UvrA9 (Aravind *et al.*, 1999), and the ribosomal processing enzyme ARB1 (Dong *et al.*, 2005).

1.1.2 The structure of the NBDs in ABCE1

Despite their diverse functions, ABC proteins share a conserved architecture. They contain a homo- or heterodimer of ABC-type NBDs that interact with additional regulative domains and substrate binding domains (Schmitt and Tampé, 2002). The structure of individual ABC ATPase domains and the dimerization of NBDs in response to ATP is well studied (Chen and

Cowan, 2003; Janas *et al.*, 2003; Schmitt *et al.*, 2003; Verdon *et al.*, 2003a), but only very few structures of full-length ABC proteins have been reported (Locher *et al.*, 2002). The crystal structure of ABCE1 from the archaeon *Pyrococcus furiosus* lacking the characteristic amino-terminal domains (residues 1-74) has been solved (Karcher *et al.*, 2005). The 1.9 Å structure in complex with ADP reveals similarities to known ABC protein structures but differs in additional hinge domains (**Figure 2**).

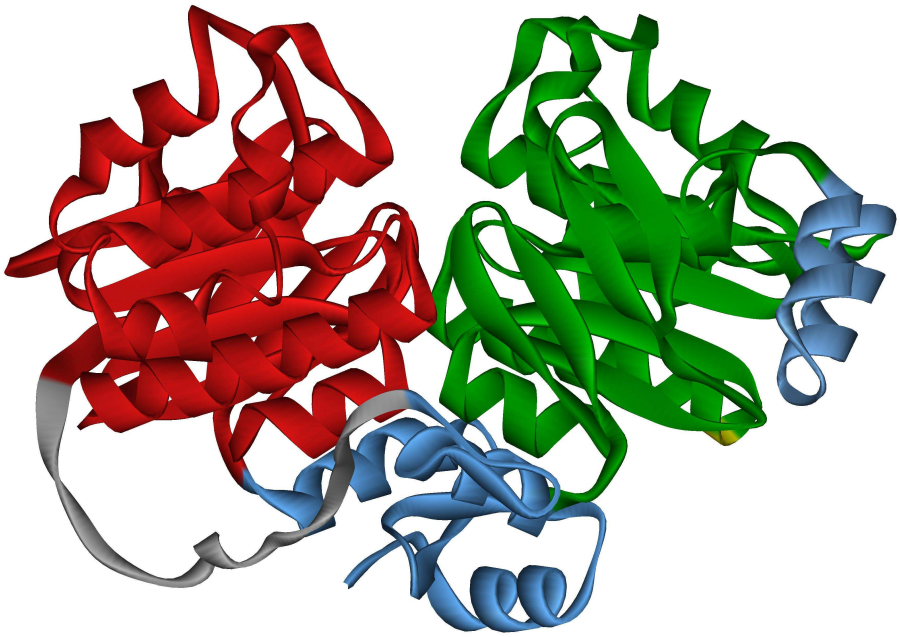

Figure 2: Structure of ABCE1 (Karcher *et al.*, 2005). A ribbon representation of the "V"-shaped crystal structure of ΔFe-S-ABCE1 from *Pyrococcus furiosus*. The two NBDs are depicted in green (NBD1) and red (NBD2). Additional domains like hinge and helix-loop-helix are shown in blue, the linker is depicted in grey.

The model indicates that the twin NBDs of ABCE1 are similarly arranged to the NBDs of other ABC proteins, e.g. the BtuCD ABC transporter. Typical NBD structures resemble an "L"-shape, which is formed by two arms that show a characteristic composition of α-helices and β-sheets (Hung *et al.*, 1998). Arm I includes the Walker A/B motifs, while arm II contains the conserved signature motif. The functional dimer in ABC proteins is composed of both NBDs arranged in a head-to-tail orientation like in Rad50 (Hopfner *et al.*, 2000). In ABCE1 the two NBDs and a hinge domain form a "V" shaped particle, in which NBD1 and NBD2 are arranged in a head-to-tail orientation with a deep cleft at the NBD1-NBD2 interface harboring both ATPase active sites (Karcher *et al.*, 2005). The hinge domain is a unique feature of

ABCE1 and is composed of hinge I and hinge II, which are tightly bound to each other by a hydrogen bond network (Karcher *et al.*, 2005). Hinge I is formed by the linker region between the two NBDs and hinge II is formed by the highly conserved C-terminal region of ABCE1. The hinge may prearrange the NBDs into a favorable orientation and facilitate ATP-driven conformational changes in the NBDs after substrate binding. In other ABC proteins it was shown that binding of ATP at the interface of two opposing NBDs induces a power stroke, consisting of two steps (van der Does and Tampé, 2004). In the first step, ATP binding to Walker A/B and Q loop motifs reorients arm I and arm II. In the second step, recognition of the ATP γ-phosphates by the signature motifs from the opposing NBD induces a clamp-like motion in the NBD dimer to form a tight NBD-2ATP-NBD sandwich. The crystal structure suggests that ABCE1 undergoes the typical ATP-induced clamp-like motion of the NBD domains.

1.1.3 Fe-S clusters

In addition to the NBDs, ABCE1 has an N-terminal Fe-S domain, which is essential for the enzymatic activity of proteins with very different functions. The Fe-S cluster acts as an electron carrier for redox reactions (Johnson, 1998) or in interactions with nucleic acids as shown in bacterial endonuclease III (Kuo *et al.*, 1992b). Besides, Fe-S clusters operate as sensors for iron and modulate protein stability (Beinert and Kennedy, 1993). Fe-S clusters constitute an ancient prosthetic group, which can be found in proteins from all living organisms. They are only composed of the inorganic components, sulfur and iron. In the most common cluster variants, [2Fe-2S], [3Fe-4S] and [4Fe-4S], the metal ions are directly coordinated by the inorganic sulfur and the adjacent cysteinyl groups from the protein backbone (Beinert *et al.*, 1997). Nevertheless, amino acids like histidine can also contribute to the iron coordination as known for [2Fe-2S] Rieske clusters. Additionally, much more complicated structural arrangements and clusters containing additional metal atoms like molybdenum exist (Howard and Rees, 2006). Furthermore, interconversion of Fe-S clusters is a widely distributed phenomenon, reflecting the dynamic arrangement (Khoroshilova *et al.*, 1995). Although Fe-S clusters can be synthesized *in vitro* (Zheng and Dean, 1994), their assembly and maturation *in vivo* requires a highly complex and regulated machinery (Lill and

Mühlenhoff, 2006). Mitochondria are the central compartment for Fe-S cluster biogenesis in eukaryotes. The maturation of Fe-S cluster proteins is the only known essential biochemical process performed by mitochondria. However, mitochondrial Fe-S cluster proteins are not required for cell viability. Several essential cytosolic proteins containing Fe-S clusters like Nar1p and Nbp35p exist, which are involved in their own Fe-S cluster maturation (Balk *et al.*, 2004; Hausmann *et al.*, 2005). Solely the cytosolic protein ABCE1 containing Fe-S clusters is not involved in Fe-S cluster assembly (Kispal *et al.*, 2005). Therefore, the production of Fe-S clusters for ABCE1 is the only crucial function of mitochondria and explains why these organelles are indispensable in all eukaryotes studied to date (Kispal *et al.*, 2005; Lill *et al.*, 2005; Lill and Mühlenhoff, 2006). Biogenesis of the essential Fe-S clusters of eukaryotic ABCE1 is dependent on the function of the mitochondrial iron-sulfur cluster (ISC) assembly machinery and Fe-S clusters are exported by the ABC transporter Atm1p from mitochondria to the cytosol (Kispal *et al.*, 1999) (**Figure 3**). Afterwards, components of the cytosolic Fe-S protein assembly apparatus e.g. the P-loop NTPases Cfd1p and Nbp35p and the iron-only hydrogenase-like protein Nar1p are required for Fe-S cluster maturation of ABCE1 (Balk *et al.*, 2004; Hausmann *et al.*, 2005).

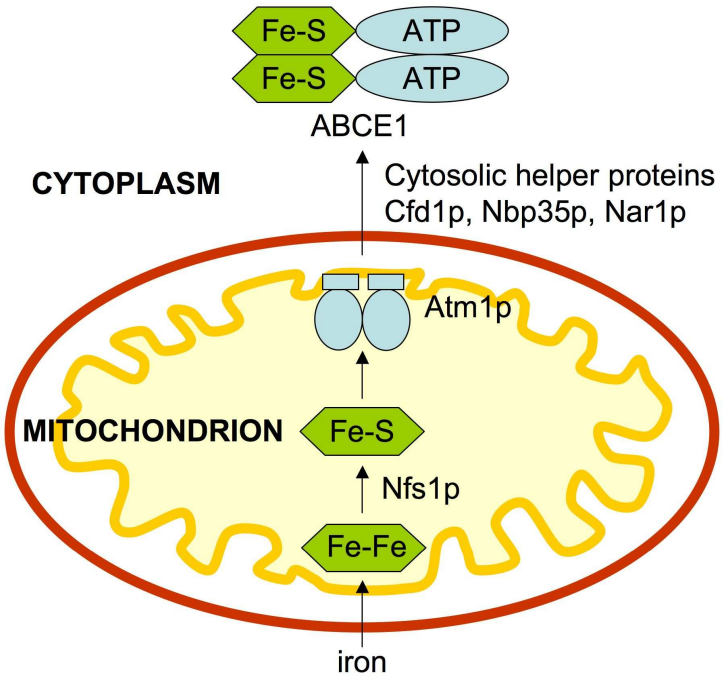

Figure 3: Maturation of cellular Fe-S proteins. In eukaryotes Fe-S clusters are assembled in mitochondria by the ISC assembly machinery.

Possibly, the Fe-S clusters of ABCE1 mediate an interaction with DNA or RNA, since both clusters contain highly conserved positively charged residues (mostly lysines) that could interact with the negatively charged phosphate backbone of RNA or DNA.

1.2 The 2-5A/RNase L pathway

Initially, ABCE1 was identified to act as an RNase L inhibitor (RLI) protecting viral RNAs from degradation by RNase L, an enzyme activated by the interferon-mediated defense system of the host (Bisbal *et al.*, 1995). Interferons are produced and secreted by mammalian cells after a viral infection. These cytokines in turn induce the transcription of a large family of genes involved in the defense against viral infections, the control of cell proliferation and differentiation, and the modulation of immune responses (Pestka *et al.*, 1987). The 2-5A/RNase L system is considered as a central pathway of interferon action and might also play a role in the regulation of RNA turnover and stability (Le Roy *et al.*, 2001; Martinand *et al.*, 1999). Interferon-α induces the 2-5A-synthetase which, upon activation by double-stranded RNA, converts ATP into 2'-5'-oligoadenylate known as 2-5A. The binding of 2-5A to RNase L produces an enzyme dimerization that activates the latent endoribonuclease, which inhibits protein synthesis by cleavage of mRNA at the 3' side of UpNp sequences (Floyd-Smith *et al.*, 1981; Kerr and Brown, 1978; Zhou *et al.*, 1993). During viral infection this antiviral pathway can be activated, since several viruses produce double-stranded RNA structures that can activate 2-5A-synthetase. The presence of 2-5A has been demonstrated in cells infected with encephalomyocarditis (EMC) virus (Williams *et al.*, 1979), vaccinia virus (Rice *et al.*, 1984), or reovirus (Nilsen *et al.*, 1982). However, several viruses seem to have developed strategies to counteract the antiviral activity or the 2-5A/RNase L pathway. An inhibition of RNase L activity has been observed during the course of human immunodeficiency virus (HIV) due to the overexpression of ABCE1, which inhibits the binding of 2-5A to RNase L (Martinand *et al.*, 1999). In this pathway ABCE1 does not induce 2-5A degradation or irreversible modification of RNase L (**Figure 4**).

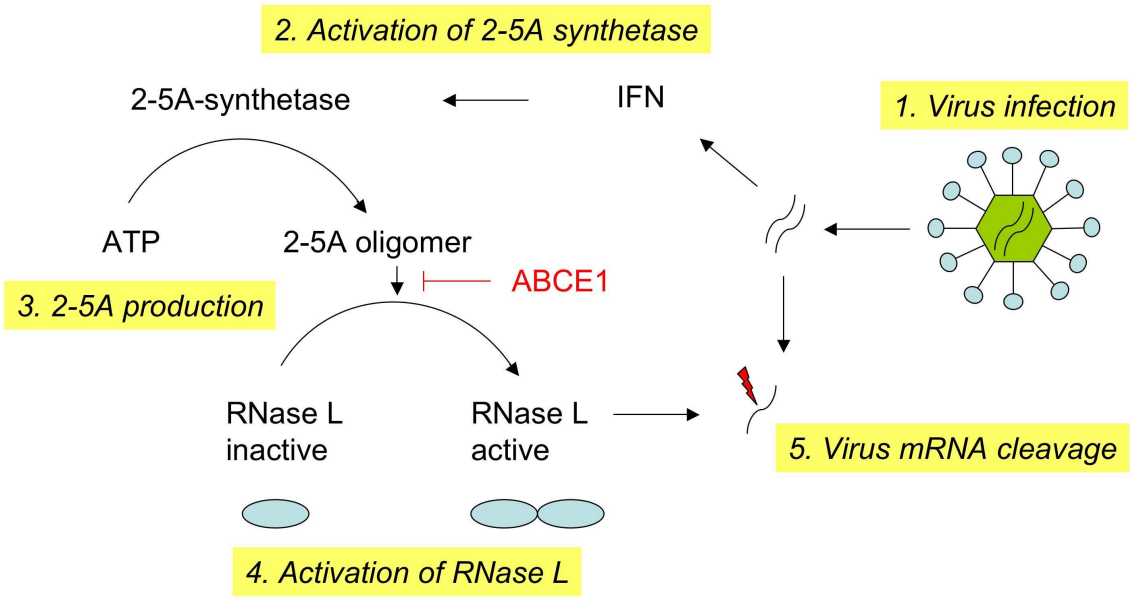

Figure 4: The 2-5A/RNase L pathway. After virus infection double-stranded RNA is released (1) and interferon production is induced. Upon interferon induction the 2-5A-synthetase is activated (2) and converts ATP into 2-5A (3). Binding of 2-5A to RNase L induces dimerization and activation of RNase L (4). ABCE1 inhibits this step of the pathway. Active RNase L degrades virus mRNA (5).

ABCE1 is also involved in mRNA stability in mammalian cells. It was shown that a fraction of cellular ABCE1 and RNase L is located in mitochondria (Le Roy *et al.*, 2001). It is speculated that the balance between RNase L and ABCE1 determines if mitochondrial mRNA is degraded. Degradation of mitochondrial mRNA leads to induction of apoptosis. Therefore, ABCE1 could counteract the interferon-α and RNase L mediated apoptosis.

ABCE1 is a highly conserved protein found in all species except in bacteria, but RNase L is only present in mammals. Therefore, the inhibition of RNase L cannot be the only function of ABCE1.

1.3 The role of ABCE1 in HIV infection

ABCE1 is induced by human immunodeficiency virus (HIV-I) infection and plays a dual role during the HIV-I life cycle. In addition to its posttranscriptional function on viral RNA of HIV, a posttranslational effect of ABCE1 in the assembly of HIV-1 capsids was demonstrated (Zimmerman *et al.*, 2002). In primate cells, assembly of a single HIV-1 capsid involves

multimerization of thousands of Gag polypeptides, the main structure proteins of HIV-1 particles, which typically assemble at the cytosolic face of the plasma membrane. ABCE1 (HP68) associates with HIV-1 Gag polypeptides and is essential for HIV-1 capsid assembly. In cells, polymerization of the capsid occurs via an ATP-dependent, stepwise pathway of discrete assembly intermediates (Dooher and Lingappa, 2004; Zimmerman *et al.*, 2002). ABCE1 interacts exclusively with intermediate complexes, but neither with unassembled Gag polypeptides nor fully assembled capsids (**Figure 5**).

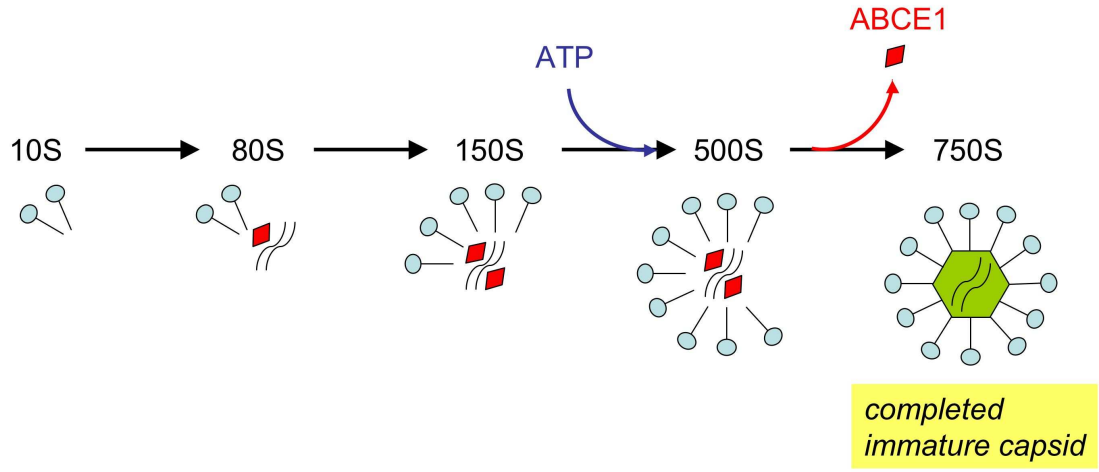

Figure 5: HIV capsid assembly. HIV-1 Gag proteins form defined assembly intermediates. ABCE1 interacts with 80S, 150S and 500S intermediates in an ATP-dependent manner, but neither with 10S nor 750S completed immature capsids.

The nucleocapsid (NC) domain of HIV-1 Gag was identified to be crucial for the interaction with endogenous primate ABCE1 (Lingappa *et al.*, 2006). This domain contains basic residues, which are not only necessary for association with endogenous ABCE1, but also for unspecific RNA binding, which promotes Gag multimerization. It was proposed that the Gag-ABCE1 interaction is not dependent on a RNA bridge and that the presence of RNA is not longer required once both proteins are associated (Lingappa *et al.*, 2006). A model suggests that ABCE1 functions as a molecular chaperone in concert with RNA and promotes ATP-dependent conformational changes important for HIV-1 Gag capsid assembly (Lingappa *et al.*, 2006). The exact mechanism how ABCE1 acts during assembly is not understood, but could include conformational changes associated with formation of the capsid shell or packaging RNA into the capsid. Recent data suggest a linkage between Gag-ABCE1

dissociation and subsequent events of virion production (Dooher *et al.,* 2007). In addition to Gag, ABCE1 also interacts with other viral factors. Such an interaction has been shown for the viral factor Vif (virion infectivity factor) (Zimmerman *et al.,* 2002). The role of ABCE1 in HIV-1 infection is certainly of high medical relevance. However, this is not its general physiological function and can hardly be the original reason for the existence of ABCE1.

1.4 ABCE1 and ribosome biogenesis

A role of ABCE1 in translation, ribosome biogenesis and processing of RNA was proposed based on sequence homology, phylogenetic distribution and conserved coexpression with orthologous groups (Braz *et al.*, 2004). Indeed, ABCE1 was shown to function in ribosome formation (Yarunin *et al.*, 2005). Eukaryotic ribosomes consist of a 60S subunit, which contains 25S, 5.8S and 5S rRNAs and ribosomal L-proteins, and a 40S subunit composed of 18S rRNA and ribosomal S-proteins. Eukaryotic ribosomes are assembled in the nucleolus before export to the cytoplasm. Ribosome formation is a highly dynamic and coordinated multistep process, which requires synthesis, processing, and modification of pre-rRNAs, assembly of ribosomal proteins and transient interaction of numerous non-ribosomal factors with the evolving pre-ribosomal particles (Tschochner and Hurt, 2003). In a first step, the 35S pre-rRNA is synthesized by RNA polymerase I forming an early precursor particle in the nucleolus. This 90S pre-ribosome includes many rRNA processing and assembly factors. Afterwards, this 90S pre-ribosomal particle undergoes a series of processing and maturation steps, of which the cleavage of the 35S pre-rRNA initiates the separation of pre-40S and pre-60S particles (Venema and Tollervey, 1999). Subsequently, these two subunits follow a separate biogenesis pathway, and the matured 60S and 40S subunits are exported to the cytoplasm. ABCE1 is associated with both pre-40S particles and mature 40S subunits (Kispal *et al.*, 2005; Yarunin *et al.*, 2005) (**Figure 6**). Depletion of ABCE1 causes a nuclear export defect of the small and large ribosomal subunits and subsequently a translational arrest (Kispal *et al.*, 2005). In contrast, no mRNA export defect was observed in ABCE1-depleted cells. ABCE1 is located both in the cytoplasm and nucleus (Dong *et al.*, 2004) and is able to shuttle between both compartments (Yarunin *et al.*, 2005). In addition, it was shown that yeast ABCE1 mutants are impaired in pre-rRNA processing, indicating that ABCE1 is involved in

pre-rRNA maturation of both the 40S and 60S subunit. ABCE1 is associated with 20S pre-rRNA, 7S pre-rRNA, 18S rRNA, 25S, 5.8S and 5S rRNA, but not with earlier pre-rRNAs (Yarunin *et al.*, 2005). The Fe-S clusters in ABCE1 have been shown to be of high importance for these functions in ribosome biogenesis (Kispal *et al.*, 2005; Yarunin *et al.*, 2005). Thus, ABCE1 links two central and ancient biosynthetic pathways, ribosome biogenesis, and maturation of Fe-S clusters. So far, the precise role of ABCE1 in RNA processing and export remains unclear.

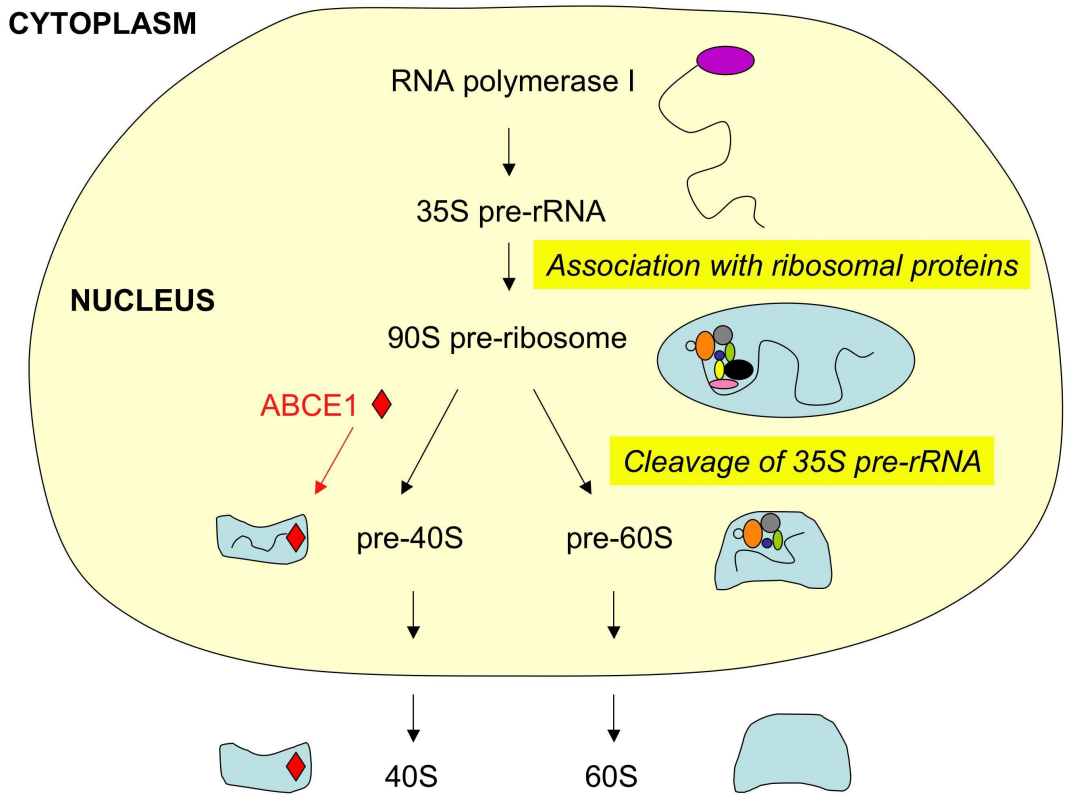

Figure 6: Ribosome assembly in eukaryotes. In the nucleolus 35S pre-rRNA is produced by RNA polymerase I. After association with various ribosomal proteins the 90S pre-ribosome is formed. After cleavage of the 35S pre-rRNA the pre-40S and pre-60S follow separate maturation pathways ending with their transport to the cytosol. ABCE1 is associated with pre-40S and 40S particles as well as with pre-rRNA and rRNA.

1.5 Function of ABCE1 in translation initiation

In addition to ribosome biogenesis, ABCE1 was shown to function in eukaryotic translation initiation (Dong *et al.*, 2004). Translation initiation is a multistep process involving the

sequential assembly of various large pre-initiation complexes. In eukaryotes translation initiation is stimulated by an array of soluble initiation factors (eIFs). The translation starts with the recruitment of initiator methionyl tRNA (Met-tRNA$_i^{Met}$) in a ternary complex with eIF2 and GTP to the 40S subunit forming the 43S preinitiation complex. This reaction is stimulated *in vitro* by eIF1, eIF1A, eIF3 (Algire *et al.*, 2002; Majumdar *et al.*, 2003). Then, the 43S complex binds to the capped 5'end of mRNAs in a reaction requiring eIF4F, eIF4A and eIF4B to produce the 48S complex. This complex scans the mRNA for an AUG start codon, which triggers GTP hydrolysis by the ternary complex, dependent on eIF5. In the last step of translation initiation, the 60S ribosomal subunit is recruited in a reaction stimulated by eIF5B generating functional 80S ribosomes before translation elongation begins (**Figure 7**). During translation polysomes are formed, which are pearl-chain like structures of ribosomes translating the same mRNA molecule simultaneously.

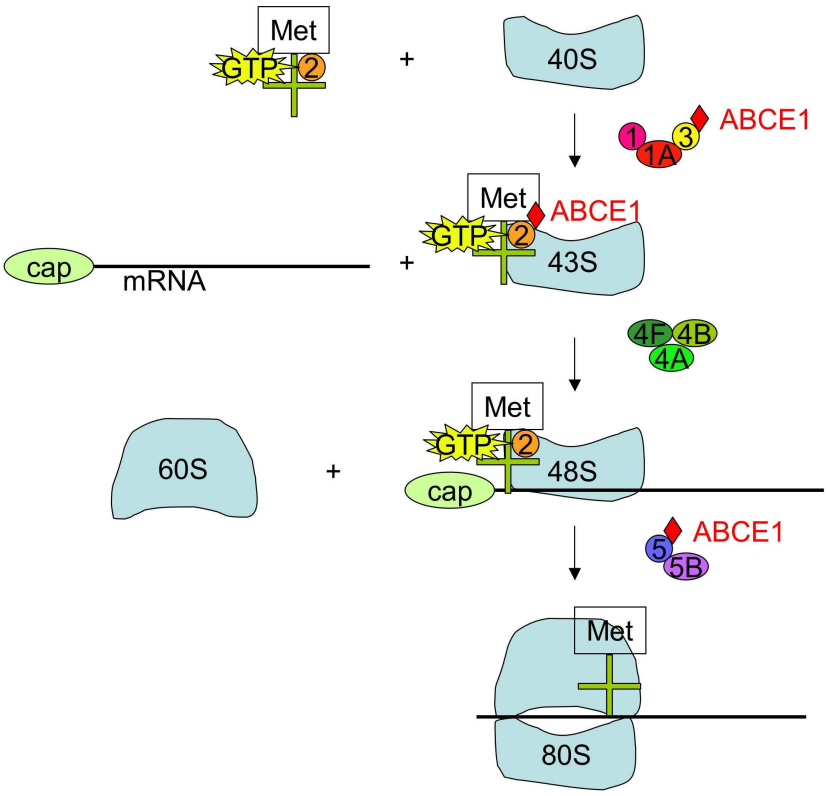

Figure 7: Translation initiation in eukaryotes. Binding of the ternary complex to the 40S subunit forms the 43S complex and is stimulated by the initiation factors eIF1, eIF1A and eIF3. Recruitment of the 5'-capped mRNA results in the 48S complex and is dependent on eIF4F, eIF4A and eIF4B. The recognition of AUG codon leads to GTP hydrolysis, which is triggered by eIF5. Binding to the 60S ribosomal subunit is promoted by eIF5B forming the 80S ribosome. ABCE1 is present only in catalytic amounts and interacts with eIF2, eIF3, eIF5 and ribosomal subunits.

ABCE1 was shown to play an important role in translation initiation of *Saccharomyces cerevisiae* (Dong *et al.*, 2004; Kispal *et al.*, 2005; Yarunin *et al.*, 2005), *Caenorhabditis elegans* (Zhao *et al.*, 2004), *Drosophila melanogaster* (where the ABCE1 gene is called *pixie*) (Andersen and Leevers, 2007; Coelho *et al.*, 2005), *Xenopus laevis* and different human cell lines (Chen *et al.*, 2006). ABCE1 is associated with 40S ribosomal subunits *in vivo* and interacts in yeast with eIF2, eIF3 and eIF5 independently of ribosomes (Dong *et al.*, 2004; Kispal *et al.*, 2005; Yarunin *et al.*, 2005). ABCE1 from Drosophila (*pixie*) also associates with eIF3 and ribosomal proteins of the small subunit (Andersen and Leevers, 2007), whereas the vertebrate ABCE1 protein interacts with eukaryotic initiation factors eIF2α and eIF5 and is essential for *in vitro* and *in vivo* translation of mRNA (Chen *et al.*, 2006). Furthermore, depletion of ABCE1 *in vivo* leads to growth arrest, decreased polysome number, a reduced average polysome size, an increase in free 80S ribosomes, and strongly impaired protein translation. ABCE1 is less abundant compared to ribosomal components and initiation factors, suggesting that ABCE1 is not a core stoichiometric component of translation. Binding of ABCE1 to the 40S subunit is likely to be a dynamic or regulated process (Kispal *et al.*, 2005). The ATP-binding cassettes (Andersen and Leevers, 2007; Dong *et al.*, 2004; Zhao *et al.*, 2004) and the Fe-S clusters (Barthelme *et al.*, 2007; Kispal *et al.*, 2005; Yarunin *et al.*, 2005) of ABCE1 were shown to play a crucial role for its catalytic function. It is speculated that the Fe-S clusters might regulate ATPase activity of the NBDs, for example in response to changing environmental conditions such as increased levels of reactive oxygen species (Kispal *et al.*, 2005).

1.6 Function of archaeal ABCE1

The function of ABCE1 in translation initiation is conserved from yeast through to higher eukaryotes. However, whether ABCE1 fulfills the same central cellular task also in the archaea has to be investigated. The evolutionary conservation of ABCE1 suggests that the protein has a universal function in translation and rRNA processing in both kingdoms. Translation is highly conserved in evolution. However, the mechanism of translation initiation diverged extensively in bacteria and eukaryotes, but very little is known about translation initiation in archaea (Londei, 2005). Bacteria and eukaryotes have widely different sets of

translation initiation factors. Surprisingly, archaea, being prokaryotes, are endowed with over 10 genes encoding proteins homologous to eukaryotic initiation factors (Bell and Jackson, 1998; Dennis, 1997). The only factors apparently restricted to the eukaryotic domain are the members of the eIF4F cap-binding complex, eIF3 and the GTPase eIF5, which were shown to interact with ABCE1 in yeast. The third factor, eIF2, which associated with yeast ABCE1, also exists in archaea, where it is called a/eIF2. This trimeric protein is responsible for guiding the met-tRNA$_i$ binding into the ribosomal P site (Londei, 2005; Pedulla *et al.*, 2005). It is interesting to understand whether ABCE1 plays a role both in eukaryotic and archaeal translation initiation. This would complete the picture of ancestral translation initiation in LUCA (Last Universal Common Ancestor) and explain the high evolutionary conservation of ABCE1.

Bacteria	**Eukaryotes**	**Archaea**
Universally conserved factors		
IF1	eIF1A	aIF1A
IF2	eIF5B	aIF2
YCiH	eIF1/SUI1	aSUI1
EFP	eIF5A	aIF5A
Domain specific factors		
IF3	-	-
-	eIF4F	-
-	eIF3	-
-	eIF2	a/eIF2
-	eIF2B	only α, β, δ subunits
-	eIF5	-
-	eIF6	aIF6

The evolutionary origin of ABCE1 is of considerable interest with regard not only to the cellular function of the protein, but also to the biogenesis of its Fe-S clusters (Kispal *et al.*, 2005). It is currently unknown, how archaea assemble their Fe-S proteins. The genomes of archaea generally do not contain homologues of the bacterial or mitochondrial ISC assembly machinery (Takahashi and Tokumoto, 2002). It is therefore unlikely that the assembly of the Fe-S clusters in archaeal ABCE1 is facilitated by a process involving ISC assembly components (Kispal *et al.*, 2005). Instead, archaeal genomes contain members of the SUF machinery which assembles Fe-S proteins in bacteria, particularly under oxidative stress and iron-deficient conditions (Zheng *et al.*, 2001). However, most archaea contain only a limited set of the *suf* genes with *sufB* and *sufC* being present in virtually all archaeal genomes

(Takahashi and Tokumoto, 2002). Despite the poor conservation of the Suf proteins, it could be possible that this machinery is responsible for the maturation of archaeal ABCE1 (Kispal *et al.*, 2005).

1.7 Objectives

The soluble ABC protein ABCE1 fulfills an essential task in the initiation of protein translation and ribosome biogenesis in all eukaryotes studied to date. Depletion of ABCE1 resulted either in embryonic lethality or in growth arrest. Furthermore, HIV capsid assembly is dependent on the cellular protein ABCE1. Both NBDs and Fe-S clusters of ABCE1 have been shown to be necessary for its function, however their precise role for activity of this highly conserved protein remains still unknown.

The current study was initiated to unravel the molecular mechanism of ABCE1. The thermoacidophilic archaeon *Sulfolobus solfataricus* was chosen as a model system. So far, functional full-length ABCE1 could not be isolated from any other organism. Therefore, my primary objective was to purify full-length ABCE1 protein using a novel homologous expression system established in *S. solfataricus*. After successful expression and purification of ABCE1 from *S. solfataricus*, I set out to investigate the functional role of NBDs and Fe-S of ABCE1, which are not characterized until now. In particular, I aimed to gain insights into the structural arrangement of the Fe-S clusters. Furthermore I studied the role of ATPase activity of the NBDs for the functionality of ABCE1. Therefore, I designed various point-mutations in functional residues as well as a domain-truncation mutant of ABCE1 and analyzed them with spectroscopic and biochemical methods. The question how the NBDs and Fe-S clusters communicate in order to coordinate ATP hydrolysis in response to cellular events is of major interest. The proposed activity of ABCE1 in eukaryotes could be mediated by RNA binding and modification, therefore I examined the RNA binding properties of ABCE1 in detail in this thesis. I planned to investigate whether high molecular structures of ABCE1 monomers are formed and whether they show a distinct activity in ATP hydrolysis and RNA binding. A major focus in this study was to analyze if ABCE1 fulfills a universal cellular function by interaction with ribosomes, RNA binding, and association with initiation factors, which is common to eukaryotes and archaea.

2 Material

2.1 Chemicals

Name	Company
[^{35}S]-Methionine	Hartmann Analytic
8-Azido-ATP-2',3'-biotin	Affinity Labeling Technologies
5-Amino-2,3-dihydro-1,4-phthalazinedione-3-aminophthal-hydrazide (Luminol)	Sigma-Aldrich
Acetic acid, 99%	Riedel de Haen
Acetone	Roth
Acryl amide	Roth
Adenosine-5'-diphosphate (ADP)	Fluka
Adenosine-5'-monophosphate (AMP)	Fluka
Adenosine-5'-triphosphate (ATP)	Fluka
Agar	GibcoBRL
Agarose	Sigma-Aldrich
D-Alanine	Sigma-Aldrich
Alumina powder type A5	Sigma-Aldrich
Ammonium chloride	Merck
Ammonium iron disulfate	Merck
Ammonium molybdate tetra hydrate	Fluka
Ammonium peroxodisulfate (APS)	Roth
Ammonium sulfate	Fluka
β-Mercaptoethanol	Roth
Bovine serum albumin (BSA)	Sigma-Aldrich
Bradford reagent	Pierce
Bromphenol blue	Merck
Calcium chloride	Merck
Chloroform	Sigma-Aldrich
Coomassie Blue G	Sigma-Aldrich
Cobalt sulfate	Merck
Copper chloride	Merck
D-Desthiobiotin	IBA GmbH
Developer solutions A & B	AGFA
Diepoxypyrocarbonate (DEPC)	Sigma-Aldrich
Dimethylpimelidate	Sigma-Aldrich
Dimethylsulfoxide (DMSO)	Fluka
di-Potassium hydrogen phosphate	Roth
di-Sodium hydrogen phosphate	Roth
1,4-Dithiothreitol (DTT)	Sigma-Aldrich
Ethanol, abs.	Riedel de Haen
Ethidium bromide	Merck
Ferric chloride	Merck
Formaldehyde, 37% (v/v)	Roth
Glycerol	Roth
Glycine	Roth
Hydrochloric acid, 37%	Merck
Hydroxyazophenylbenzoic acid (HABA)	Sigma-Aldrich
Imidazole	Fluka

Isopropanol	Roth
Isopropyl-β-D-thiogalactopyranoside (IPTG)	MBI Fermentas
1-(4-Isothiocyanatobenzyl)ethylenediamine-N,N,N',N'-tetraacetic acid (EDTA)	Roth
Magnesium acetate	Roth
Magnesium chloride	Riedel de Haen
Magnesium sulfate	Merck
Malachite green	Sigma-Aldrich
Manganese chloride	Sigma-Aldrich
Methanol	Riedel de Haen
3-N-morpholino-propanesulfonic acid (MOPS)	Roth
N-(2-hydroxyethylpiperazine)-N'-2-ethanesulfonic acid (HEPES)	Sigma-Aldrich
Nickel sulfate	Merck
Nicotineamide adenine dinucleotide hydrate (NAD)	Sigma-Aldrich
N,N,N',N'-Tetramethylethylenediamin (TEMED)	Sigma-Aldrich
Phenylmethane sulfonyl fluoride (PMSF)	Sigma-Aldrich
Ponceau Red S	Sigma-Aldrich
Potassium chloride	Roth
Potassium acetate	Roth
Potassium dihydrogen phosphate	Roth
Pyronin Y	Sigma-Aldrich
Rubidium chloride	Roth
Salmon testes DNA	Sigma-Aldrich
Silver nitrate	Roth
Skim milk powder	Roth
Sodium acetate	Roth
Sodium azide	Roth
Sodium borate	Merck
Sodium chloride	Fluka
Sodium dithionite	Fluka
Sodium dodecyl sulfate (SDS)	Roth
Sodium molybdate	Merck
Sodium thiosulfate	Roth
Sodium hydroxide	Riedel de Haen
Sulfuric acid, 96%	Roth
SybrGold	Invitrogen
trans-4-Hydroxycinnamic acid (p-Coumaric acid)	Sigma-Aldrich
Trichloroacetic acid (TCA)	Roth
Tricine	Roth
Triethanolamine	Roth
Triethylamine	Roth
Tris-(hydroxymethyl)-aminomethane (Tris)	Roth
Tween-20	Roth
Vanadate sulfate	Merck
Zinc sulfate	Merck

2.2 Enzymes, Markers and Kits

Name	Company
*Afl*III	New England Biolabs
ANTI-RNase	Ambion
*Apa*I	MBI Fermentas
ClaI	New England Biolabs
Coomassie Plus Bradford Assay Kit	Pierce
DNase I	Invitrogen
dNTP mix	MBI Fermentas
*Eco*RI	MBI Fermentas
Gene Ruler 1 kb Ladder	MBI Fermentas
*Hind*III	MBI Fermentas
*Nco*I	MBI Fermentas
PCR Extraction Kit	Qiagen
Pfu Turbo DNA Polymerase	Stratagene
Proteinase K	New England Biolabs
Ribonuclease Inhibitor	MBI Fermentas
RNase A	MBI Fermentas
Taq Polymerase	MBI Fermentas
T4 DNA Ligase	MBI Fermentas
T4 Polynucleotide Kinase	MBI Fermentas
T7 RNA Polymerase	New England Biolabs
Peroxidase-conjugated Extravidin	Sigma-Aldrich
Protein Molecular Weight Marker	MBI Fermentas
Prestained Protein Molecular Weight Marker	MBI Fermentas
NucleoSpin Plasmid Kit	Machery-Nagel
NucleoSpin RNA II Kit	Machery-Nagel
QIAquick Gel Extraction Kit	Qiagen
TOPO Cloning Kit	Invitrogen

2.3 Cells and Media

Name	Company/Source
Ampicillin	Roth
BL21(DE3) (*E. coli*)	Novagen
C41(DE3) *(E. coli)*	Novagen
Chloramphenicol	Roth
D(-)-Arabinose	Sigma-Aldrich
Kanamycin	Sigma Aldrich
Peptone/Tryptone from Casein	Roth
Saccharomyces cerevisiae, R1158 Tet-Rli (genotype: URA::CMV-tTA MaTa his-3-1 leu2-0 met 15-0)	Open Biosystems
Sulfolobus solfataricus P2, P1 (DSM 1616), M16(ΔpyrEF/lacS) PH1-16	Provided by S. Albers (Martusewitsch *et al.*, 2000)
Tryptone Bacto™	BD Bioscience
Yeast extract	Roth

2.4 Antibodies

Antibody	Source	Dilution	Company
Anti-ABCE1	Rabbit	(1:10000)	Eurogentec
Anti-rabbit-HRP	Goat	(1:20000)	Dianova
Anti-mouse-HRP	Goat	(1:17000)	Sigma-Aldrich
Anti-His_6	Mouse	(1:2000)	Novagen
Anti-a/eIF2α	Mouse	(1:1500)	Eurogentec

2.5 Vectors

Vector	Relevant characteristics	Source
pCR4	For TOPO cloning	Invitrogen
pSVA1	pBR05 *E. coli* entry vector with terminator sequence separated	Provided by S. Albers (Albers *et al.*, 2006)
pSA4	Modified pET15b	Provided by S. Albers (Albers *et al.*, 2003)
pSVA5	pSVA1 containing the lacS gene under control of araS promoter	Provided by S. Albers (Albers *et al.*, 2006)
pSVA30	SSO0287-StrepII-His_{10} inserted into pSVA5, *E. coli* donor vector for SSO0287	This study (Barthelme *et al.*, 2007)
pSVA31	PMJ05 containing expression cassette from pSVA30	This study (Barthelme *et al.*, 2007)
pMJ05	Virus based shuttle vector for *S. solfataricus/E. coli*	Provided by S. Albers (Jonuscheit *et al.*, 2003)
pRS423	Yeast multi-copy plasmid	(Barthelme *et al*., 2007)
pCR4TOPO	TOPO cloning Kit	Invitrogen
pET401	Cloning vector based on pTRC99	Karel van Wely, unpublished
pET32c	Expression vector in *E. coli*	Novagen
pRKISC	Increases the production of apo-Fe-S proteins in *E. coli*	Provided by Y. Takahashi, (Kriek *et al.*, 2003)
pRKSUF017	Increases the production of apo-Fe-S proteins in *E. coli*	Provided by Y. Takahashi, (Takahashi and Tokumoto, 2002)
pRKEhNNif	Coding for NIF (nitrogen fixation)-like system for Fe-S cluster formation of non-nitrogenase Fe-S proteins to form under anaerobic conditions	Provided by T. Nozaki (Ali *et al.*, 2004)
pRARE	Coding for rare tRNAs	Novagen
pSD1	SSO0287-His_6 inserted into pSVA4 *E. coli* expression vector	This study (Barthelme *et al.*, 2007)
pSD2	ΔFe-S-SSO0287(69-600)-His_6 inserted into pSVA4 *E.coli* expression vector	This study (Barthelme *et al.*, 2007)

2.6 Oligonucleotides

Name	Sequence (5'-3')	Purpose
P1f	CCATATCCCATGGTGAGAGTTGC	Cloning of SSO0287 for expression in *E. coli* and *S. solfataricus*
P2r	CCATATGGATCCCTGGGTAGAAAGAACCAAGGAG	Cloning of SSO0287 for expression in *E. coli*
P3f	GCGGCCATGGTGCTGCCAGACGAGTTAGAAGGA	Cloning of truncated SSO0287 for expression in *E. coli*
P4r	GGGCCCTTAATGGTGATGGTGATGGTGATGGTGTTTTTCAAAT TGTGGATGTGACCAATTCTGGGTAGAAAGAACCAAGGAG	Cloning of SSO0287 for expression in *S. solfataricus*
P5f	ATGGTCGACGCCCTCGTATCTGCAACG	Cloning of ABCE1 in *S. cerevisiae*
P5r	ATACCCGGGAGTACGGATCACCGAAGAGG	Cloning of ABCE1 in *S. cerevisiae*
E238Q	GCAGATGTATACATATTTGATCAACCTTCTTCTTATCTAGATG	Point mutation
E485Q	GATCTTTACGTTTTGGATCAACCTTCCTCTTATCTCG	Point mutation
K112A	GGGAAGAATGGAGTAGGGGCAACCACAGTACTTAAAATAC	Point mutation
K381A	CCAAACGGAATTGGAGCGACAACTTTCGCAAGAATA	Point mutation
Sulf1	TTCTGGAGGAGGACTT	Sequencing primer
T7	TAATACGACTCACTATAGGG	Sequencing primer
T7 term	GCTAGTTATTGCTCAGCGG	Sequencing primer
M13F	TGTAAAACGACGGCCAGT	Sequencing primer
M13R	CAGGAAACAGCTATGACC	Sequencing primer

2.7 Equipment

Apparatus	Company
AEKTA explorer	GE Healthcare
Autoclave 5075 ELVC	Tuttnauer Systec
Cary 50 Bio UV/Vis spectrophotometer	Varian
Cell disruption system	BasicZ, IUL Instruments
ELISA reader, PolarStar Galaxy	BMG Labtechnologies
EXTRA IIA spectrometer	Atomica instruments
Gel electrophoresis apparatus	Biorad/Hoefer
Incubator Kelvitron	Heraeus
Incubator	HT
Ino Lab pH-meter	WTW
Kern 770 microbalance	Kern
Lumi imager F1™	Roche
Magnetic stirrer	Ikamag
Membrane vacuum pump	Kobe

Mettler PM 460 balance	Mettler
Microwave T.D.S.	Samsung
Milli Q-Plus water system	Millipore
Multipipette	Eppendorf
NanoDrop ND-1000 UV/Vis spectrophotometer	Peqlab Biotechnologie GmbH
PCR machine, T personal	Biometra
Semi-dry Blot apparatus	Biorad
SMART chromatography system	GE Healthcare
Sonicator	Branson
Superdex 200 HiLoad 16/60	GE Healthcare
Superdex 200 PC 3.2/30	GE Healthcare
Thermomixer	Eppendorf
UV table, UVT-20 M/W	Herolab
Vortexer, Vortex Genie 2™	Bender & Hobein AG

2.8 Centrifuges and Rotors

Centrifuge	Rotor
Eppendorf centrifuge 5417R	F-45-30-11
Heraeus Sepatech Megafuge 1.0 R	BS4402/A
Sorvall RC 5B Plus	GSA
Beckman L-50	Ti50, Ti60, Ti80, SW27, SW41

2.9 Supplementary material

Material	Company
Cuvettes, plastic	Fisher Scientific
Cuvettes, quartz glass	Hellma
Dynabeads Protein G	Dynal Biotech
Eppendorf tubes	Greiner
Filter paper	Whatman
Gloves, latex	Terumo Teruglove
Gloves, nitril	Servoprax
HisSelect™ columns	Sigma-Aldrich
HiTrap™ chelating columns	GE Healthcare
Micro Bio-Spin P-6 columns	BioRad
Microliter syringes	Hamilton
Multiwell plates	Greiner
Nitrocellulose membrane	Schleicher & Schüll
Pasteur pipettes	Merck
PCR tubes	Sarstedt
PD-10 desalting columns	GE Healthcare
Pipette tips	Greiner
Pipettes	Abimed
Spin concentrators (Amicon)	Millipore
Strep-Tactin Superflow Cartridge	IBA GmbH
Syringes, plastic	Braun
Test tubes, plastic, sterile 15 ml and 50 ml	Greiner

3 Methods

3.1 Molecular biology

3.1.1 Construction of plasmids

For site-directed mutagenesis, primers were phosphorylated using T4 polynucleotide kinase for 30 min at 37°C. After inactivation for 10 min at 70°C, ligase chain reaction was performed with *Pfu*-polymerase and *Amp*-ligase using plasmid DNA as template and 20 pmol of the phosphorylated primers in PCR-buffer containing 2 mM $MgSO_4$, 0.2 mM dNTPs and 1 mM NAD. The PCR was started with 1 min denaturation at 95°C followed by 30 cycles of 1 min denaturation at 95°C, 1 min annealing at 55°C, and 15 min extension at 65°C. The mutated plasmid was isolated with the PCR extraction Kit (Qiagen) following the manufacturer's instructions. Subsequently, the plasmid was incubated for 2 h at 37°C with *Dpn*I to remove the parental methylated DNA and transformed into competent DH5α cells.

Plasmids were isolated with the NucleoSpin Plasmid Kit (Machery-Nagel), following the manufacturer's instructions. Plasmid-DNA was eluted with 30 µl of ddH_2O and stored at -20°C. Restriction of plasmids was done using the amount of enzymes, buffers and incubation times as suggested by the manufacturer. To separate DNA fragments after restriction 1% agarose gels were prepared in TAE-buffer (20 mM Tris/acetate, pH 8, 1 mM EDTA) containing ethidium bromide for staining. Samples were mixed with 6 × loading dye (Fermentas) and loaded onto the gel. Gels were run at 100 V for 40 min. DNA fragments were extracted from the gel by using the QIAquick Gel Extraction Kit (Qiagen) following the manufacturer's instructions. Ligation of inserts into the appropriate vector was performed with 3 × fold excess of insert DNA to vector using T4 DNA ligase overnight at 16°C in ligation buffer containing 2 mM ATP. Subsequently the mixture was transformed into competent *E. coli* cells. For cloning and amplification of plasmids the strain DH5α was used and for protein expression the ligation mixture was transformed into the *E. coli* strain BL21(DE3). Plasmids were verified by restriction analysis and positive clones by DNA sequencing, performed by the company Scientific Research and Development GmbH.

3.1.2 Cloning of the ABCE1 gene for expression in *E. coli*

The open reading frame (ORF) of the *Sulfolobus solfataricus* ABCE1 gene SSO0287 was amplified by PCR using genomic DNA and the primers, P1f and P2r, and cloned into the *Nco*I and *Bam*HI sites of the pSA4 expression vector (modified pET15 vector with T7 promoter). The resulting plasmid (pSD1) codes for the wild-type ABCE1 protein of *S. solfataricus* with a carboxy-terminal His_6-tag. A truncated version of *S. solfataricus* ABCE1 (amino acids 69-600) comprising the two nucleotide binding domains was generated by PCR using the wild-type construct pSD1 and the primers, P3f and P2r, yielding pSD2. The conserved glutamate residue downstream of the Walker B motif in both NBDs of the wild-type construct was changed to glutamine (E238Q and/or E485Q) and the conserved lysine converted to alanine (K112A and/or K381A) by site-directed mutagenesis.

3.1.3 Cloning of the ABCE1 gene for expression in *S. solfataricus*

For over-expression of affinity-tagged ABCE1, a stable and selectable shuttle vector based on the virus SSV1 of *Sulfolobus shibatae* was used (Albers *et al.*, 2006). The ORF SSO0287 (ABCE1) was amplified by PCR using genomic DNA of *S. solfataricus* and the primers, P1f and P4r. This resulted in the introduction of *Nco*I and *Apa*I restriction sites in the flanking regions of the gene and a tandem-affinity tag at the carboxy-terminus (His_8-tag and StrepII-tag). The gene was cloned into pSVA5 using the *Nco*I and *Apa*I sites resulting in pSVA30. To transfer the araS promoter together with the gene to be expressed into the virus-based vector, the *Bln*I/*Eag*I insert from pSVA30 was ligated into pMJ05, resulting in the plasmid pSVA31.

3.2 Microbiology

3.2.1 Competent *E. coli* cells

An overnight culture of *E. coli* cells was diluted 1:200 in 200 ml of LB medium and grown at 37°C to an OD_{550} of 0.5. The culture was incubated on ice for 10 min and harvested at 2000 × g at 0°C for 10 min. The cell pellet was carefully resuspended in 35 ml ice-cold TFB I buffer (30 mM potassium acetate, 100 mM RbCl, 50 mM $MnCl_2$, 10 mM $CaCl_2$,

15% glycerol, pH 5.8) and incubated on ice for 1 h. After centrifugation at 3000 × g at 0°C for 10 min, the cell pellet was resuspended in 6 ml of ice-cold TFB II buffer (10 mM MOPS, 10 mM RbCl, 75 mM $CaCl_2$, 15% glycerol, pH 6.8). Cell aliquots of 100 µl were frozen in liquid nitrogen and stored at -80°C.

3.2.2 Transformation of competent *E. coli*

100 µl of *E. coli* DH5α or BL21 competent cells were incubated with 1 µl plasmid DNA on ice for 30 min. Heat shock was performed for 45 sec at 42°C and subsequently cells were incubated for 1 min on ice. 900 µl of LB medium (10 g/l tryptone, 5 g/l yeast extract, 5 g/l NaCl) were added and regeneration was done for 45 min at 37°C in a thermomixer. 100 µl of the regenerated cells were plated on LB-Agar-plates containing the appropriate antibiotic and incubated overnight at 37°C.

3.2.3 Electroporation of *S. solfataricus*

Electroporation of *S. solfataricus* was performed as described earlier (Schleper *et al.*, 1992). A mid-logarithmic culture (OD_{600} 0.2-0.3) of *S. solfataricus* M16 (pyrEF/lacS double mutant) was cooled on ice and pelleted in 50 ml tubes by low speed centrifugation. The cell pellet was washed once in an equal volume of cold 20 mM sucrose in double-distilled water, pH 5.6. To decrease the amount of residual salts from the growth medium, the cells were washed again in ½ and then in 1/50 of the original culture volume. Finally, the pellet was resuspended in 20 mM sucrose at a concentration of about 10^{10} cells per ml. Ice-cold aliquots (50 µl) were mixed with 1µl of DNA (100-300 ng) and transferred to plastic electroporation cuvettes with an electrode gap of 1 mm. The cuvettes were closed and cooled on ice for 5 min. The high-voltage electroporation was performed for 9.1 ms at a field strength of 1.5 kV/cm with a Gene Pulser apparatus. After electroporation the mixture was immediately diluted with 1 ml of growth medium. Cells were regenerated at 75°C for 1 h. 50 ml Brock medium containing uracil (10 µg/ml) was inoculated with the electroporated cells. After 2-3 days of growth cells reached an OD_{600} of 0.5 and were transferred to selective medium without uracil.

3.2.4 Isolation of single transformants of *S. solfataricus*

To obtain single transformants cells were plated on media without uracil and incubated for 5 days at 80°C. For solid media, gelrite (gellan gum) was added to a final concentration of 0.6% to tryptone medium. Magnesium and calcium were added to 10 mM and 3 mM, respectively. Chromosomal DNA was isolated as described earlier (Schleper *et al.*, 1992). Integration of the viral vector into the genome was confirmed by Southern blot analysis using standard procedures.

3.2.5 Heterologous expression of *S. solfataricus* ABCE1 in *E. coli*

The *E. coli* strain BL21(DE3) was co-transformed with ABCE1 constructs and the pRARE plasmid coding for rare tRNAs and grown in LB medium supplemented with 100 µg/ml ampicillin and 25 µg/ml chloramphenicol at 37°C. Expression was induced at an OD_{600} of 0.6 for 3 h at 30°C by adding 0.2 mM IPTG.

3.2.6 Homologous expression of ABCE1 in *S. solfataricus*

S. solfataricus PH1-16 cells containing pSVA31 were inoculated from a frozen stock culture and grown in 50 ml Brock's medium containing 0.1% tryptone. After two days of growth (OD_{600}~0.4) at 80°C and pH 3, cells were transferred to two flasks each filled with 400 ml medium containing 0,1% tryptone and 0.2% arabinose to induce expression of ABCE1. After the cells reached OD_{600}~0.4, the culture was splitted in eight flasks each filled with 1500 ml Brock medium containing 0.1% tryptone and 0.2% arabinose. After two additional days of growth (OD_{600}~0.7), the cells were harvested at 4,000 × g for 20 min at 4°C and resuspended in 20 mM NaH_2PO_4, 300 mM NaCl, 20 mM imidazole, pH 7.4, frozen in liquid nitrogen, and stored at -80°C.

Brock I stock solution	**Brock II stock solution**	**Brock III stock solution**	**Fe solution**
0.48 mM $CaCl_2$ autoclave	1 M $(NH_4)_2SO_4$ 100 mM $MgSO_4$ 0.15% H_2SO_4 1:1 autoclave	410 mM KH_2PO_4 10 nM $MnCl_2$ 120 nM $Na_2B_4O_7$ 640 nM $ZnSO_4$ 0.5 nM $CuCl_2$ 0.1 nM $NaMoO_4$ 0.03 nM $CoSO_4$ 0.09 nM $NiSO_4$ 0.15% H_2SO_4 1:1 autoclave	7.4 mM $FeCl_3$ sterilize with filter

Brock medium	
Brock I	0.1%
Brock II	1%
Brock III	0.5%
Fe solution	0.1%
Tryptone	0.2%
adjust pH to 3.5 with H_2SO_4	

3.2.7 Expression and site-directed mutagenesis of ABCE1 in yeast

For generation and analysis of yeast ABCE1 mutants a yeast strain was used in which the endogenous, chromosomal promoter of ABCE1 was replaced by a tetracycline-regulated promoter (Hughes, 2000). The cells were transformed with the multi-copy plasmid pRS423 harboring the wild-type or the mutated gene. A plasmid coding for the ABCE1 homologue in *S. cerevisiae* ABCE1 was generated by PCR using the primers P5f and P5r with chromosomal DNA as template. The amplified construct was inserted into the *Sal*I and *Sma*I restriction sites of the vector pRS423. The protein was expressed under the control of the endogenous promoter.

The highly conserved amino-terminal cysteine residues C16, C21, C25, C29, C55, C58, C61 and C65 as well as the non-conserved cysteine C38 were exchanged to serines or to alanines by site-directed mutagenesis. Single, double, and triple mutations of these cysteines as well as a double mutation of C29 in combination with S28 to alanines were generated and transformed into yeast cells. After doxycycline treatment, the chromosomal expression of ABCE1 was repressed and the plasmid-encoded ABCE1 mutants were expressed substituting the mutated endogenous protein in the cells. For control, yeast cells were either transformed by the ABCE1 gene or the vector alone.

3.3 Protein isolation methods

3.3.1 Purification of ABCE1 via His-Tag

Cell pellets of *S. solfataricus* were thawed and PMSF (end concentration 1 mM) was added. The cells were disrupted by sonication on ice and centrifuged for 1 h at 114,000 × g. Subsequently, ABCE1 was purified to homogeneity via metal affinity chromatography (HisSelect, Sigma) by washing with 20 mM and eluting with 300 mM imidazole.

For purification of ABCE1 expressed in *E. coli* frozen cells were thawed, resuspended in buffer B (20 mM Tris/HCl, 100 mM NaCl, 1 mM EDTA, 1 mM DTT, pH 7.4), and disrupted by sonication. After centrifugation at 114,000 × g for 30 min, the supernatant was heated for 10 min at 75°C and additionally centrifuged for 1 h at 114,000 × g. Subsequently, the solution was applied to metal affinity chromatography (HiTrap, GE Healthcare). ABCE1 was purified by washing with 60 mM imidazole and final elution with 200 mM imidazole. Fractions containing ABCE1 were pooled, dialyzed against buffer C (20 mM Tris, 100 mM NaCl, pH 7.4), and concentrated to ~2 mg/ml using a Centricon 30 device.

Wild-type and mutant proteins were purified to homogeneity (>95%) as assessed by silver-stained SDS-PAGE (10%). The identity of ABCE1 was verified by MALDI-TOF MS. The protein concentration was determined by using the Coomassie Plus Bradford Assay Kit (Pierce) following the manufacturer’s instructions.

3.3.2 Purification of ABCE1 via StrepII-tag

Cell pellets of *S. solfataricus* were disrupted by sonication on ice and centrifuged for 1 h at 114,000 × g. Subsequently, 1 mg of Avidin was added to the supernatant and loaded onto a Strep-Tactin Cartridge equilibrated in buffer W (100 mM Tris/HCl, pH 8, 150 mM NaCl). ABCE1 protein was eluted with buffer W containing 25 mM desthiobiotin. The Strep-Tactin Cartridge was regenerated with buffer W containing 1 mM HABA and stored in buffer W.

3.3.3 Standard SDS-PAGE (polyacrylamide gel electrophoresis)

The stacking gel buffer was composed of 0.5 M Tris/HCl, pH 8.8 and 0.4% (w/v) SDS, the separating gel buffer contained 1.5 MTris/HCl, pH 6.8 and 0.4% (w/v) SDS. The acrylamide solution consists of 30% (v/v) acrylamide and 0.8% N, N' methylenbisacrylamide. The running buffer was composed of 25 mM Tris/HCl, 192 mM glycine, 0.01% (w/v) SDS and the sample buffer (5×) contained 250 mM Tris/HCl, pH 8, 21.25% (v/v) glycerol, 7.5% (w/v) SDS, 2.5% (v/v) β-mercaptoethanol and 0.025% (w/v) bromphenol blue. Samples were denatured in sample buffer for 5 min at 95°C and gels were run at 200 V for 1 h.

Using the MiniProtean-system (Biorad) gels were poured according to the following table:

	Separating gel (10%)	**Stacking gel (4%)**
Separating gel buffer	3.95 ml	-
Stacking gel buffer	-	1.1 ml
Acrylamide solution	3.1 ml	650 µl
H_2O	3.95 ml	2.7 ml
APS	60 µl	45 µl
TEMED	30 µl	15 µl

3.3.4 Gel shift assay and native gel electrophoresis

For gel shift assays, 50 pmol of each of the potentially interacting proteins were incubated in binding buffer (10 mM HEPES, 0.1 mM $MgCl_2$, 0.2 mM GTP) at 65°C for 5 min. Sample buffer (5×) was composed of 40% glycerol containing pyronin Y. Samples were analyzed in a native acrylamide gel, consisting of 12.5% separating gel, pH 4.3 and 4% stacking gel, pH 6.8. The separating gel contained 120 mM K-acetate and 720 mM acetic acid. The running buffer was composed of 130 mM acetic acid and 350 mM D-alanine. The gel run was performed at 150 V for 90 min at inversed polarity, followed by coomassie blue-staining.

Using the Hoefer gel system gels were poured according to the following table:

	Separating gel (12.5%)	**Stacking gel (4%)**
Acrylamide solution	4 ml	1.4 ml
Potassium acetate (1 M)	1.2 ml	1.2 ml
Acetic acid	43 µl	7 µl
H_2O	4.8 ml	7.4 ml
APS	150 µl	150 µl
TEMED	4 µl	14 µl

3.3.5 Coomassie blue and silver staining

For coomassie blue staining the gels were incubated for 20 min in 0.25% (w/v) Coomassie brilliant blue solution and excessive dye was removed by washing in destain solution (40% Ethanol, 10% acetic acid). Gels were rinsed in water afterwards. Gels were incubated for at least 1 h in destain solution and washed two times for 10 min in water. Subsequently, the gels were incubated for 1 min in 0.02% sodium thiosulfate and washed two times for 1 min in ddH_2O. Staining was done in 0.1% silver nitrate for 20 min, followed by two washing steps in ddH_2O for 1 min. Afterwards gels were incubated in developing solution (2% sodium carbonate, 0.04% formaldehyde) until protein staining became visible.

3.3.6 Western Blotting

Gels were transferred onto nitrocellulose membrane in blotting buffer (190 mM glycine, 25 mM Tris/HCl, 0.1% (w/v) SDS) using the Semi-Dry Blot apparatus (BioRad) for 35 min at 100 mA per gel. To determine the efficiency of the protein transfer, the membrane was stained for 5 min in Ponceau Red S solution and washed in water until defined bands were visible. The nitrocellulose membrane containing the transferred proteins was incubated for 1 h in 5% skim milk powder in TBST (20 mM Tris/HCl, pH 8, 150 mM NaCl, 0.2% Tween-20). Subsequently, the membrane was washed 3 times for 5 min in TBST. The first antibody was incubated at the appropriate dilution in 5% skim milk powder in TBST for 1 h. After washing the membrane 3 times for 5 min in TBST the protein bands were visualized using horseradish peroxidase-conjugated second antibody, which was incubated at the appropriate dilution in TBST for 1 h. After washing the membrane three times in TBST for 5 min, the membrane was incubated in freshly prepared detection solution (100 mM Tris/HCl, pH 8.5, 2.5 mM luminol, 0.4 mM coumaric acid, 0.02% H_2O_2) for 1 min. Chemiluminescence was detected using the LumiImager or chemiluminescence film.

For reusing of immunoblots membranes were incubated for 30 min in 250 mM glycine, pH 2.8 and washed extensively in TBST (20 mM Tris/HCl, pH 8, 150 mM NaCl, 0.2% (v/v) Tween-20), subsequently.

3.3.7 Antibody generation

Polyclonal antibodies against ABCE1 purified from *E. coli* were generated in rabbits (Eurogentec).

3.4 Biochemical and biophysical analytical methods

3.4.1 8-azido-ATP crosslinking

Photo affinity labeling of heterologously expressed wild-type and mutant ABCE1 was performed in a final protein concentration of 2 µM and 1 µM of 8-azido-ATP-2',3'-biotin in binding buffer (20 mM Tris/HCl, pH 7.4, 100 mM NaCl, 5 mM $MgCl_2$). Binding of biotinylated ATP was competed by adding either unlabeled ATP or AMP (5 mM) and incubation for 20 min on ice. To induce crosslinking, samples were UV-radiated at 295 nm for 5 min on ice. Photo-crosslinked protein was analyzed by SDS-PAGE and Western blotting using peroxidase-conjugated Extravidin.

3.4.2 ATP hydrolysis assay

ATPase activities were measured by the colorimetric malachite green assay as described previously (Baykov *et al.*, 1988). ATP hydrolysis was measured in triplets in 25 µl of binding buffer (20 mM Tris/HCl, pH 7.4, 100 mM NaCl, 5 mM $MgCl_2$) with ABCE1 (0-10 µM) and ATP (0-5 mM) for 5 min at 80°C. The reaction was terminated by addition of 175 µl of ice-cold 20 mM H_2SO_4 and incubation on ice. After transferring samples onto multiwell plates, 50 µl of freshly prepared staining solution (0.28 mM malachite green solution, 0.17% (v/v) Tween-20, 1.48% (w/v) ammonium molybdate tetrahydrate) were added simultaneously to all samples and incubated for 15 min at RT. Absorption was measured at 620 nm against a phosphate standard (0-6 nmol phosphate) and values of controls (ATP in buffer without protein) were subtracted.

3.4.3 Analytical gel filtration

ABCE1 (~30 µM) purified from *S. solfataricus* and *E. coli* were applied to a Superdex 200 PC 3.2/30 gel filtration column at a flow rate of 50 µl/min in 20 mM Tris/HCl, 100 mM NaCl, pH 7.4) on a SMART system. The absorption was recorded at 280 nm, 260 nm and 410 nm. Dextran blue 2000 (V_0), apoferritin (440 kDa) and bovine serum albumin (66 kDa) were used as molecular weight standards. Fractions of 35 µl were collected and analyzed by SDS-PAGE and Coomassie staining.

3.4.4 Total reflection x-ray analysis

Total reflection x-ray fluorescence, a trace multi-element analytical method was applied to quantify the iron and sulfur content of the purified ABCE1 proteins from *S. solfataricus* and *E. coli*. The measurement was performed using an EXTRA IIA spectrometer with a sample volume of 4 µl in 50 mM Tris-acetate buffer, pH 7.5. The protein solution (~20 µM) was placed onto siliconized quartz carrier plates and evaporated to dryness. By excitation with the Mo(Kα) line for 1000 seconds, a multi-element fluorescence spectrum was obtained. The intensities of the sulfur and iron peaks were related to a rubidium peak as an internal standard. The iron and sulfur content was calculated from the fluorescence spectrum.

3.4.5 Pulsed electron paramagnetic resonance

X-band EPR spectra were measured on a Bruker cavity (MD5-W1) equipped with an Oxford helium flow cryostat (CF935). The pulses were amplified using a 1 kW pulsed traveling wave tube amplifier. A conventional two pulse ($\pi/2 - \tau - \pi$) sequence was used. The field sweep EPR spectrum was obtained by integrating the area under the Hahn echo as a function of the magnetic field. The measurement was performed at 10 K at a microwave frequency of 9.745446 GHz using a Π/2 pulse length of 8 ns, a τ of 120 ns and a shot repetition rate of 1 ms.

3.5 RNA methods

3.5.1 Isolation of total RNA

Total RNA at a concentration of 1 mg/ml was isolated from crude *S. solfataricus* cell extract by using the NucleoSpin RNA II Kit following the manufacturer's instructions.

3.5.2 Isolation of 16S and 23S rRNA

16S and 23S rRNA were obtained by loading ~25 µg of total RNA purified from crude *S. solfataricus* cell extract onto 12 ml linear 5-25% (w/v) sucrose density gradients and centrifuged in a Beckman SW41 rotor operated at 36,000 rpm for 4 h at 4°C. Absorption was measured at 260 nm and fractions corresponding to 16S and 23S peaks were separately pooled and precipitated by addition of 1/10 volume of 3 M sodium acetate and 2.5 volumes of 95% ethanol for 30 min at -20°C. After low spin centrifugation (30 min, 14,000 rpm, 4°C) pellets were washed with 70% ethanol and dried pellets were resuspended in DEPC-treated water.

3.5.3 Isolation of total tRNA

Crude cell extracts (S-30) were centrifuged in a Spinco Ti 50 rotor at 50,000 × g for 2 h at 4°C to separate ribosomes from a supernatant (S-100) containing total cellular tRNAs and cytoplasmatic proteins. Crude total tRNA was obtained by extracting the post-ribosomal supernatants three times with phenol and by precipitation of the last aqueous phase with 2.5 volumes of 95% ethanol.

3.5.4 *In vitro* transcription

For run-off transcription, the constructs were linearized with the appropriate enzyme. Subsequently, the linearized DNA was incubated at 37°C for 90 min with T7 RNA polymerase and 0.5 mM of rNTPs. The reaction mixture was incubated with 10 units of

DNaseI at 37°C for 30 min. The transcribed RNA was purified by three rounds of phenol-chloroform extraction, precipitated and resuspended in DEPC-H_2O.

3.5.5 RNA detection

The size and integrity of the transcribed RNA was checked in 1% agarose gels. RNA concentrations were determined by measuring the absorption at 260 nm using the NanoDrop System.

3.6 Cell biology

3.6.1 Preparation of crude cell extracts

About 5 g of *S. solfataricus* P2 (wild-type) cells were disrupted by grinding with 10 g of alumina powder while gradually adding 2.5 ml/g wet weight of cells of ribosome extraction buffer (20 mM Tris/HCl pH 7.0, 10 mM $Mg(OAc)_2$, 40 mM NH_4Cl, 3 mM DTT, 2.5 µg/ml RNase-free DNase). To avoid contact with RNases the mortar was washed with ANTI-RNase and autoclaved. Alumina and cellular debris were removed by centrifugation twice at 30,000 × g for 30 min. The cleared supernatant (S-30) was stored at -80°C.

3.6.2 Preparation of ribosomes

Crude cell extract (S-30) was centrifuged in a Spinco Ti 50 rotor at 50,000 × g for 2 h at 4°C to separate ribosomes from a supernatant (S-100) containing total cellular tRNAs and cytoplasmatic proteins. Initiation factor free ribosomes were obtained by resuspending the ribosome pellets in a high-salt buffer (20 mM Tris/HCl, pH 7.0, 2 M NH_4Cl, 10 mM $Mg(OAc)_2$, 2 mM DTT). The ribosome suspension was then layered onto a 7.0 ml cushion of 0.5 M sucrose made in high-salt buffer and centrifuged in a Spinco Ti 50 rotor at 45,000 × rpm for 3 h at 4°C. The salt-washed ribosomes (70S) were resuspended at OD_{260} = 500 in ribosome extraction buffer (20 mM Tris/HCl pH 7.0, 10 mM $Mg(OAc)_2$, 40 mM NH_4Cl, 3 mM DTT, 2.5 µg/ml RNase-free DNase) containing 10% (v/v) glycerol.

3.6.3 Isolation of ribosomal subunits

Ribosomal subunits (30S and 50S subunits) were separated by directly centrifuging the salt-washed ribosomes on preparative sucrose gradients. Therefore ribosomes were resuspended in 20 mM Tris/HCl pH 7.0, 40 mM NH_4Cl, 10 mM $Mg(OAc)_2$, 2 mM DTT. 1 ml aliquots of the ribosome suspension (OD_{260} = 40) were layered onto 38 ml linear, 10-30% (w/v) sucrose density gradients made in ribosome-suspending buffer. The gradients were centrifuged in a Beckman SW27 rotor operated at 18,000 × rpm at 4°C for 18 h. When separating ribosomal subunits from crude cell lysate or after *in vitro* translation, samples were loaded onto 12 ml linear 10-30% (w/v) sucrose density gradients and centrifuged in a Beckman SW41 rotor operated at 36,000 rpm for 4 h at 4°C. Absorption was measured at 260 nm and fractions corresponding to 30S and 50S peaks were separately pooled and precipitated by addition of 2 volumes of ice-cold acetone. After low-speed centrifugation, the pellets were resuspended in ribosome extraction buffer containing 10% (v/v) glycerol and stored at -20°C.

3.6.4 Co-immunoprecipitation

Co-immunoprecipitations were performed with Dynabeads Protein G according to the manufacturer's instructions. 50 µl magnetic Dynabeads were washed two times in 500 µl of 100 mM Na_2HPO_4-buffer, pH 6.7. 100 µl of α-ABCE1 antibodies were bound for 80 min at RT while gentle mixing. Subsequently, beads were washed three times with 100 mM Na_2HPO_4-buffer, pH 6.4 containing 0.05% (v/v) Tween-20. The beads were washed two times in 1 ml of 200 mM triethylamine, pH 8.2. Antibodies were crosslinked to the beads by incubation for 30 min at RT in 1 ml of freshly prepared 20 mM dimethylpimelidate in 200 mM triethylamine buffer. The reaction was stopped with 1 ml of 50 mM Tris/HCl, pH 7.4. After 15 min at RT, beads were washed three times with 100 mM Na_2HPO_4-buffer, pH 6.4 containing 0.05% (v/v) Tween-20. 80 µl of *S. solfataricus* cell extract were incubated on the antibody-coupled beads for 1 h at 4°C. The supernatant contained the ABCE1-depleted cell lysate. The magnetic beads were washed three times with 1 ml of 100 mM Na_2HPO_4-buffer, pH 6.7. Bound proteins were eluted by adding of 20 µl SDS-loading buffer, vortexing and incubation at 95°C for 10 min.

3.6.5 *In vitro* translation

Samples contained 3-4 µg of *in vitro* transcribed mRNA, 5 µg of bulk *S. solfataricus* tRNA, 3 µl of [^{35}S]-methionine (1200 Ci mmol^{-1} at 10 mCi mL^{-1}), 10 µl of *S. solfataricus* cell lysate (preincubated for 10 min at 70°C), 20 mM KCl, 20 mM TEA/HCl, pH 7.5, 20 mM Mg acetate, 6 mM ATP and 2 mM GTP in a final volume of 25 µl. The samples were incubated for 1 h at 75°C. 10 µl of the reaction were analyzed by SDS-PAGE (17.5%). The radioactive bands were detected and quantified by autoradiography.

4 Results

4.1 Expression of archaeal ABCE1

4.1.1 Expression of ABCE1 in *S. solfataricus*

To examine the function of ABCE1, *S. solfataricus* ABCE1 was expressed heterologously in *E. coli* and homologously in *S. solfataricus*. Noteworthy, ABCE1 is one of the first examples for recombinant protein production in the hyperthermophilic crenarchaeote *S. solfataricus*, a model organism for archaea with a growth optimum at 80°C. While many systems exist for the production of recombinant proteins in bacterial and eukaryotic model organisms, only a few transformation systems have been developed for archaea so far. Until now, there is no other system available for overexpression of proteins in hyperthermophilic archaeal organisms. However, it is likely that the Fe-S cluster containing protein ABCE1 folds into its native state only under natural conditions of high temperature or in the presence of its native cofactors. For the purpose of high-level gene expression in *S. solfataricus* a virus-based shuttle vector was designed with an arabinose-inducible promoter of the arabinose-binding protein AraS (Albers *et al.*, 2006). In this shuttle vector the complete DNA of the virus SSV1 was combined with pUC18 for replication/selection in *E. coli*, the genes *pyrEF* of *S. solfataricus* for complementation of uracil auxotrophic mutants of *Sulfolobus* and the gene of ABCE1 (SSO0287) (**Figure 8**).

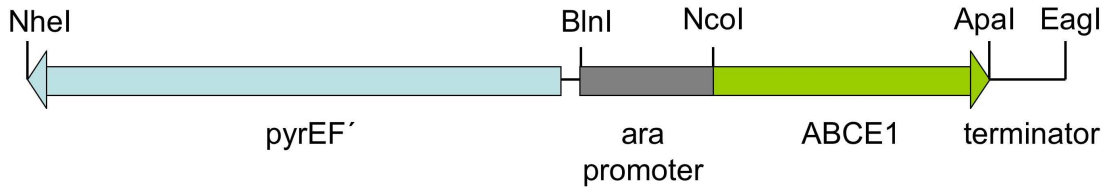

Figure 8: Schematic representation of the *S. solfataricus* shuttle vector. The diagram shows the regions of the pSVA5 vector with the pyrEF gene cassette as a selection marker, the arabinose-inducible promoter and the restriction sites used to clone ABCE1 down the promoter sequence.

SSV1 was originally isolated as 15 kbp plasmid from *Sulfolobus shibatae* and its DNA is packed into lemon-shaped particles that were shown to infect the closely related strain *S. solfataricus* (Schleper *et al.*, 1992). Upon infection, SSV1 DNA integrates site-specifically

into the 3’ end of a tRNA gene in the host chromosome, but it is also detected as a plasmid with approximately three or five copies per chromosome (Reiter *et al.*, 1988; She *et al.*, 2002). Infection and propagation of the virus does not result in cell lysis, but in a significant growth retardation of the host (Martin *et al.*, 1984; Schleper *et al.*, 1992). The pyrEF genes of the shuttle vector allow stable propagation of the vector by growing transformants under selective conditions (Jonuscheit *et al.*, 2003). In order to optimize ABCE1 production, various conditions were tested. The expression of ABCE1 was started with cultures containing 0.1% tryptone without arabinose. Highest protein yield of ABCE1 was achieved when the cultures were induced at OD_{600} = 0.4 by arabinose and grown to OD_{600} = 0.7. When cells were grown to higher densities (OD_{600} > 1.0), degradation products of the ABCE1 protein were observed. The highest yield and purity of ABCE1 protein was obtained, when the cultures were grown with tryptone and arabinose instead of only arabinose at induction time (data not shown). The expression of ABCE1 was scaled up to fermentation in 45 liters (Albers *et al.*, 2006). A fermentor containing medium with 0.1% tryptone and 0.2% arabinose was inoculated with 1.6 liters of ABCE1 expressing *S. solfataricus* culture. After 2 days of growth (OD_{600} = 0.7), the cells were pelleted and the protein was purified. The yields per liter (0.5 to 0.75 mg) were comparable to those from small cultures.

4.1.2 Expression of ABCE1 in *E. coli*

Expression of ABCE1 mutants was performed in the *E. coli* system, due to its easy genetic accessibility. Unfortunately, ABCE1 is prone to degradation in *E. coli*. C-terminal fragments containing the His-tag of ABCE1 were co-purified via metal affinity chromatography and could not be separated by size exclusion chromatography as confirmed by MALDI-TOF. To minimize degradation of the ABCE1 protein, cells were grown at 30°C after induction with IPTG. Different growth conditions were tested: Usage of LB media containing 5% (v/v) ethanol, change of media at induction, ABCE1 expression at 16°C for 20 h or usage of the pET32c expression vector did not prevent degradation (data not shown). A large fraction of expressed ABCE1 was present in inclusion bodies. ABCE1 was purified from the minor soluble fraction to avoid a refolding process. In order to minimize the degradation of ABCE1, which could be due to misfolded Fe-S clusters, different plasmids (pRKISC, pSUF, pNIF) coding for Fe-S cluster assembly proteins were co-transformed with ABCE1 into *E. coli*

C41(DE3) cells. The C41 strain is efficient in overexpressing toxic proteins from all classes of organisms. However, no effect was seen concerning the degradation pattern of ABCE1 (**Figure 9**). For the results presented in this work, ABCE1 was expressed together with rare tRNAs (coded by the pRARE plasmid) to compensate the different codon usage of *S. solfataricus* in *E. coli*.

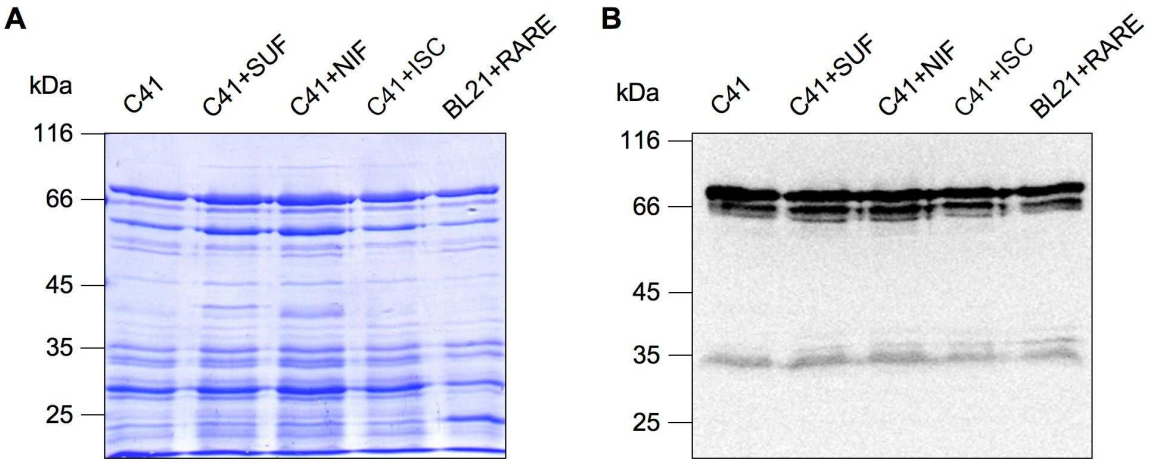

Figure 9: Optimization of ABCE1 expression. The expression of ABCE1 was tested in 100 ml C41(DE3) or BL21(DE3) cells grown for 3 h at 30℃ with or without additional plasmids coding for Fe-S cluster assembly machineries or rare tRNAs. Cells were pelleted and disrupted by sonication. After centrifugation, lysates were incubated for 20 min at 75℃ and centrifuged again. Samples were analyzed by SDS-PAGE (10%). **(A)** Coomassie blue staining, **(B)** Western Blot with α-ABCE1 antibodies.

4.2 Isolation of archaeal ABCE1

ABCE1 was purified via the C-terminal tandem affinity tag (His_8-tag or StrepII-tag) in the homologous expression system and the C-terminal His_6-tag in the heterologous expression system (**Figure 10**). In both systems the isolation was optimized to obtain ABCE1 protein with the highest purity (>95%). To minimize degradation products of ABCE1 purified from *E. coli* different strategies were followed. The isolation procedure and the buffer composition were optimized in order to inhibit protein cleavage and degradation by proteases. Heating the *E. coli* cell lysate for 10 min to 75°C efficiently deactivated proteases and significantly reduced the number of impurities by precipitating *E. coli* proteins. The lowest number of degradation products was obtained with a centrifugation step before heating the cell lysate. The buffer composition was optimized using buffer containing 1 mM EDTA, which blocked

metalloproteases. Adding the protease inhibitor mixture Complete (Roche) or 1 mM PMSF to the cell lysate did not affect ABCE1 protein degradation. Some of the mutant ABCE1 proteins (E238Q/E485Q and K112A/K381A) showed higher degradation profiles than wild-type protein. Metal affinity chromatography was performed using HiTrap chelating columns (GE Healthcare). Impurities were separated by a washing step with 60 mM imidazole, further washing steps or elution with an imidazole gradient showed no further improvement. C-terminal ABCE1 fragments eluted slightly before full-length ABCE1, when proteins were eluted with 200 mM imidazole. For this reason the first eluting fractions of full-length ABCE1 were discarded as decided by SDS-PAGE and Coomassie-staining.

ABCE1 expressed in *S. solfataricus* was isolated via the His_8-tag using the HisSelect-cartridge (Sigma). For purification from *S. solfataricus* cells this column material proved to be much better than the HiTrap Chelating column (Ge Healthcare) in respect to impurities. Isolation of ABCE1 protein from *S. solfataricus* via the StrepII-tag with the Strep-Tactin cartridge (IBA) resulted in very pure ABCE1 protein. Gel filtration experiments revealed that the isolation via His_8- or StrepII-tag lead to different oligomeric states of ABCE1 (see 4.7). Purified ABCE1 protein exhibited a brownish color. About 0.5 mg of purified protein at 2-3 mg/ml was obtained per liter of *S. solfataricus* or *E. coli*. The identity of the protein was confirmed by MALDI-TOF MS.

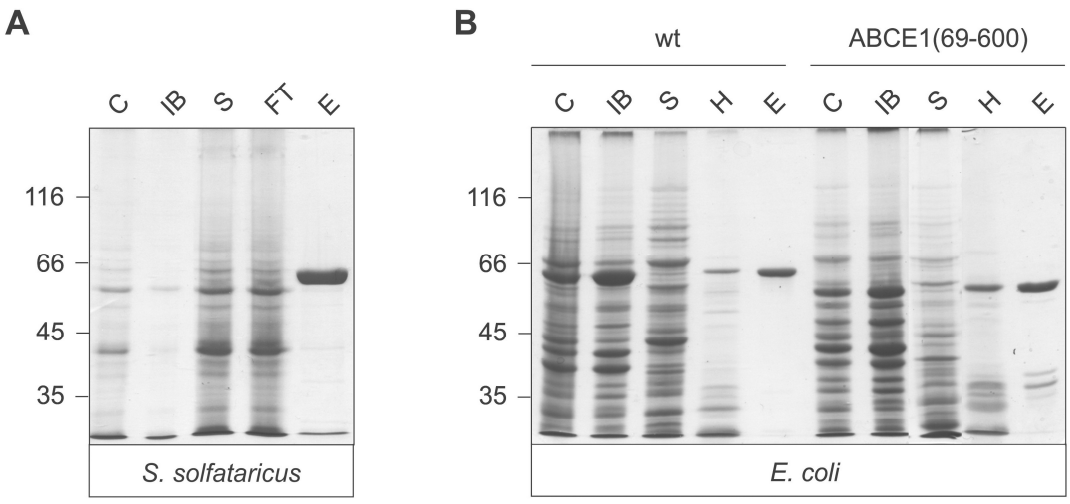

Figure 10: Expression and purification of archaeal ABCE1. ABCE1 was expressed and purified via immobilized metal affinity chromatography (IMAC) from *S. solfataricus* **(A)** and from *E. coli* **(B)** and analyzed by SDS-PAGE (10%, Coomassie-stained). C, cell lysate; IB, inclusion bodies or unbroken cells; S, supernatant after centrifugation; H, supernatant after heat shock; FT, flow through; E, elution.

4.3 ABCE1 is active in ATP hydrolysis

In ABC transporters the NBDs bind and hydrolyze ATP to drive the transport of substrates across membranes. The fact that ABCE1 is not membrane-associated raises questions about the role of the NBDs in this protein. Therefore, the ATPase activity of ABCE1 was analyzed. Wild-type ABCE1 purified from *S. solfataricus* was active in ATP hydrolysis with a K_m of 0.7 mM and a turnover of 10 ATP/min at 80°C. No cooperativity was observed (Hill coefficient of 1.0). As expected for a protein from a hyperthermophilic organism, the ATPase activity of ABCE1 showed a bell-shaped curve with an optimum at temperatures around 80°C (**Figure 11**). The truncated mutant lacking the Fe-S clusters revealed a similar ATPase activity as wild-type ABCE1 purified both from *E. coli* or *S. solfataricus*. In conclusion the amino-terminal Fe-S cluster domains did not affect ATP hydrolysis.

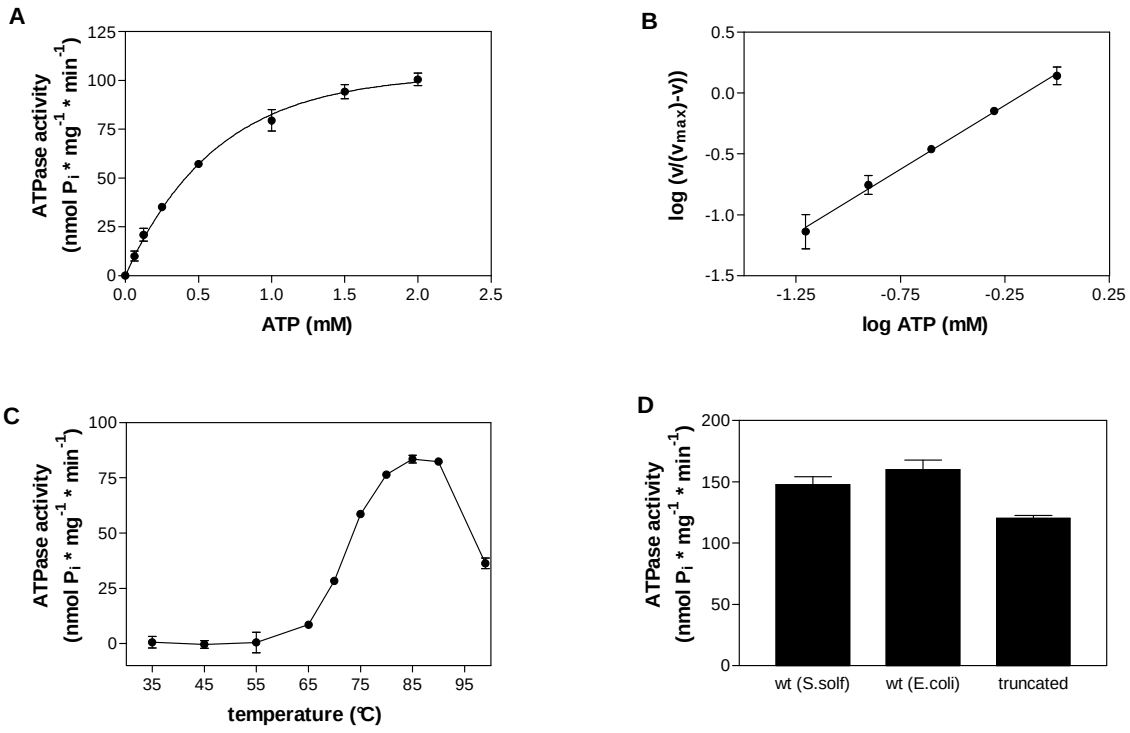

Figure 11: ATPase activity of archaeal ABCE1. The release of inorganic phosphate was determined with purified ABCE1. **(A)** Purified wild-type ABCE1 from *S. solfataricus* (4.3 µM) was incubated for 5 min at 80°C with increasing amounts of ATP. A K_m value of 0.7 mM, v_{max} of 137 nmol $P_i \times mg^{-1} \times min^{-1}$, and k_{cat} of 10 min^{-1} was determined. **(B)** Hill plot of the results shown in (A) with a Hill coefficient of n = 1. **(C)** Wild-type ABCE1 (4.3 µM) purified from *S. solfataricus* was incubated with 1 mM ATP for 5 min at different temperatures. **(D)** Wild-type or mutant ABCE1 from *E. coli* and wild-type ABCE1 from *S. solfataricus* (4.3 µM) were incubated for 5 min at 80°C with 5 mM ATP to determine v_{max}. All ATPase data are corrected for background hydrolysis (identical conditions without protein). The data represent the mean of three independent measurements and the error bars indicate the standard deviation.

4.4 The two NBDs in ABCE1 are functionally non-equivalent

To address the functional role of each NBD, conserved catalytic residues were mutated. First, a catalytic glutamate residue downstream of the Walker B motif was replaced by a glutamine. It is well accepted that mutation of this conserved residue in other ABC proteins does not affect ATP binding but leads to a severely impaired ATPases activity of the NBD (Janas *et al.*, 2003; Moody *et al.*, 2002). Second, a conserved residue in the Walker A motif was replaced by an alanine, which causes impaired nucleotide-binding properties in other ABC transporters. In most examples blocked ATP hydrolysis results in a stable NBD dimer. In ABC transporters, dimer formation of the NBDs upon ATP binding is required for a transport cycle (van der Does *et al.*, 2006; van der Does and Tampé, 2004). Since ABCE1 contains two NBDs, intramolecular dimerization of both NBDs or intermolecular association of two ABCE1 molecules is possible. The E/Q or K/A mutation in each of the NBDs of ABCE1 either alone or in both NBDs was introduced, to address the functional role of both NBDs. The mutants of ABCE1 were expressed and isolated from *E. coli* in equal amounts as the wild-type protein. As expected, the double E/Q and K/A mutants showed almost no residual ATPase activity (**Figure 12**). When the mutation was introduced in the first NBD (E238Q or K112A), the protein exhibited a reduced ATPase activity compared to wild-type ABCE1 (2-fold decrease). Strikingly, a 15-fold increase in ATPase activity was observed after mutating the corresponding glutamate or lysine in the second NBD (E485Q or K381A).

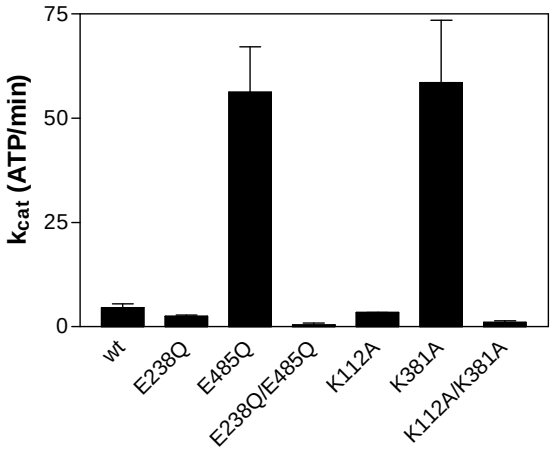

Figure 12: ATPase activity of mutant NBD domains in ABCE1. The turnover number (ATP/min) was calculated from the release of inorganic phosphate determined at 80°C and 2 mM ATP. ATPase activity was performed with 2.9 µM of wild-type, E238Q, E238Q/E485Q, K112A, K112A/K381A and 0.4 µM of E485Q and K381A ABCE1 purified from *E. coli*. The data represent the mean of three independent measurements and the error bars indicate the standard deviation.

This could be caused by stable intermolecular dimerization of two ABCE1 molecules or stable intramolecular dimerization of the NBDs. In order to examine whether active ABCE1 is composed of one or two ABCE1 molecules, the dependency of protein concentration on ATPase activity was analyzed in wild-type and in the hyperactive mutants. In a dynamic equilibrium of ABCE1 monomers causing intermolecular interactions, a non-linear relation to protein concentration is expected, which however, was not observed in these experiments. In contrast, wild-type ABCE1 and the hyperactive mutants exhibited a linear relationship of protein concentration on ATPase activity (**Figure 13**).

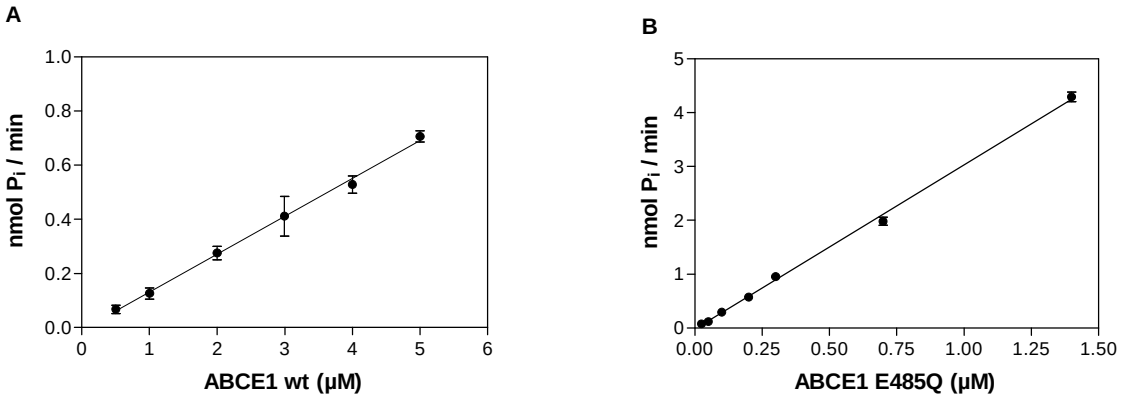

Figure 13: Linear dependency of the release of inorganic phosphate on protein concentration. (A) wild-type ABCE1 (corresponding to a K_{cat} of 3.5-5 ATP/min). (B) ATPase hyperactive E485Q mutant (corresponding to a K_{cat} of 60-110 ATP/min).

The non-equivalence of the ABCE1-NBDs in ATP hydrolysis could be explained by different functional roles of both NBDs. The ATP binding properties of each mutant were analyzed in order to exclude that different ATP binding properties result in the observed increased ATPase activity of NBD2. For this purpose the E/Q and K/A ABCE1 mutants were crosslinked with 8-azido-ATP, which was competed by non-labeled ATP. In this assay, the NBDs of ABCE1 were shown to bind ATP (wt shown in **Figure 15**) even after introduction of the E/Q or K/A mutation (**Figure 14**). The hyperactive K381A-mutant showed only weak 8-azido-ATP crosslinking, which however was not due to lower protein amounts. Protein levels were equal in all analyzed samples judged by Western blotting against ABCE1. In the K381A-mutant the bound 8-azido-ATP was also competed by ATP.

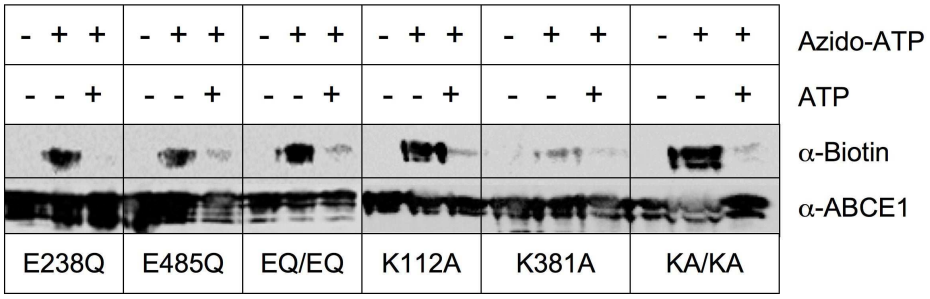

Figure 14: Nucleotide binding properties of NBD mutants. 2 µM of mutant ABCE1 purified from *E. coli* were incubated with 5 mM ATP and/or 1 µM of 8-azido-ATP-2',3'-biotin in 10 mM $MgCl_2$ for 15 min on ice. Photo affinity labeling was performed for 5 min on ice. Samples were analyzed by SDS-PAGE (10%) and Western blotting (wt shown in Figure 16).

4.5 Nucleotide binding properties of ABCE1

As a functional hallmark, many ABC proteins contain two NBDs with very distinct roles in ATP binding and hydrolysis. Binding of nucleotides to ABCE1 was investigated by a photo-crosslinking assay competing 8-azido-ATP by non-labeled nucleotides. Both wild-type and a truncated mutant of ABCE1 lacking the Fe-S domains purified from *E. coli* exhibited the same binding properties, verifying that nucleotide binding is attributed to the NBDs, excluding binding of nucleotides to the amino-terminal domains (**Figure 15**). Since ABC transporters usually do not bind AMP, AMP was used as a control. Strikingly, 8-azido-ATP was competed by ATP or AMP. If ATP and AMP bind to the same site of ABCE1, AMP should be a competitor of ATPase activity. Indeed, after addition of 2 mM AMP, the ATPase activity of ABCE1 was decreased by 30% (data not shown).

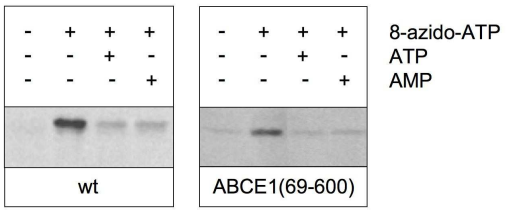

Figure 15: Nucleotide binding of ABCE1 by photo-crosslinking. Photo affinity labeling with 8-azido-ATP-2',3'-biotin (1 µM) of wild-type, and truncated ABCE1(69-600) (2 µM each) purified from *E. coli*. 8-Azido-ATP photo-crosslinking was competed with ATP or AMP (5 mM). Samples were analyzed by SDS-PAGE (10%) and Western blotting using α-biotin antibodies.

4.6 ABCE1 harbors two diamagnetic Fe-S clusters

In addition to the two ABC ATPase domains, ABCE1 harbors a unique N-terminal region containing eight conserved cysteines with the $CX_4CX_3CX_3CPX_nCX_2CX_2CX_3CP$ consensus sequence, predicted to coordinate iron-sulfur clusters. For ABCE1, a specific incorporation of iron and the interaction with members of the Fe-S cluster assembly machinery was demonstrated indicating a functional importance of two of these eight cysteine residues (position 3 and 7) (Kispal *et al.*, 2005). However, information regarding the type and structural organization of the Fe-S clusters is not available until now (Barthelme *et al.*, 2007). To address these issues this study was initiated in collaboration with Dominik Barthelme and Dr. Urte Scheele.

The first indication for the presence of Fe-S clusters in ABCE1 was the brownish color and its UV/VIS spectrum, which revealed a shoulder at 410 nm (**Figure 16**). Absorption centered around 410 nm can be attributed to thiolate-to-iron charge-transfer transitions from cysteines coordinating Fe-S clusters (Porello, 1998). The absorption spectrum of wild-type ABCE1 isolated from *E. coli* differed only by the lower extinction coefficient ε_{410}. Importantly, a truncated version of the ABCE1 protein, which lacks the amino-terminal cysteine-rich domains, ABCE1(69-600), did not show any absorption above 280 nm (**Figure 22**). As presented below, homologously expressed ABCE1 existed in an oligomeric and a monomeric state (see 4.7). The presence of Fe-S clusters in both peak fractions (440 and 68 kDa) was demonstrated by the absorbance at 410 nm in analytical gel filtration. The ratio of absorption at 280 nm and 410 nm was 8:1 in the oligomeric state and 4:1 in the monomeric fraction.

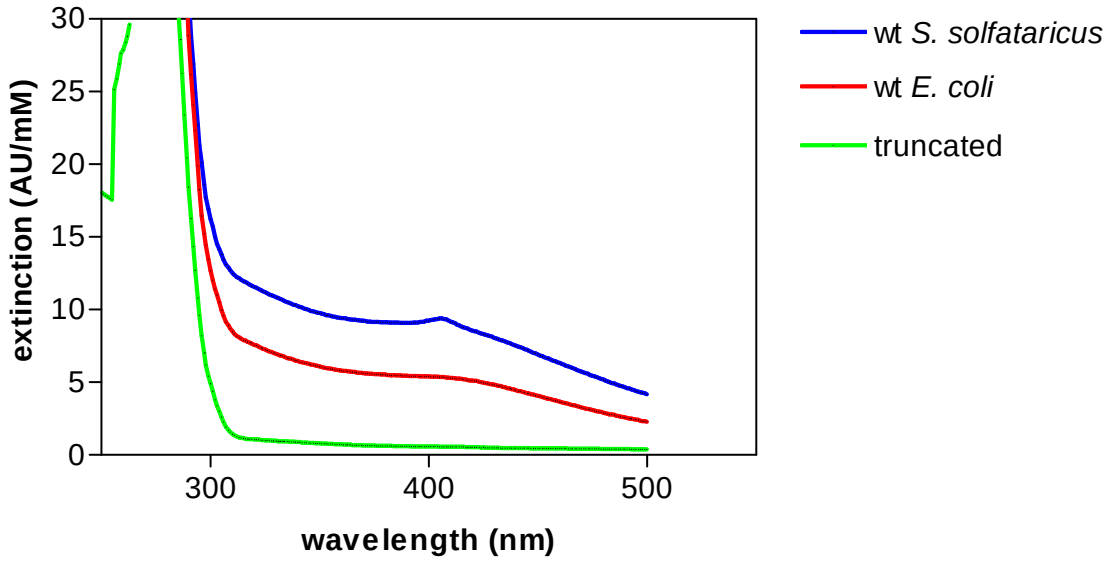

Figure 16: UV/Vis absorption spectra of wild-type ABCE1 purified under aerobic conditions from *S. solfataricus* or *E. coli* as well as amino-terminally truncated ABCE1(69-600).

To quantify the amount of metal ions incorporated in the clusters of ABCE1, total x-ray reflection fluorescence (TXRF) spectroscopy was performed. If ABCE1 contains the two predicted [4Fe-4S]-clusters, 8 iron atoms per ABCE1 molecule should be detected. In wild-type ABCE1 5-7 iron atoms per ABCE1 molecule were found, depending on the kind of preparation. When ABCE1 was purified from *E. coli* under aerobic conditions 4.5 iron atoms were determined. Purification from *E. coli* cells under exclusion of oxygen resulted in ABCE1 containing 6.0 iron atoms. When ABCE1 was purified from *S. solfataricus* under aerobic conditions 5.5 iron atoms were detected, while purification under exclusion of oxygen led to 6.8 iron atoms per ABCE1 molecule. Considering a small amount of impurities and the intrinsic error in protein quantification, it is likely that the iron and sulfur content are slightly underestimated. Especially for the protein isolated from *E. coli* a small population of non-assembled Fe-S cluster was found. Nickel, zinc, copper, molybdenum and wolfram were not detected above background, while ABCE1 purified from *S. solfataricus* contained 11 phosphor atoms per ABCE1 molecule. In the truncated version of ABCE1(69-600), no iron above background was detected. Together with the UV/VIS data, these findings indicate that wild-type ABCE1 contains either two cuban or one cuban and one cuboidal Fe-S clusters.

To characterize the type of Fe-S clusters in ABCE1, the protein purified from *S. solfataricus* was subjected to electron paramagnetic resonance (EPR) spectroscopy. After purification of ABCE1 under aerobic conditions a substoichiometrical characteristic signal for a $[3Fe\text{-}4S]^{+}$ cluster in the oxidized state of ABCE1 was detected (**Figure 17**). The relatively isotropic g-tensor of g(x) = 2.0220; g(y) = 2.0196, and g(z) = 2.0053 was indicative for a $[3Fe\text{-}4S]^{+}$ cluster (Ackrell *et al.*, 1984; Elsasser *et al.*, 2002). The EPR signal disappeared upon reduction with 10 mM sodium dithionite. Paramagnetic [4Fe-4S] clusters usually exhibit much broader spectra due to their anisotropic g-tensor, while $[4Fe\text{-}4S]^{2+}$ clusters are EPR silent. After purification of wild-type ABCE1 from *S. solfataricus* and *E. coli* under anaerobic conditions, the two Fe-S clusters identified in ABCE1 were EPR-silent and therefore in a diamagnetic state. This demonstrates the presence of two diamagnetic $[4Fe\text{-}4S]^{2+}$ clusters in ABCE1, one of which is sensitive to oxidation shown by the formation of a $[3Fe\text{-}4S]^{+}$ cluster upon oxidative degradation during aerobic preparation.

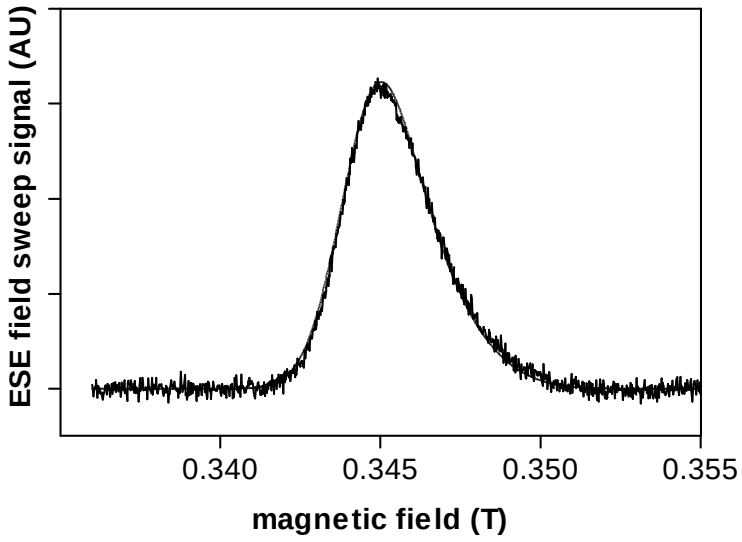

Figure 17: Field sweep electron spin echo (ESE) spectroscopy. Pulsed EPR X-band spectrum (dark line) of ABCE1 purified under aerob conditions from *S. solfataricus* (50 µM). For simulation (grey line), G-tensor principal values g(x) = 2.0220, g(y) = 2.0196, and g(z) = 2.0053 were used.

In collaboration with Dr. Urte Scheele we analyzed whether all eight cysteines are essential to build up the Fe-S clusters. A [4Fe-4S] center is formed by four inorganic and four organic sulfur atoms, the latter provided by four cysteine residues, whereas only three cysteines are essential for a [3Fe-4S] cluster. As *S. solfataricus* cannot be easily genetically accessed, *S. cerevisiae* was used as a screening system for viability of yeast ABCE1 mutants, in which each of the eight conserved cysteines was individually or in combination exchanged to alanine or serine, respectively. Plasmids encoding ABCE1 including these mutations were transformed into a yeast strain, in which the endogenous promoter of ABCE1 was replaced by a tetracycline-repressible promoter. After repression of endogenous ABCE1 by addition of doxycycline, single clones were analyzed for viability. Remarkably, only five out of the eight conserved cysteines (C16, C25, C55, C61 and C65; position 1, 3, 5, 7, 8) were found to be essential for cell survival (**Figure 18**). Surprisingly, the C21S, C29S and C58S mutants (position 2, 4, 6) were still viable. Since it is known that serine residues can coordinate Fe-S clusters in certain cases, each of these three cysteine residues were mutated to alanine. Here, C29A and C58A (position 4 and 6) were still viable, but the C21A mutant (position 2) was lethal. In conclusion, six coordinating cysteines, of which serine at position 2 can partially be accepted, are strictly required for the formation of Fe-S clusters. Double and triple mutations of C21, C29 and C58 were not viable. In contrast to ABCE1 from *S. solfataricus*, yeast ABCE1 contains a non-conserved cysteine (C38) in addition to the eight conserved cysteine residues. Mutation of the non-conserved C38 to alanine was without a phenotype in yeast, but was lethal in combination with the mutation of C29A (**Figure 18**). In a process called ligand swapping a cysteine, originally not involved in Fe-S cluster coordination, can take over the function of a missing or mutated cysteine residue. In conclusion, only the cysteine at position 6 is not essential for the assembly of the Fe-S cluster. This demonstrates that ABCE1 contains two [4Fe-4S] clusters one of which can be interconverted to a [3Fe-4S] cluster, with seven cysteines serving as essential ligands in order to maintain cell viability (**Figure 18**).

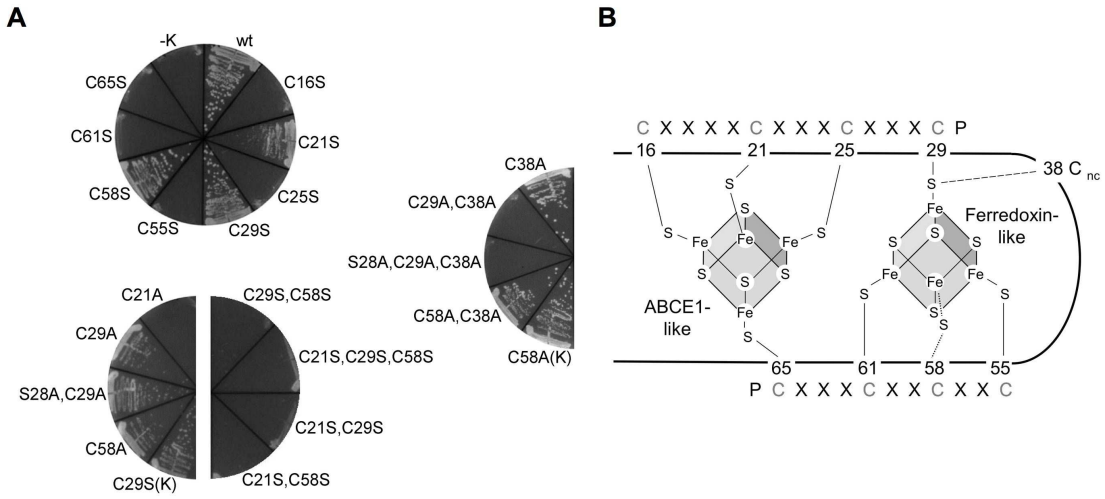

Figure 18: ABCE1 contains two [4Fe-4S] clusters. (A) Functional analysis of cysteine mutants in *S. cerevisiae*. Indicated mutants were transformed into a yeast strain, in which the endogenous promoter of ABCE1 was replaced by a tetracycline repressible promoter. The plasmid containing wild-type ABCE1 (wt) served as a positive control, the empty vector as a negative control (-K). **(B)** A model of Fe-S cluster organization in ABCE1 is shown. The conserved first (C16), second (C21), third (C25) and eighth (C65) cysteine residues form the unique RLI cluster $C(X)_4C(X)_3C(X)_nCP$, while the conserved fourth (C29), fifth (C55), sixth (C58), and seventh (C61) cysteine form the ferredoxin-like cluster $CP(X)_nC(X)_2C(X)_2C$. The dotted line indicates the dispensable nature of the sixth conserved cysteine (C58) in the latter cluster and the dashed line shows the substitution of the fourth (C29) cysteine by the non-conserved cysteine C38 within the ferredoxin-like cluster (ligand swapping).

4.7 Oligomerization of ABCE1

Upon His_8-tag purification of homologously expressed ABCE1 from *S. solfataricus* the protein eluted from the gel filtration column in two distinct populations. The first peak contained a large oligomeric complex of ABCE1 of the same size as apoferritin (440 kDa), which would be consistent with a hexamer (~420 kDa). The second peak was assigned to the 68 kDa monomeric protein corresponding to a size of BSA. Notably, the oligomeric complex contained no other protein except ABCE1 as demonstrated by SDS-PAGE silver-staining (**Figure 19**). Interestingly, such an oligomeric complex was not observed when homologously expressed ABCE1 was isolated via the StrepII-tag.

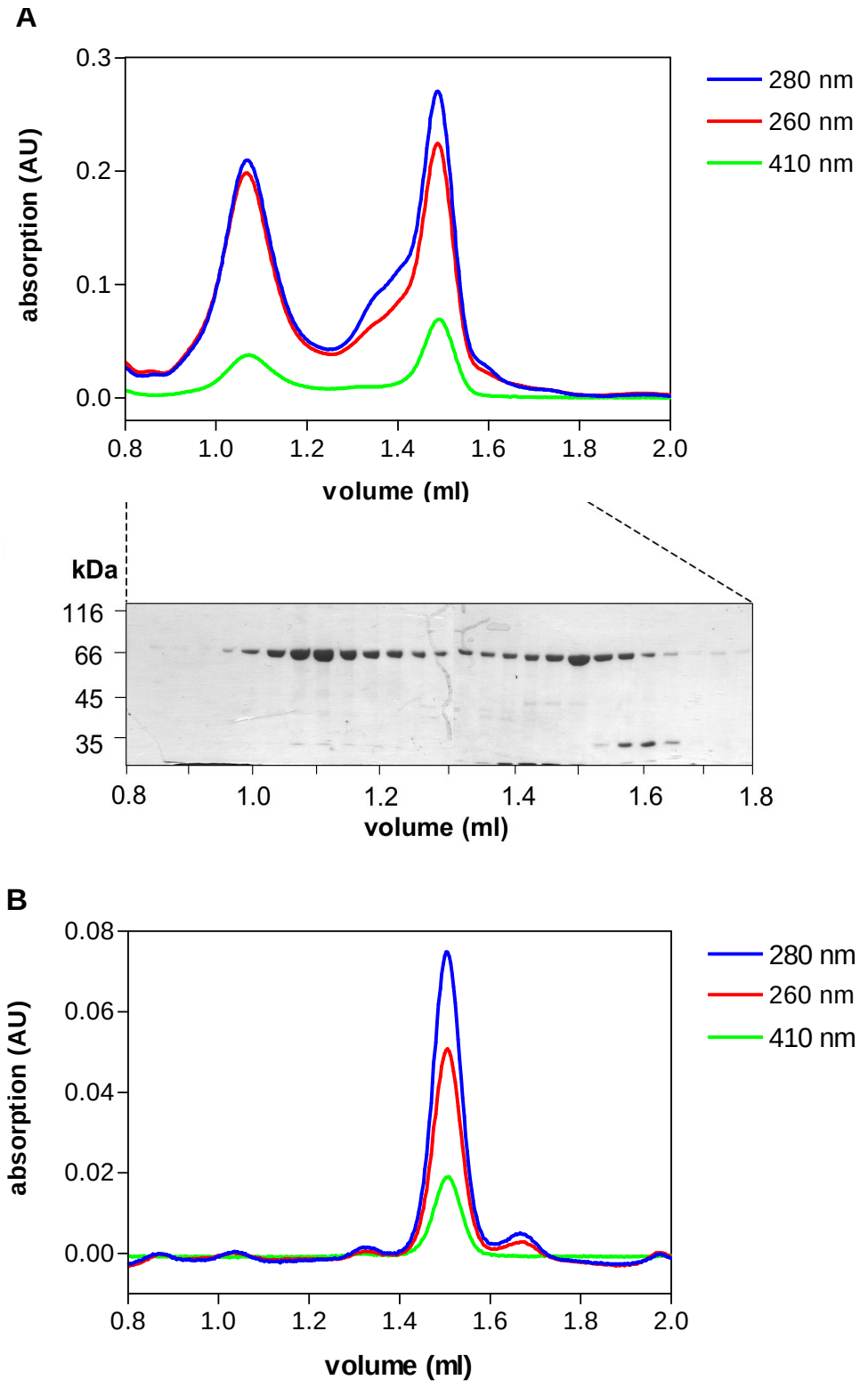

Figure 19: Analytical gel filtration profile of wild-type ABCE1 from *S. solfataricus*. 50 µl of isolated ABCE1 (~40 µM) were analyzed at RT with a flow-rate of 50 µl/min on a Superdex 200 PC 3.2/200 gel filtration column using a SMART-system. **(A)** After His_8-tag isolation a high molecular fraction eluted at 1.1 ml (440 kDa) and a low molecular fraction eluted at 1.5 ml (70 kDa). Peak fractions (0.8 ml-1.8 ml) were analyzed by SDS-PAGE (10%, silver-stained). **(B)** After StrepII-tag purification ABCE1 eluted as a monodispersed peak at 1.5 ml.

This observation indicates that the different purification procedures affect the oligomeric status of ABCE1. This phenomenon was investigated in further detail. To exclude that nickel ions present in the His_8-tag purification induce oligomerization, the gel filtration was performed with monomeric ABCE1 in nickel containing buffer. The oligomeric complex was not induced by addition of 20 mM $NiSO_4$. In contrast the oligomer from the His_8-tag purified ABCE1 could be disassembled by addition of 2.5 mM desthiobiotin. The oligomeric ABCE1 fraction was also not observed in the heterologously expressed protein purified via the His_6-tag from *E. coli*. Here, the protein eluted from the column in a monodisperse peak with an apparent molecular weight of 70 kDa (**Figure 20**).

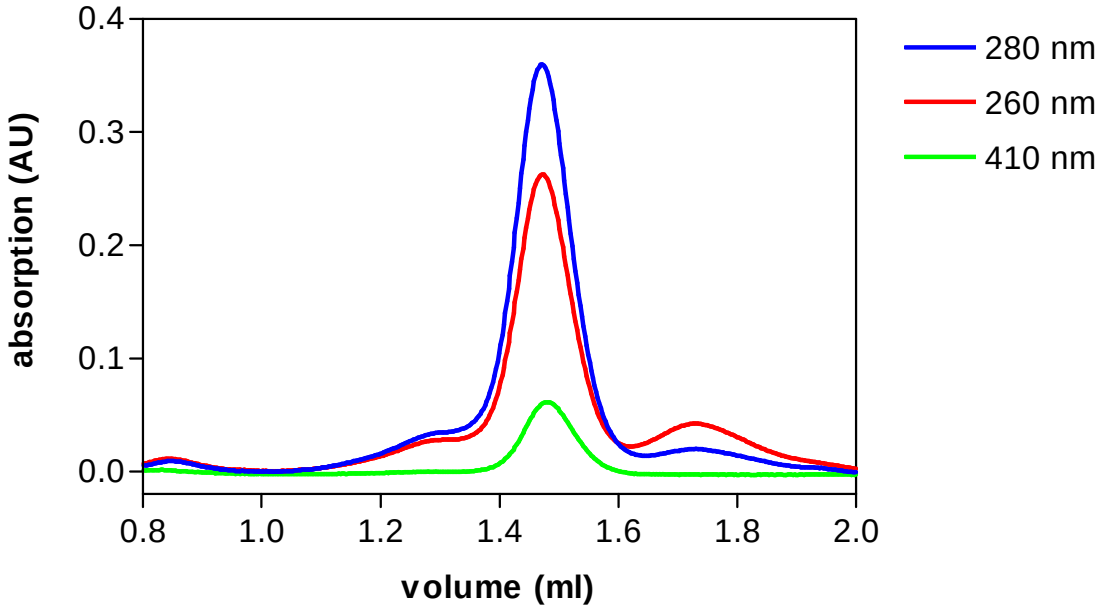

Figure 20: Analytical gel filtration profile of wild-type ABCE1 purified from *E. coli*. 50 µl of isolated ABCE1 (~40 µM) were analyzed at RT with a flow-rate of 50 µl/min on a Superdex 200 PC 3.2/200 gel filtration column using a SMART-system. ABCE1 eluted as monodisperse peak at 1.5 ml.

While the absorption at 280 nm was higher than at 260 nm in the monomeric fraction, the ratio of absorption at 260 nm and 280 nm indicates that the 440 kDa complex might contain nucleic acids. To investigate, whether oligomeric ABCE1 was associated with RNA/DNA, ABCE1 was incubated with either RNase A or DNase I and subsequently analyzed by gel filtration. The oligomeric complex completely dissociated after incubation with RNase A, while DNase I did not influence the complex (**Figure 21**). Thus, it seems plausible that the oligomeric fraction of ABCE1 contains RNA.

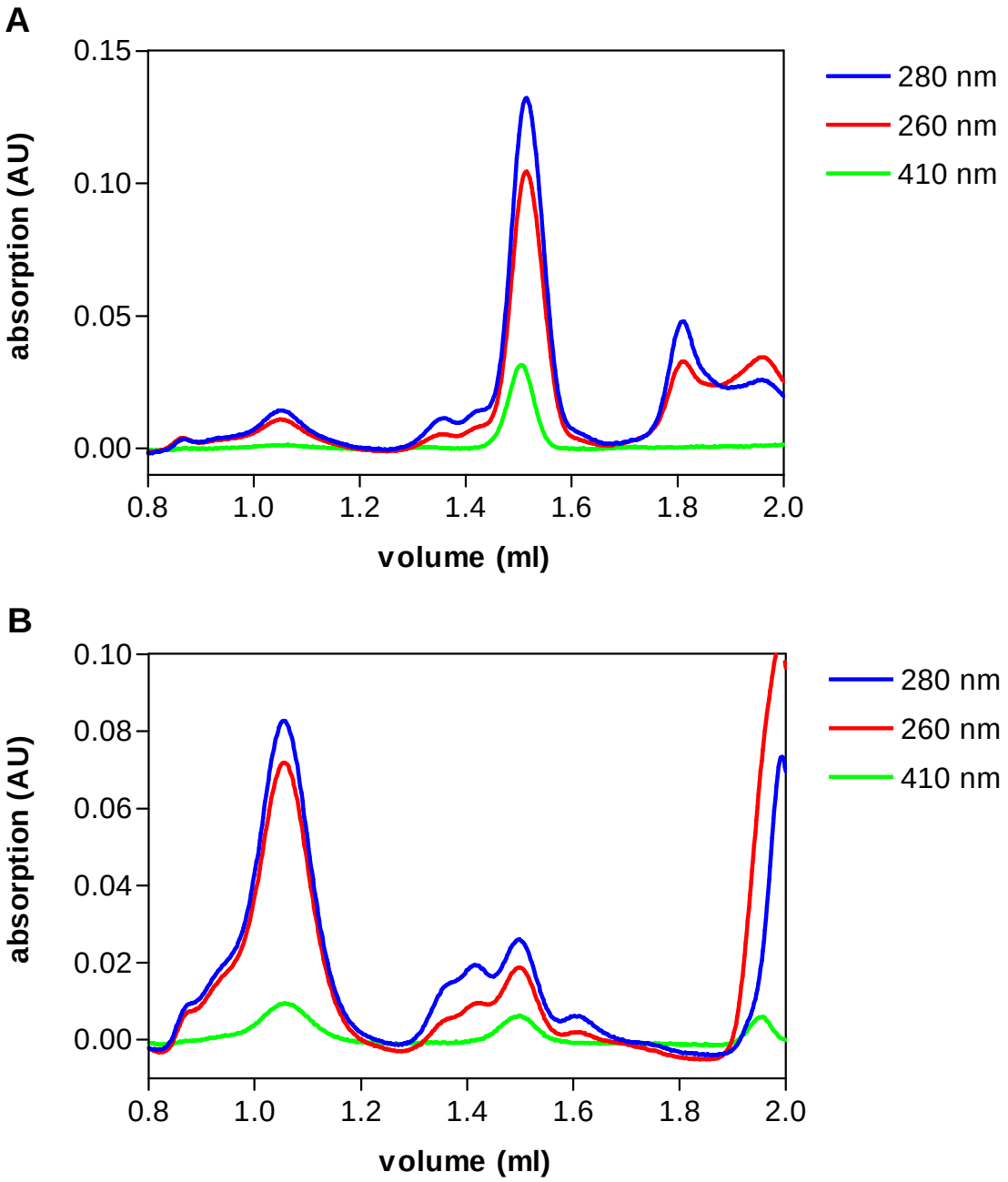

Figure 21: Influence of RNase A and DNase I on oligomerization status of ABCE1. Analytical gel filtration was performed at RT on a Superdex 200 PC 3.2/200 gel filtration column using a SMART-system. His_8-tag isolated ABCE1 was incubated for 1 h at 37℃ **(A)** with 2 U RNase A or **(B)** 1 U DNase I. After RNase A treatment the oligomeric ABCE1 fraction significantly decreased.

If oligomerization of ABCE1 is dependent on RNA binding, it should be possible to induce oligomerization of monomeric ABCE1 by addition of RNA. Therefore monomeric wild-type ABCE1 was incubated with different RNAs and oligomerization was analyzed by gel

filtration. But neither 16S nor 23S rRNA purified from total RNA from *S. solfataricus* by sucrose density gradients could shift the monomer into an oligomeric fraction. Furthermore, *in vitro* transcribed mRNA, 5S rRNA, tRNA or artificial 23mers could not induce oligomerization of ABCE1.

The influence of ionic strength, oxidation, and chelators on oligomerization of ABCE1 was analyzed by gel filtration. High or low ionic strength had no influence on oligomerization of ABCE1, because the oligomer was not disassembled when buffer containing 300 mM NaCl or 300 mM KCl was used. The addition of chelators, like 100 mM EDTA or 100 mM EGTA, led to the dissociation of the oligomer. Low concentrations of chelator (e.g. 5 mM EDTA) did not influence the oligomerization of ABCE1. Addition of 15 mM β-mercaptoethanol could partially disassemble the oligomeric ABCE1 fraction. In contrast, oxidation of ABCE1 (several days at 4°C or addition of 1 mM ferricyanid) could shift the oligomer/monomer ratio to a higher amount of oligomeric ABCE1.

Additive	**Effects on oligomer**
5 mM EDTA	No effect
100 mM EDTA	Dissociation (97%)
15 mM β-mercaptoethanol	Dissociation (50%)
1 mM ferricyanid	Association (50%)
50 mM arginine + 50 mM glutamate	Dissociation (95%)
2.5 mM desthiobiotin	Dissociation (100%)
0.15 µg avidin	No effect
2 Units RNase A	Dissociation (95%)
1 Unit DNase I	Association (20%)

Tab. 1: Effects of different additives on oligomerization. Additives were incubated with homologously expressed ABCE1 for 30 min at 37°C in 20 mM Tris/HCl pH 7.4, 100 mM NaCl and analyzed on a Superdex 200 PC 3.2/200 gel filtration column using a SMART-system.

Based on these observations it seemed possible that oligomerization was dependent on redox-processes mediated by its Fe-S clusters. Therefore, a truncated ABCE1 mutant lacking the Fe-S clusters was analyzed. Like the wild-type protein purified form *E. coli* heterologously expressed truncated ABCE1 exhibited no oligomerization (**Figure 22A**). In contrast, homologously expressed truncated ABCE1 purified via the His_8-tag showed oligomerization (50% of wild-type levels) after time-dependent aging of the protein (several days at 4°C) (**Figure 22B**). A dimeric fraction was visible in truncated ABCE1 from *S. solfataricus* in

addition to the oligomer. Possibly, the process of oligomerization is slower in truncated ABCE1, explaining why an intermediate dimer state became visible. Importantly, truncated ABCE1 expressed in both organisms showed no absorption at 410 nm. Thus, the detected absorption at 410 nm in full-length ABCE1 can be attributed to the Fe-S clusters of ABCE1.

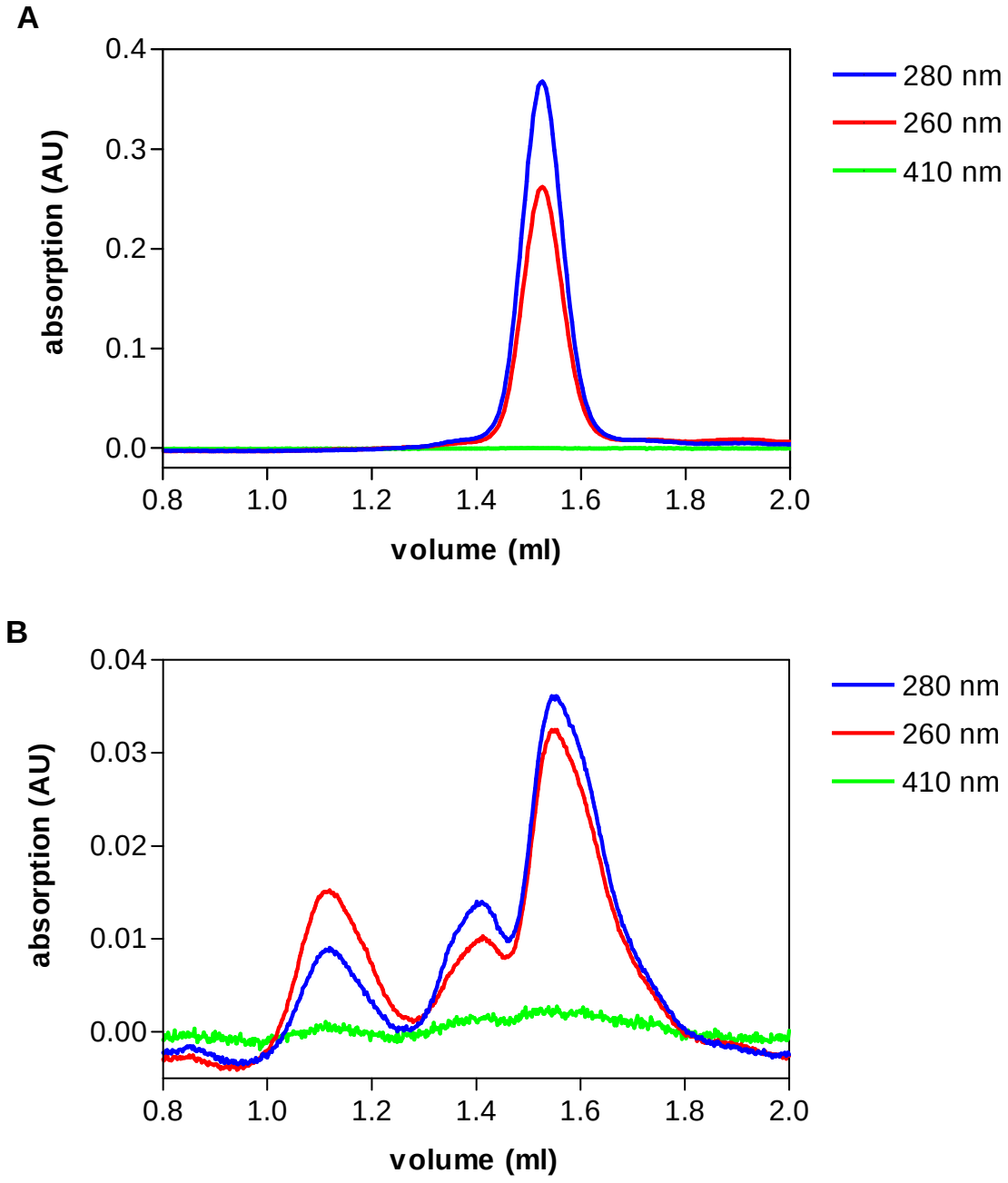

Figure 22: Analytical gel filtration profile of truncated ΔFe-S ABCE1. 50 µl of isolated ABCE1 **(A)** purified from *E. coli* (~40 µM) and **(B)** purified from *S. solfataricus* (~10 µM) were analyzed at RT on a Superdex 200 PC 3.2/200 gel filtration column using a SMART-system. At 410 nm no absorption was detected.

Interestingly, the oligomeric fraction could be significantly (90%) reduced by incubation with 2 mM ATP for 5 min at 65°C. Subsequently, the ATPase activities of monomeric and oligomeric ABCE1 were analyzed. Oligomeric ABCE1 fractions showed two-fold higher ATPase activity than monomeric fractions, while wild-type ABCE1 containing both fractions exhibited a mean value of both fractions in ATPase activity (**Figure 23**).

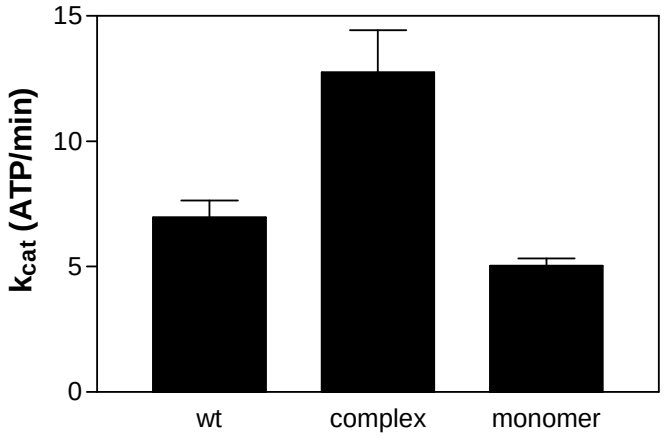

Figure 23: ATPase activity of different oligomeric states of ABCE1. The release of inorganic phosphate was measured at 80°C for 5 min with 2 mM ATP and 2.9 µM ABCE1. Oligomeric and monomeric ABCE1 purified from *S. solfataricus* were separated by gel filtration. The turnover number was calculated for the oligomeric complex with 12.7 ATP/min, for the monomer with 5 ATP/min, and for the mixed ABCE1 population with 6.9 ATP/min.

The ABCE1 oligomer was not only observed in gel filtration experiments. ABCE1 was also crosslinked in hexameric and intermediate states with diepoxybutan (DEB) analyzed by SDS-PAGE (Barthelme, unpublished data). DEB causes unspecific crosslinking of sulfhydryl-, amino- or reactive groups in nucleic acids. In the control without DEB, only monomeric ABCE1 was present. Although oligomeric ABCE1 was observed in gel filtration and crosslinking experiments the hexamer could not be visualized by electron microscopy so far. The physiological relevance of an oligomeric status of ABCE1 needs further investigation.

4.8 RNA-Binding properties of ABCE1

All known functions of ABCE1 are associated with RNA binding. Therefore, together with Dominik Barthelme I examined, whether endogenous, purified ABCE1 is associated with

RNA. In analytical gel filtration the peak fractions (440 kDa and 66 kDa) of the oligomeric and monomeric states of ABCE1 were analyzed for the presence of either RNA or DNA. As shown above, the oligomeric complex was RNase A-sensitive, but DNase I-resistant (**Figure 21**). Although we did not succeed to induce oligomerization by addition of RNA, it could be possible that ABCE1 is associated with a specific endogenous RNA after isolation from *S. solfataricus*. After proteinase K treatment and phenol/chloroform extraction with Trizol^{TM}, the nucleic acids were analyzed in a denaturing 8 M urea gel (Barthelme, unpublished data). In the 440 kDa fraction RNA could be visualized by the fluorescent dye SybrGold (specific for RNA/DNA) (**Figure 24**). The RNA fragments ranged from 20 to 200 nt and were RNase A sensitive. In addition, DNA molecules around 500 bp were visible, which were degraded upon DNase I treatment. No distinct bands were detected, but a mixed population of either RNA or DNA molecules. These experiments clearly demonstrate that ABCE1 purified from *S. solfataricus* is associated with nucleic acids.

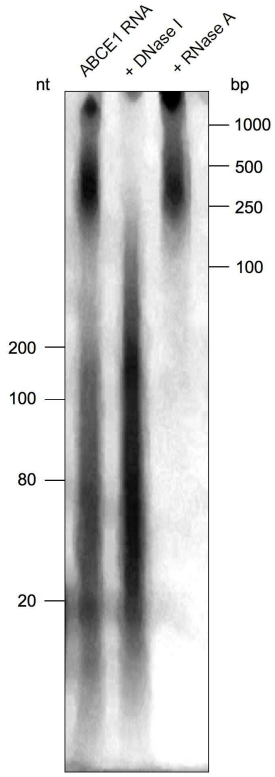

Figure 24: Separation of ABCE1 associated nucleotides. 20 µl of ABCE1 isolated from *S. solfataricus* (30 µM) were incubated for 1 h with 1.2 units proteinase K. After heat inactivation of proteinase K the nucleic acids were incubated at 37°C for 1 h with DNase I or RNase A. After electrophoretic separation on a 10% 8 M TBE urea gel, the nucleic acids were visualized with the dye SybrGold.

Further attempts to characterize the bound RNA identified the 5S rRNA and 7S RNA of the signal recognition particle and six small nucleolar RNAs (Barthelme, unpublished data). In contrast, the large ribosomal RNAs, 16S rRNA and 23S rRNA and three transfer RNAs for methionine were not identified by RT-PCR with gene-specific primers from the protein-associated RNA mixture.

As ABCE1 associates with ribosomes (see 4.9), binding of ABCE1 to ribosomal proteins or to ribosomal RNA is possible. Here, binding of ABCE1 to ribosomal RNA was examined *in vitro*. For this purpose total RNA purified from *S. solfataricus* was incubated with purified ABCE1 and separated on 5-25% sucrose density gradients. The largest population in total RNA are 16S and 23S rRNA, which segregated in two distinct peaks in 5-25% sucrose density gradients. Free ABCE1 was located on top of the sucrose gradient, while RNA bound ABCE1 migrated together with the 16S and 23S rRNA into the sucrose gradient Binding of ABCE1 to the 16S and 23S rRNA containing fractions was detected by Western blots with α-ABCE1 directed antibodies. (**Figure 25**).

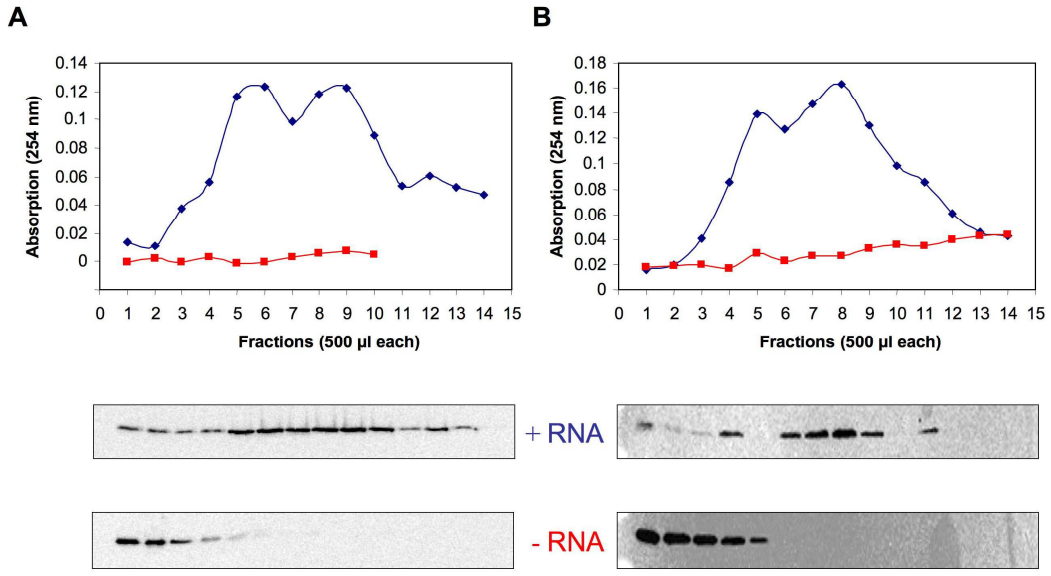

Figure 25: Association of ABCE1 with RNA *in vitro*. Wild-type **(A)** or truncated **(B)** ABCE1 isolated from *S. solfataricus* (1.5 µM each) were incubated for 5 min at 65℃ with 22 µg total RNA purified from *S. solfataricus* in 5 mM MgAcetate, 20 mM NH_4Cl, 20 mM Tris/HCl, pH 7.4 and loaded onto a 5-25% sucrose density gradient, which was run for 16 h at 18,000 rpm in a Beckman SW27 rotor at 4℃. After fractionation (500 µl), absorption was measured at 254 nm and each fraction was precipitated with 2 µg BSA and 1 ml acetone. Each fraction was subjected to SDS-PAGE (10%) and Western blotting using α-ABCE1 antibodies.

ABCE1 also associated with rRNA when 16S and 23S rRNA were separated prior to ABCE1 binding. In order to examine, which domain of ABCE1 binds to the large ribosomal RNAs, the experiment was performed with truncated ABCE1 lacking the Fe-S domains. Truncated ABCE1 was also detected in the fractions containing rRNA (**Figure 25**). These experiments show that the Fe-S clusters are not necessary for RNA-binding, and the NBDs are responsible for RNA-binding *in vitro*.

The next step was to analyze whether the ATPase activity of ABCE1 was dependent on RNA. After incubation of wild-type ABCE1 purified from *S. solfataricus* with RNase A, only a small decrease in ATPase activity was observed. Addition of DNase I did not alter ATPase activity. When ABCE1 was incubated with tRNA a two-fold increase of ABCE1 ATPase activity was detected. In contrast, mRNA could not alter the ATPase activity of ABCE1. In summary, ATPase activity of ABCE1 seemed not to be significantly dependent on RNA (**Figure 26**).

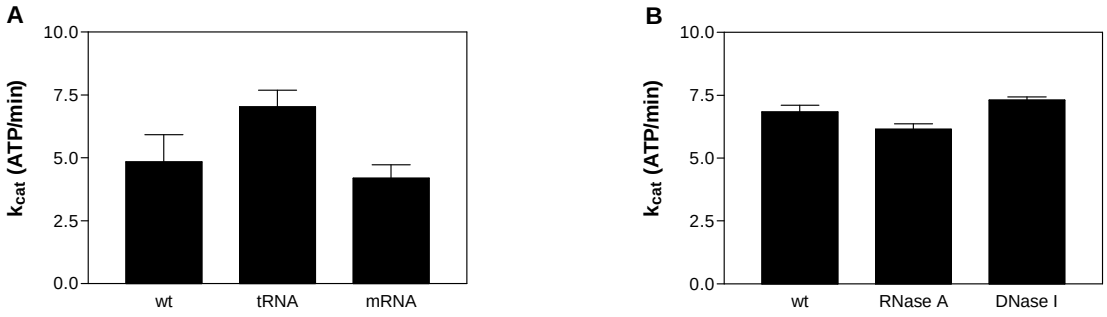

Figure 26: Effect of RNA on ATPase activity of ABCE1. The turnover number (ATP/min) was calculated from the release of inorganic phosphate after incubation of 2.9 µM ABCE1 isolated from *S. solfataricus* for 5 min at 80°C with 2 mM ATP. **(A)** After addition of 1 mM of RNA k_{cat} was calculated for tRNA with 7 ATP/min, for mRNA with 4.2 ATP/min and without RNA with 4.8 ATP/min. **(B)** After incubation with 1 unit of RNase A the turnover number was 6.1 ATP/min, with 1 unit of DNase I 7.3 ATP/min and without RNase A/DNase I 6.8 ATP/min.

4.9 ABCE1 associates with ribosomes

The association of ABCE1 with ribosomes was investigated in order to unravel the physiological function of ABCE1 in archaea. For this purpose the sedimentation profile in sucrose gradients of endogenous ABCE1 in *S. solfataricus* cell lysate was determined (**Figure 27A**). Immunoblotting analysis of the gradient fractions revealed that ABCE1 was associated with the 30S and 50S ribosomal subunits. A substantial proportion of ABCE1 was also found in non-ribosomal fractions at the top of the gradient. This was also shown for the ABCE1 *Drosophila* homologue *pixie* and other initiation factors or proteins associated with ribosomes (Andersen and Leevers, 2007; Tyzack *et al.*, 2000). In the next step, it was determined whether ABCE1 purified from *S. solfataricus* could interact with isolated ribosomes from *S. solfataricus* independently of factors in the cell lysate. Again, ABCE1 associated with 30S and 50S ribosomal subunits and co-localized with soluble proteins on top of the gradient (**Figure 27B**). Since ABCE1 contains two NBDs and two Fe-S clusters, the domains of ABCE1 responsible for the ribosomal interaction were analyzed. A truncated ABCE1 (69-600) mutant without the N-terminal Fe-S domain was tested for interaction with ribosomes in sucrose gradients (**Figure 27C**). Truncated ABCE1 also associated with 30S and 50S ribosomal subunits, demonstrating that the Fe-S domains of ABCE1 are not responsible for the interaction with ribosomes in archaea.

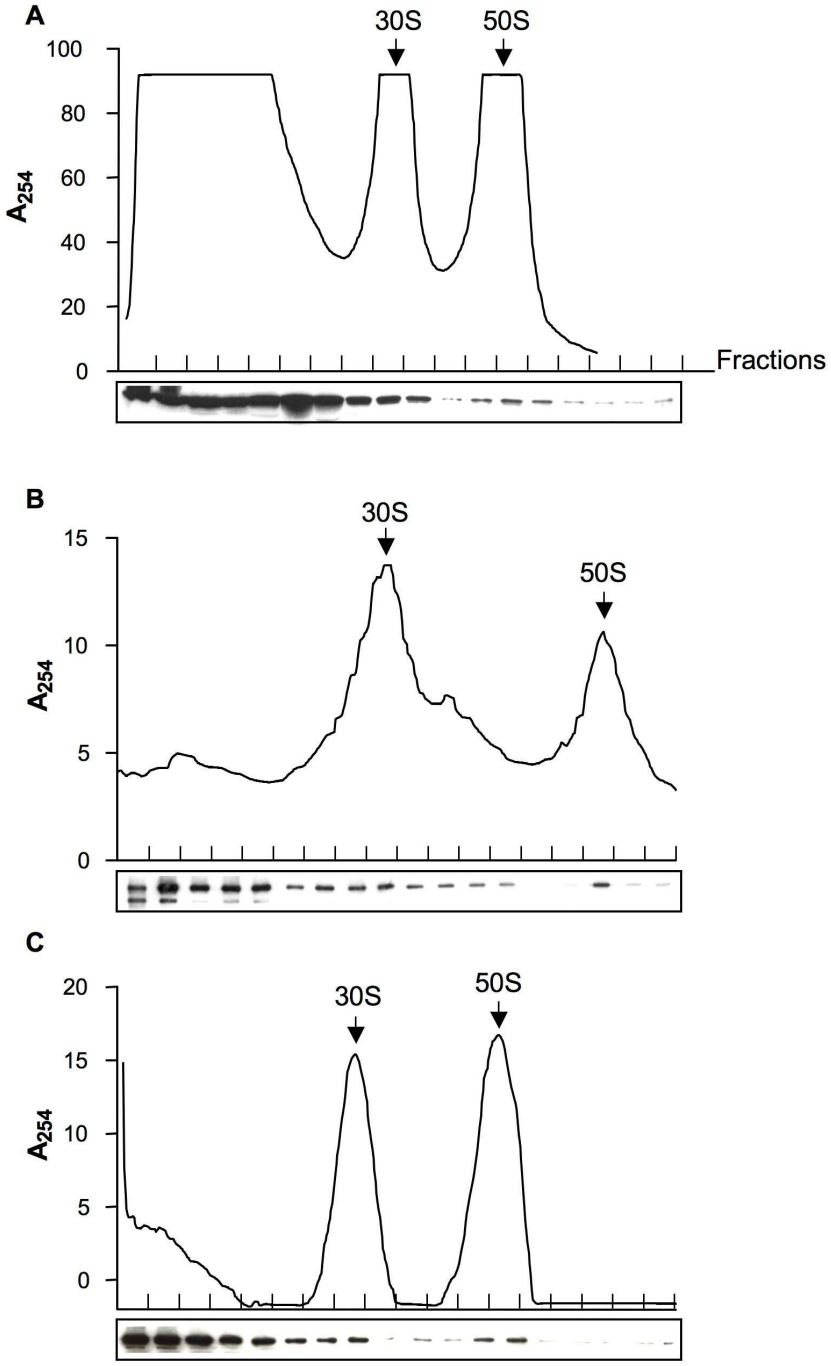

Figure 27: Interaction of ABCE1 with ribosomes. 10-30% sucrose density gradients were made in 30 mM KCl, 20 mM triethylamine pH 7.0, 10 mM Mg acetate, and were run at 36,000 rpm for 4 h in a Beckman SW41 rotor. The gradients were fractionated and the position of the ribosomal subunits was determined by optical density measurements at 254 nm. Subsequently, the fractions were analyzed for the presence of ABCE1 by Western Blotting. **(A)** About 100 µl of *S. solfataricus* cell extract were loaded onto the gradient. **(B)** 200 pmol of wild-type ABCE1 isolated from *S. solfataricus* was preincubated with 20 pmol of purified 70S ribosomes for 10 min at 65℃ and loaded onto the gradient. **(C)** 200 pmol of truncated ABCE1 (69-600) isolated from *E. coli* was preincubated with 20 pmol of purified 70S ribosomes for 10 min at 65°C and loaded onto the gradient.

In contrast to ABC50 and *pixie* (Andersen and Leevers, 2007; Tyzack *et al.*, 2000), addition of 2 mM ATP did not alter the ribosomal association of ABCE1. Interestingly, addition of 2 mM ATP to the cell lysate favored the formation of a strong double ABCE1 band in immunoblotting of the sedimentation profile, pointing to an ATP-dependent modification of endogenous ABCE1 (**Figure 28**). Strikingly, ABCE1 with a lower molecular mass (~5 kDa) was present in the gradient performed with ATP, which was significantly stronger in the fraction interacting with the ribosomal 50S subunit.

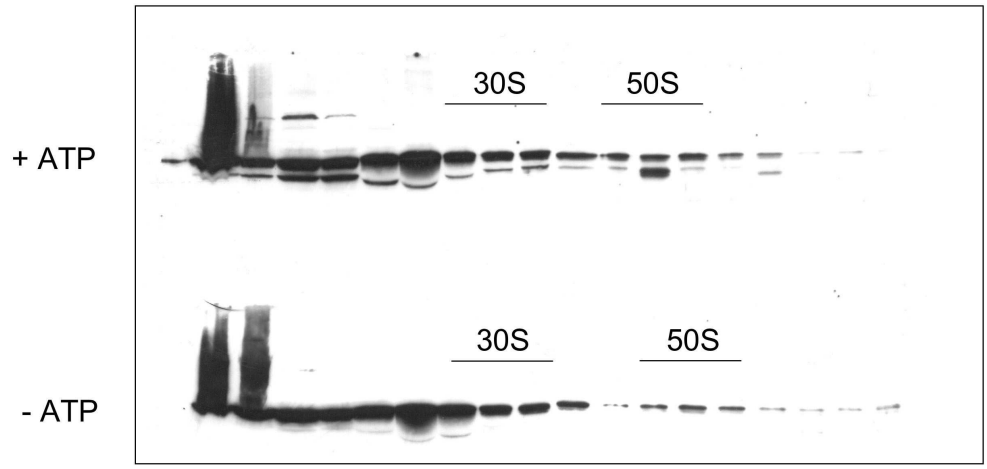

Figure 28: Influence of ATP on ribosome association of ABCE1. About 100 µl of *S. solfataricus* cell extract with or without 2 mM ATP were loaded onto a 10-30% sucrose density gradient, made in 30 mM KCl, 20 mM triethylamine pH 7.0, 10 mM Mg acetate and centrifuged at 36,000 rpm for 4 h in a Beckman SW41 rotor. Subsequently, the gradients were fractionated and analyzed for the presence of ABCE1 by Western Blotting.

The association of NBD mutants of ABCE1 with purified ribosomes was also examined. No difference in ribosomal binding was observed (**Figure 29**), but binding was dependent on native ABCE1 protein.

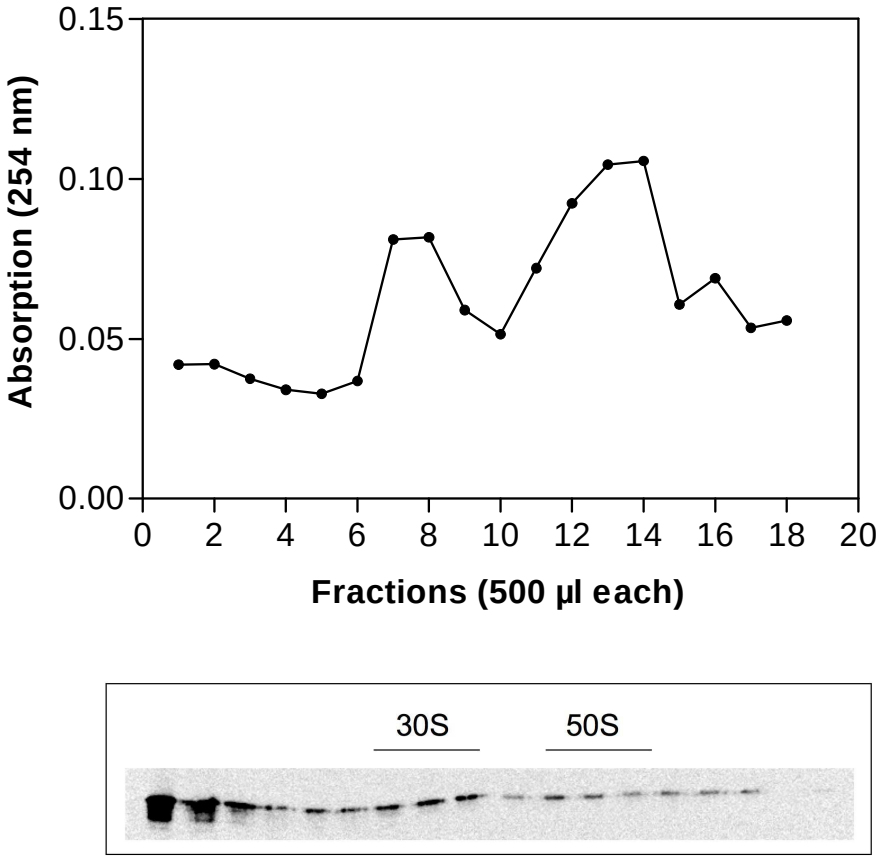

Figure 29: Association of the hyperactive E485Q mutant with ribosomes. 200 pmol of E485Q ABCE1 isolated from *E. coli* was preincubated with 20 pmol of purified 70S ribosomes for 10 min at 65°C and loaded onto a 10-30% sucrose density gradient made in 30 mM KCl, 20 mM triethylamine pH 7.0, 10 mM Mg acetate, and run at 18,000 rpm for 17 h in a Beckman SW27 rotor. The gradient was fractionated and the position of the ribosomal subunits was determined by optical density measurements at 254 nm. Subsequently, the fractions were analyzed for the presence of ABCE1 by Western Blotting.

4.10 ABCE1 does not interact with archaeal initiation factors

Earlier experiments demonstrated that ABCE1 co-purifies with the eukaryotic initiation translation factors eIF2, eIF3 and eIF5 in yeast (Dong *et al.*, 2004; Kispal *et al.*, 2005; Yarunin *et al.*, 2005). Although archaeal translation initiation is more related to eukaryotes than to prokaryotes, no homologues of eIF3 and eIF5 are found in archaea. The only factor, which was shown to interact with ABCE1 in yeast and also exists in archaea is eIF2 (Dong *et al.*, 2004). The archaeal homologue, a/eIF2 functions in binding of met-$tRNA_i$ like its eukaryotic relative (Londei, 2005). The aim was to investigate if ABCE1 plays a universal

role in translation initiation by binding to the trimeric archaeal protein a/eIF2. Binding of ABCE1 to the separated α, β and/or γ subunits of a/eIF2 was analyzed. As shown in **Figure 30**, only a very weak interaction between ABCE1 and the α subunit of a/eIF2 was detected. The α subunit is phosphorylated in *P. horikoshii* (Tahara *et al.*, 2004), thereby inhibiting translation. Moreover, no significant interaction of ABCE1 and β and γ a/eIF2 subunits could be detected by native gel electrophoresis. This might be due to the low solubility of ABCE1 in this native gel system or simply explained by the fact that ABCE1 does not interact with a/eIF2 in archaea.

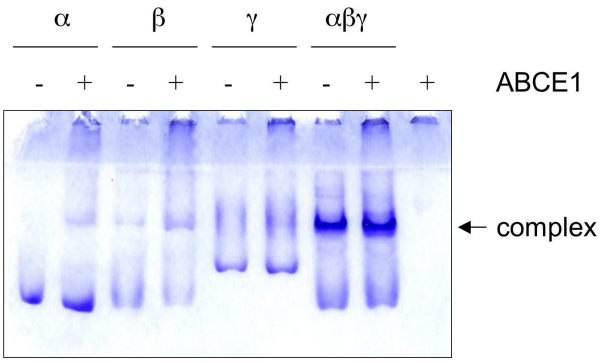

Figure 30: Interaction of a/eIF2 and ABCE1. Purified recombinant *S. solfataricus* a/eIF2 α, β and/or γ subunits and ABCE1 purified from *S. solfataricus* (each 50 pmol) were mixed and incubated at 65℃ for 5 min. Interaction of subunits was judg ed on an acetic acid native gel (23.5%, Coomassie blue stained).

4.11 The role of ABCE1 in archaeal translation

Since ABCE1 associates with ribosomes, this highly conserved protein could be essential for archaeal protein synthesis. The following experiments were performed in collaboration with Dr. Dario Benelli in the group of Prof. Dr. Paola Londei (Rome). A cell-free protein synthesizing system was utilized, in which the *S. solfataricus* cell lysate was preincubated with polyclonal antibodies raised against ABCE1 in order to deplete the lysate of endogenous ABCE1 (**Figure 31A**). Translational activity was judged by the presence of the translational product of a reporter mRNA, which was produced by *in vitro* transcription.

Depletion of ABCE1 did not reduce protein synthesis of the reporter protein. Like the control lysate, which was incubated with rabbit pre-immune serum, the ABCE1-depleted lysate maintained its translational activity (**Figure 31B**). Thus, either ABCE1 is not essential for

translation in archaea or the remaining amounts of ABCE1 in the depleted cell lysate (~ 5%) is still sufficient to enable translation in the cell-free system.

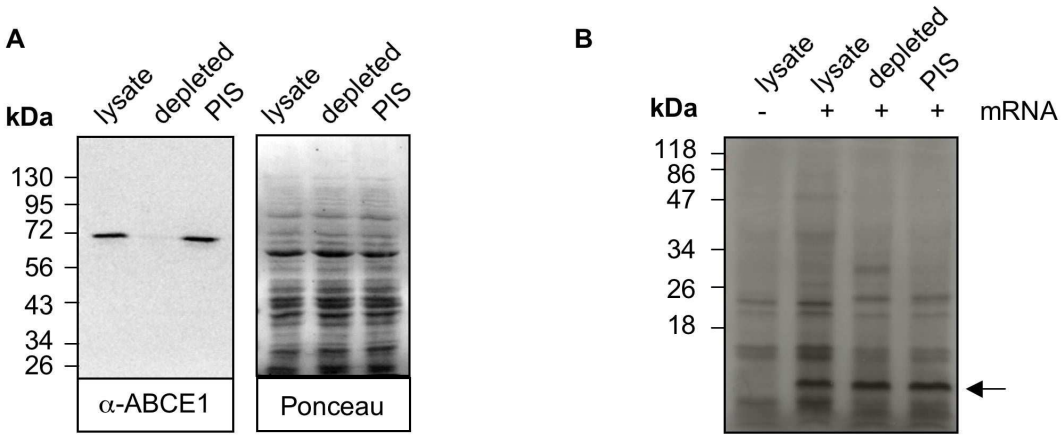

Figure 31: ABCE1 is not essential for archaeal translation. (A) Left panel: Western Blot directed against ABCE1 before (first lane) and after (second lane) depletion of *S. solfataricus* lysate with α-ABCE1 antibodies or after incubation of beads with pre-immune serum PIS (third lane). On the right panel the ponceau-staining of the same Western Blot is shown as a loading control. **(B)** The control sample of the *S. solfataricus* cell-free protein synthesizing system contained only endogenous mRNAs and no reporter mRNA. The samples were incubated for 1 hour at 75°C and analyzed by autoradiography on SDS-PAGE (17.5%). The arrow indicates the newly synthesized protein. Lysate (lane 1 and 2), ABCE1-depleted lysate (lane 3) and lysate treated with pre-immune serum (PIS) (lane 4) were analyzed.

5 Discussion

5.1 The NBDs of ABCE1

ABCE1 is one of the most conserved proteins among eukaryotes and archaea. Sequence and structural homology strongly suggest its classification to the ABC protein family. Until now, this is the first study providing results that the NBDs of ABCE1 bind and hydrolyze ATP with thermodynamic and kinetic values similar to other ABC proteins. The turnover number of wild-type ABCE1 is comparable to the values obtained for isolated NBDs of ABC transporters (ABCE1 10 min^{-1}, MJ0796 12 min^{-1}, Mdl1 25 min^{-1}, CFTR 6.7 min^{-1}) (Annereau *et al.*, 2003; Janas *et al.*, 2003; Moody *et al.*, 2002). Noteworthy, the Fe-S clusters do not affect ATP hydrolysis.

However, unique properties of ABCE1 for an ABC protein were discovered. Both NBDs not only bind ATP, but also AMP, which typically is neither a substrate nor a reaction product of ABC protein-catalyzed reactions. ATP and AMP seem to bind to the same site within the NBDs of ABCE1 as shown by a competition assay in which ATP was displaced by AMP. Binding of AMP was also reported in cystic fibrosis transmembrane conductance regulator (CFTR), which is an anion channel of the ATP binding cassette (ABC) transporter family. Like other ABC transporters it can hydrolyze ATP. While ATP hydrolysis influences channel gating, it was puzzling why CFTR would require this reaction, since anions flow passively through CFTR. Moreover, no other ion channel is known to require the energy of ATP hydrolysis to gate. It was found that CFTR has an adenylate kinase activity (ATP + AMP ↔ ADP + ADP) that regulates gating (Randak *et al.*, 1997; Randak and Welsh, 2003). Thus, channel activity could be regulated by two different enzymatic reactions, ATPase and adenylate kinase, which share a common ATP-binding site in the second nucleotide binding domain. At physiological nucleotide concentrations, adenylate kinase activity rather than ATPase activity may control gating, and therefore require little energy consumption (Randak and Welsh, 2003). In addition, the ATPase domains of Rad50, a protein related to the ABC transporter family were shown to share structural similarities with adenylate kinases. Rad50 is the catalytic component of a highly conserved DNA repair complex that functions in many aspects of DNA metabolism involving double-strand breaks. It was demonstrated that Mre11/Rad50 complexes from three organisms catalyze the reversible adenylate kinase

reaction *in vitro* (Bhaskara *et al.*, 2007). Mutation of the conserved signature motif decreased the adenylate kinase activity of Rad50 but did not reduce ATP hydrolysis. This mutant resembles a Rad50 null strain with respect to meiosis and telomere maintenance in *S. cerevisiae*, correlating adenylate kinase activity with *in vivo* functions. An adenylate kinase inhibitor blocked Mre11/Rad50-dependent DNA tethering *in vitro* and in cell-free extracts, indicating that adenylate kinase activity of Mre11/Rad50 promotes DNA-DNA associations. A model for Rad50 was proposed that incorporates both ATPase and adenylate kinase reactions as critical activities that regulate Rad50 functions (Bhaskara *et al.*, 2007). Possibly, ABCE1 possesses adenylate kinase activity as described for CFTR and Rad50.

In ABC proteins the conserved glutamate in the signature motif "LSGGQ" residue was proposed to act as the catalytic base (Moody *et al.*, 2002), while a conserved lysine is responsible for coordinating ATP. Typically, such mutations strongly impair ATP hydrolysis and promote dimerization of the NBDs (Janas *et al.*, 2003; Moody *et al.*, 2002; Verdon *et al.*, 2003b). Mutations of these conserved residues in NBD2 of ABCE1 (EQ mutation downstream of the Walker B motif and KA mutation in the Walker A motif) resulted in increased enzymatic activity, while nucleotide binding properties were not altered. In contrast, mutation of the conserved residues in NBD1 did not change the ATPase activity significantly compared to wild-type. This finding is similar to Rad50, where mutation of the signature motif did not decrease ATPase activity but exclusively reduced adenylate kinase activity (Bhaskara *et al.*, 2007). A possible adenylate kinase activity of ABCE1 could be affected by this mutation in NBD1. Similarly, in CFTR both NBD1 and NBD2 bind ATP, but NBD1 has little if any enzymatic activity, whereas NBD2 can function as an ATPase (Aleksandrov *et al.*, 2002; Berger *et al.*, 2002). When both active sites were mutated, no ATPase activity was detected. In ABCE1, *in vivo* data obtained in *S. cerevisiae* showed that EQ and KA mutations in either of the two NBDs resulted in non-viable yeast cells (Dong *et al.*, 2004; Karcher *et al.*, 2005). Thus, both a reduced and an elevated ATPase activity of ABCE1 mutants (E238Q and E485Q respectively) resulted in lethal phenotypes in *S. cerevisiae*. Furthermore, studies reported by Dong *et al.* (2004) demonstrated that mutation of the active site of the ATPase in NBD2 strongly inhibited protein translation. In the ABCE1 fly orthologue *pixie* the EQ-mutation in NBD2 led to constitutive association with the 40S ribosomal subunit, while a

pixie deletion mutant lacking the second ABC domain abolished association with the 40S ribosomal subunit (Andersen and Leevers, 2007).

According to the results obtained in this thesis a model in which the NBDs of wild-type ABCE1 dimerize upon ATP binding and dissociate after ATP hydrolysis would be plausible, as proposed for the ATP reaction cycle of MJ0796 (Smith *et al.*, 2002). Each active site is formed by a Walker A/B motif from one NBD and by the signature motif from the opposing NBD. In ABCE1 both NBDs are connected by a flexible linker and form a "V"-shaped particle, where NBD1 and NBD2 are arranged in a head-to-tail orientation (Karcher *et al.*, 2005). The active form of ABCE1 is an intramolecular dimer, based on the linear dependency of wild-type ABCE1 on protein concentration. The hyperactivity of NBD2-mutants could be explained by functional differences of both NBDs. Possibly, NBD1 and maybe its position inside the ABCE1 protein contributes the major activity for ATP hydrolysis, while NBD2 plays a more regulatory role. This hypothesis could explain why mutation of NBD2 would result in hyperactive ABCE1. But additional mutation or swapping mutants are required to characterize the distinct function of both NBDs. Alternatively, an altered, "closed" conformation of ABCE1 could be responsible for the hyperactivity of the NBD2-mutants (**Figure 32**). When the E/Q or K/A residues in NBD2 are mutated, hydrolysis cannot take place in NBD2 and the active site stays in a "closed" state. In consequence the dimer does not dissociate completely and NBD1 is in a favored position to hydrolyze ATP with a higher turnover number leading to hyperactive mutants.

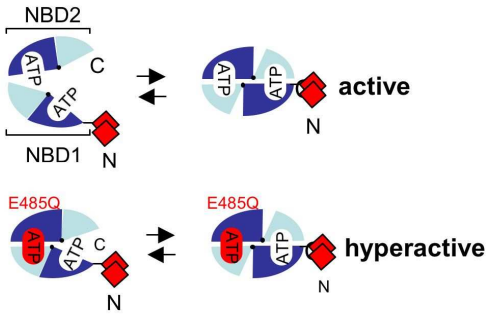

Figure 32: Proposed model of the ATP-driven reaction cycle in wild-type and mutant ABCE1. In the active state NBD1 and NBD2 of ABCE1 open and close during an ATP hydrolysis cycle. In the hyperactive mutant, NBD1 and NBD2 stay in close proximity, thereby enabling increased ATP hydrolysis.

Based on these findings it can be concluded that the precise fine-tuning of the ATPase activity and possibly adenylate kinase activity of the two NBDs are crucial for its essential cellular function. In future experiments it has to be analyzed whether ABCE1 functions as adenylate kinase and whether inhibitors blocking adenylate kinase activity change the function of ABCE1.

5.2 The Fe-S clusters of ABCE1

While the NBDs classify ABCE1 as a member of the large ABC protein family, the amino-terminal Fe-S clusters are a unique feature of this protein. So far, little is known about the nature and structural organization of the Fe-S clusters. In this study, the type, coordination and functional relevance of the Fe-S clusters in ABCE1 of archaea and eukaryotes were determined. Other studies have proved the indispensable role of these clusters for protein function and cell viability by mutating two of the conserved cysteine residues thought to be involved in iron coordination. Each point mutation resulted in the complete loss of iron incorporation into ABCE1 (Kispal *et al.*, 2005).

The first indication for the presence of Fe-S clusters in ABCE1 was the brownish color of isolated ABCE1. In addition, UV/Vis absorption spectra of purified wild-type ABCE1 protein revealed a shoulder at 410 nm typical for Fe-S centers, while no absorption at 410 nm was measured in the truncated ABCE1 mutant lacking the Fe-S domain. Assumed that ABCE1 contains two [4Fe-4S] clusters 8 iron atoms should be detectable. In this study only 6.5 iron atoms were obtained by TXRF analysis. The lower amount of detectable iron atoms can be explained by the fact that the iron and sulfur contents are slightly underestimated by this method due to a small population of non-assembled Fe-S cluster, impurities, and the intrinsic error in protein quantification. Further, the type of Fe-S clusters present in ABCE1 was analyzed by EPR. ABCE1 was EPR silent, which is typical for proteins containing $[4Fe\text{-}4S]^{2+}$ cluster. After partial aerobic degradation, a substoichiometrical signal for a $[3Fe\text{-}4S]^{+}$ center was detected, indicating that ABCE1 is sensitive to oxidation.

Results in this study clearly demonstrated the presence of two diamagnetic $[4Fe\text{-}4S]^{2+}$ clusters in ABCE1 and highlighted the essential role of the conserved cysteines for Fe-S cluster assembly. The eight cysteine residues involved in cluster formation are strongly conserved,

six of which (C16, C21, C25, C55, C61 and C65) proved to be strictly necessary for protein function since mutation to serine or alanine was lethal. Sequence comparison showed that the Fe-S cluster coordination in ABCE1 partially resembles those of 8 Fe ferredoxins, e.g. in *Desulfovibrio africanus* ferredoxin III or *Azotobacter vinelandii* ferredoxin I (Busch *et al.*, 1997; Tilley *et al.*, 2001). Based on homology, we postulated that ABCE1 contains one ferredoxin-like $[4Fe\text{-}4S]^{2+}$ cluster formed by the cysteines at position 4/5/6/7 (Barthelme *et al.*, 2007). In fact, these residues perfectly matched the consensus sequence $CP(X)_nCX_2CX_2C$. The latter three cysteine residues formed a loop and coordinated the irons of the cuban-type cluster from three sides, while the fourth position is occupied by a more distant residue. The coordination of the second Fe-S cluster in ABCE1 (cysteines 1/2/3/8) has not been described in any other protein. A unique ABCE1-type $[4Fe\text{-}4S]^{2+}$ cluster is proposed with the consensus sequence $CXPX_2CX_3CX_nKCP$ (Barthelme *et al.*, 2007).

The systematic mutagenesis of all conserved cysteines in yeast ABCE1 revealed that, surprisingly, two cysteine-to-alanine mutants (C29A, C58A) at position 4 and 6 are not lethal (Barthelme *et al.*, 2007). The initial result showing that mutation of the fourth cysteine to serine or alanine was viable in yeast was puzzling. However, all eukaryotic ABCE1 proteins contain a conserved extra cysteine within the N-terminal Fe-S cluster domain, which can rescue C29 (position 4) by ligand swapping (Barthelme *et al.*, 2007). Hence, C29 at position 4 is indeed involved in the formation of the ferredoxin-like cluster. Position 6, which is part of the ferredoxin-like cluster, is dispensable for the essential ABCE1 function. Remarkably, a mutant at position 6 was extremely unstable, resulting in a loss of iron and acid-labile sulfur (Barthelme *et al.*, 2007). This finding supports the assumption that the two Fe-S clusters in ABCE1 are assembled simultaneously depending on each other in an “all-or-nothing” manner (Kispal *et al.*, 2005). Strikingly, the ferredoxin-like cluster can also exist in $[3Fe\text{-}4S]^{+}$ state. Although interconversion between [4Fe-4S] and [3Fe-4S] clusters has been reported in ferredoxin II from *Desulfovibrio gigas* (Moura *et al.*, 1982) or ferredoxin III from *Desulfovibrio africanus* (Busch *et al.*, 1997) it is not clear, whether this state exists in ABCE1 *in vivo*. The iron-responsive element binding protein (IRE-BP) contains a labile Fe-S cluster that can be interconverted between [4Fe-4S] and [3Fe-4S] forms (Beinert *et al.*, 1997; Beinert and Kennedy, 1993; Haile *et al.*, 1992). Alteration of the cluster coincides with the loss of enzymatic activity, while RNA binding activity is acquired in the cluster-free form of IRE-BP.

The fact that the ferredoxin-like cluster of ABCE1 is functional in different states, indicates that this inorganic complex may represent a very ancient molecular switch and sensing device. The Fe-S clusters within ABCE1 could serve as sensors for changing environmental conditions such as increased levels of reactive oxygen species (ROS) (Andersen and Leevers, 2007; Kispal *et al.*, 2005). The concentration of ROS inside the cell is a very important variable parameter. In response to oxidative stress, ABCE1 could efficiently down regulate both ribosomal biogenesis and initiation of translation, adapting the cell to fluctuating environmental and intercellular conditions (Kispal *et al.*, 2005). Another possibility is that the Fe-S clusters of ABCE1 fulfill a structural rather than a redox-catalytic function like in *E. coli* endonuclease III (Kuo *et al.*, 1992b). In this enzyme, the Fe-S cluster serves as a scaffold for positioning catalytic amino acids involved in DNA recognition and binding. Notably, the N-terminal Fe-S clusters of ABCE1 are rich in conserved basic residues, which could, similarly to the *E. coli* endonuclease III or MutY, sense and modify nucleic acids (Kuo *et al.*, 1992a; Porello *et al.*, 1998; Thayer *et al.*, 1995). Despite the potential role in scaffolding a ligand-binding site, the Fe-S clusters of ABCE1 are not required for the folding and the structural integrity of the twin ABC ATPase domains (Karcher *et al.*, 2005). From the X-ray structure it was anticipated that the two NBDs perform an ATP-driven clamp-like motion. In the results presented in this study the Fe-S clusters of ABCE1 did not affect ATP-hydrolysis. Nevertheless, the impact of the Fe-S domain on the functionality of ABCE1 needs to be addressed in further detail.

5.3 Oligomerization of ABCE1

A hexameric arrangement of RecA-like domains is observed in many proteins, including e.g. F1-ATPase, TrwB, T7gp4 helicase, Rho transcriptional terminator and HslU protease (Ye *et al.*, 2004). These proteins are structurally related to ABCE1 containing a RecA-like fold, which is found in the NBDs of ABC proteins. In some cases a macromolecule – either DNA or a polypeptide – is moved through the central pore of this molecular machine. A loading process with a substrate may require opening and closing or disassembly and reassembly of the ring structure. ATP binding and hydrolysis are major driving forces for processive translocation and rearrangement of these protein rings. In some examples RNA binding leads

to a hexameric arrangement as described for Rho (Skordalakes and Berger, 2003) or the RNA processing exosome (Lorentzen *et al.*, 2005).

Most likely, RNA binding induces an oligomerization of ABCE1. The oligomer was disassembled after RNase treatment pointing to a complex of ABCE1 with RNA in the oligomeric structure. Often, oligomerization directly influences the activity and protein function. However, in ABCE1, the oligomeric state had no significant influence on ATPase activity as shown in this thesis. Possibly, another unknown enzymatic function of ABCE1, e.g. adenylate kinase activity or RNA unwinding or modification, is influenced by oligomerization. Further, the factors necessary for *in vitro* oligomerization were determined. However, oligomerization of monomeric ABCE1 could not be induced by different RNA molecules as investigated in this thesis. Probably, an unknown very specific, modified or unfolded RNA substrate could be necessary to induce oligomerization of ABCE1. Maybe some additional factors such as chaperones are missing to induce oligomerization of monomeric ABCE1 *in vitro*. This is plausible, because ABCE1 oligomerization was observed after isolation from *S. solfataricus* cells, but not after purification from *E. coli* cells. Further experiments are required to identify such a RNA molecule inducing ABCE1 oligomerization.

Potentially, the Fe-S could mediate oligomerization by RNA binding or redox processes. Indeed, in this thesis it was demonstrated that oligomerization was influenced by redox processes. While oxidation led to oligomerization, reduction of ABCE1 decreased the oligomeric population. This finding supports the hypothesis that the Fe-S clusters mediate the function of ABCE1 e.g. by oligomerization. However, oligomerization was also detected in truncated ABCE1 lacking the Fe-S clusters. In the truncated ABCE1 mutant oligomerization was time-dependent, meaning that ABCE1 molecules oligomerized only after several days pointing to a diminished ability of ABCE1 monomers to oligomerize. Oligomeric structures as shown in other RecA-like proteins are essential for their enzymatic activity and regions outside the RecA-like fold were responsible to maintain such an oligomeric state of the ATPase domain (Ye *et al.*, 2004). For many ABC transporters e.g. BtuCD, the transmembrane domains are essential to preserve the oligomeric state of the ATPase. Indeed, several isolated ATPase domains of ABC transporters are monomeric in the absence of the transmembrane domain (Karpowich *et al.*, 2001; Schmitt and Tampé, 2002). In the ABC protein ABCE1 the Fe-S clusters could present the additional domain outside the NBDs responsible to stabilize

efficiently oligomeric structures. However, due to the fact that oligomerization is neither clearly associated with the function of the Fe-S cluster domain nor with the ATPase activity of the NBDs of ABCE1, it cannot be excluded that the observed oligomer of ABCE1 is an artifact of experimental isolation methods. In contrast, the oligomer disassembly after RNase treatment points to a specific organized structure. Further experiments are necessary to characterize the oligomeric state of ABCE1. The RNA substrate leading to ABCE1 oligomerization in *S. solfataricus* cell lysate has to be identified and oligomerization of monomeric ABCE1 with this RNA molecule has to be shown. In addition, further approaches to visualize ABCE1 oligomers by electron microscopy should be made.

5.4 RNA binding properties of ABCE1

Ribonucleic acids function in many different processes in each organism. RNA molecules carry genomic information, fulfill structural tasks in the ribosome and are active as ribozymes. Besides, small non-coding RNAs exist (Aravin *et al.*, 2006; Zago *et al.*, 2005). These RNA molecules are found to function in RNA splicing (U snRNAs), RNA modification (snoRNAs) and regulation of gene expression (siRNAs, miRNAs, piRNAs). It is speculated that ABCE1 interacts with RNA to fulfill its postulated function in RNase L inhibition, HIV-I capsid assembly, translation initiation, and ribosome biogenesis. Although ABCE1 sequence and structure does not include any typical classical RNA/DNA binding motifs such as zinc finger (Coleman, 1992), DEAD box, RNA recognition motif (RRM) or KH domain (Messias and Sattler, 2004), the Fe-S clusters were reported as a direct RNA binding motif in other proteins (Lee *et al.*, 2004). Until now, no detailed studies investigating the RNA binding properties of ABCE1 are published. An interaction of ABCE1 with rRNA (5S, 5.8S, 7S, 18S, 25S) was shown exclusively in *S. cerevisiae* (Yarunin *et al.*, 2005). To verify the function of ABCE1 in RNA binding two different approaches were performed in *S. solfataricus* in this study. First, it was investigated whether ABCE1 is associated *in vivo* with ribonucleic acids after isolation from *S. solfataricus* cells. In addition, *in vitro* RNA binding properties of ABCE1 were examined. Analysis of bound RNA to ABCE1 revealed that the protein is *in vivo* associated with a mixed population of nucleic acids. Bound RNA of a size of 20-150 nt and DNA of 250-1000 bp was detected. Besides, ABCE1 associated *in vitro* with 16S and 23S ribosomal RNA

as shown in sucrose gradients. In additional experiments ABCE1 also bound to smaller RNAs like 5S rRNA, 7S of the signal recognition particle and six snoRNAs. The broad range of bound nucleotides suggests that ABCE1 binds nucleic acids unspecifically.

RNA binding was observed independently of ATP. RNA did not affect ATPase activity of ABCE1. Some ABC transporters show a substrate-stimulated ATPase activity (Gorbulev *et al.*, 2001). In ABCE1 the ATPase activity could potentially be stimulated by RNA. As isolated ABCE1 already contained RNA, RNA was removed by RNase treatment. However, RNase treatment prior to activity measurements did not decrease ATPase activity. Interestingly, also the truncated ABCE1 mutant lacking the Fe-S domains also associated with RNA. Therefore, the Fe-S clusters of ABCE1 are not directly involved in RNA binding. Most likely, RNA is bound by the NBDs or the linker region of ABCE1. Possibly, only a certain type of RNA can induce ATPase activity of ABCE1. If ABCE1 functions like a helicase it moves along nucleic acid strands and uses the energy of ATP hydrolysis for unwinding base-paired duplexes of bound RNA. Putative ATP-dependent RNA helicases have also been implicated in ribosome biogenesis (Dez *et al.*, 2004; Harnpicharnchai *et al.*, 2001; Nissan *et al.*, 2002). The gp4 helicase of the bacteriophage T7 DNA replication system functions as a hexamer to unwind duplex DNA at replication forks, moving a single-stranded DNA through the central pore. The closed hexameric ring seen in the x-ray structure of a helicase fragment is a dimer of trimers (Singleton *et al.*, 2000). The transcriptional terminator Rho also shows a hexameric arrangement (Skordalakes and Berger, 2003). In most RecA-like motor ATPases, which includes the AAA+ family, the ABC family and helicase superfamilies I, hydrolysis requires residues from a neighboring RecA-like domain, explaining why the ATPase activity in the oligomeric state is often much higher than in the monomer (Ye *et al.*, 2004). However, in the case of ABCE1, the oligomeric population showed only slightly higher ATPase activity.

5.5 Association with ribosomes and the function of ABCE1 in translation

Translation is a highly regulated process important to development and pathologies such as cancer, making ABCE1 a potential target for therapeutics (Chen *et al.*, 2006). In eukaryotes, ABCE1 has been shown to function in the initiation of protein synthesis, though the

molecular mechanism in which ABCE1 is involved remains unclear. In humans, ABCE1 interacts exclusively with eIF2α and eIF5 (Chen *et al.*, 2006), but not with eIF3. Remarkably, in *S. solfataricus* ABCE1 neither coimmunoprecipitates with a/eIF2α nor interacts *in vitro* with purified α, β, or γ subunits of a/eIF2 in native gel electrophoresis. Nevertheless, ABCE1 associates with 30S and 50S ribosomes *in vivo* and independently of initiation factors *in vitro*, although a large fraction of ABCE1 was localized in the soluble fractions of the cell lysate. It could be possible that ABCE1 is only required at a defined time point in translation. In this study, the twin NBDs including the linker domain of ABCE1 were identified as the part of the protein, which is essential for ribosome binding. Furthermore, ribosomal 16S and 23S RNA without ribosomal proteins seem to be sufficient for association with ABCE1. Further studies could be directed to map the exact ribosomal binding site in the NBDs of ABCE1. Next, it needs to be investigated if ABCE1 also associates with 70S ribosomes or exclusively binds to 30S or 50S ribosomal subunits. This can be performed by crosslinking the ribosomal subunits with formaldehyde after incubation with ABCE1 and subsequent analysis in a sucrose gradient.

Several soluble ABC proteins (GCN20, YEF3, ARB1 and ABCE1) have been reported to interact with ribosomes and function in protein synthesis or ribosome biogenesis in yeast. The ABC protein ARB1 is a shuttling factor that stimulates 40S and 60S ribosome biogenesis (Dong *et al.*, 2005). Mutations of conserved ARB1 residues expected to function in ATP hydrolysis were lethal. The mammalian homologue of GCN20, ABC50, contains twin NBDs like ABCE1, but no Fe-S clusters. ABC50 interacts with eukaryotic initiation factor 2 and associates with the ribosome in an ATP-dependent manner (Tyzack *et al.*, 2000). The association of ABC50 with ribosomal subunits is increased by ATP and decreased by ADP. In yeast, ABCE1 mutations of conserved residues expected to function in ATP hydrolysis are lethal (Dong *et al.*, 2004; Karcher *et al.*, 2005). Introduction of the EQ-mutation in the second NBD of ABCE1 is predicted to bind, but not hydrolyze ATP. The EQ- and KA-mutant in the second NBD of ABCE1 obtained in this thesis showed highly increased ATPase activity. Interestingly, introduction of the EQ-mutation in NBD2 of yeast ABCE1 had a dominant negative phenotype, decreasing the rate of translation initiation *in vivo*, and the mutant protein inhibited translation of a luciferase mRNA reporter in wild-type cell extracts (Dong *et al.*, 2004). The *Drosophila* homologue, *Pixie*, was shown to associate with the 40S subunit on

sucrose density gradients in an ATP-dependent manner (Andersen and Leevers, 2007). *Pixie* did not associate with the 40S subunit under standard conditions and the addition of ADP or ATP had no effect on the distribution of *Pixie* on sucrose gradients. Importantly, adding non-hydrolysable AMP-PNP to cell extracts caused a redistribution of some *Pixie* into the fractions containing the 40S subunit. In contrast, an ABCE1 fly mutant lacking the second ABC domain did not bind the 40S subunit in the presence of AMP-PNP. In *Drosophila*, ABCE1 containing the EQ-mutation in NBD2 was constitutively associated with the 40S ribosomal subunit (Andersen and Leevers, 2007). Like yeast ABCE1, the archaeal homologue associated with 30S ribosomes in absence of ATP. Unlike ABC50, addition of 2 mM ATP did not significantly alter the binding of ABCE1 to ribosomal subunits in *S. solfataricus*. This suggests that the functional motifs in the NBDs of ABCE1 are required for association with ribosomes, but ribosome association is controlled differently in each organism. Interestingly, after addition of excess ATP a distinct double band of ABCE1 was visible. It is unlikely that the lower ABCE1 band represents a degradation product, because it was found also in endogenous ABCE1 of cell lysates. Possibly ABCE1 is phosphorylated or carries another modification switching between a functional and de-activated ABCE1 form. Further studies could analyze whether ABCE1 is phosphorylated using antibodies directed against phosphorylation sites.

It is striking that yeast ABCE1 affects the efficiency of translation in cell-free extracts (Dong *et al.*, 2004). Similarly, depletion of yeast ABCE1 impairs protein synthesis in cells grown in glucose-containing rich medium, which is a blend of peptone, yeast extract, and dextrose in optimal proportions for growing most *Saccharomyces cerevisiae* strains. In contrast no effects were observed after growth in minimal medium (Kispal *et al.*, 2005). The effect in rich medium was explained by the more efficient depletion of ABCE1, as under these conditions cells undergo more divisions than in minimal medium. In addition, human ABCE1 plays an essential role in the translation of mammalian mRNAs (Chen *et al.*, 2006). Antisera to ABCE1 inhibited *in vitro* translation of luciferase mRNA by 90% in rabbit reticulocyte lysates but not to polyU molecules which can be translated independent of initiation factors (Chen *et al.*, 2006). Results in this study proved that ABCE1 was not essential for *in vitro* “leadered” translation in *S. solfataricus*. In *S. solfataricus*, “leadered” mRNA including a Shine-Dalgarno sequence and “leaderless” without a 5’-untranslated region (UTR) were shown to be

translated. Also, “leaderless” mRNAs appeared to be universally translatable by bacterial, eukaryotic and archaeal ribosomes. It is not clear, why “leaderless” translation is so widespread in the archaea, especially in the hyperthermophiles, while being rather exceptional in bacteria and eukaryotes (Londei, 2005). Possibly, but unlikely, ABCE1 is only required for “leaderless” translation in *S. solfataricus*. It is possible that the remaining ABCE1 protein carried out its catalytic function in translation after depletion of endogenous protein in *S. solfataricus* cell lysate (~5%). But most likely, ABCE1 is not necessary for translation in archaea, as ABCE1 was not associated with the initiation factor a/eIF2. Nevertheless, the ABCE1 gene is one of the few genes conserved between archaea and eukaryotes and probably fulfills a universal task, which is unknown so far. Further investigations in archaea are required to unravel the physiological role of ABCE1 in the metabolism of archaea.

Abbreviations

ABC	ATP binding cassette
Å	Angstrom
ABCE1	ABC protein subfamily E1
AAA	ATPases associated with a variety of cellular activities
ADP	Adenosine diphosphate
AMP	Adenosine monophosphate
APS	Ammonium peroxodisulfate
Atm1p	ABC transporter exporting precursors of Fe-S clusters
ATP	Adenosine triphosphate
BCA	Bicinchonic acid
BLAST	Basic Local Alignment Search Tool
bp	base pair DNA
BSA	Bovine serum albumin
BtuCD	Vitamin B_{12} import system permease
CFIDS	Chronic fatigue immune dysfunction syndrome
CFTR	Cystic fibrosis transmembrane conductance regulator
Da	Dalton
ddH_2O	Double distilled water
DEB	Diepoxybutan
DEPC	Diepoxypyrocarbonate
DMSO	Dimethylsulfoxide
DNA	Deoxyribonucleic acid
DTT	1,4-Dithiothreitol
EDTA	1-(4-Isothiocyanatobenzyl)ethylenediamine-N,N,N’,N’-tetraacetic acid
eIF	Eukaryotic initiation factor
Fe-S	Iron sulfur
g	Gram or gravity constant
GTP	Guanosine triphosphate
h	Hour
HABA	Hydroxyazophenylbenzoic acid
HEPES	N-(2-hydroxyethylpiperazine)-N’-2-ethanesulfonic acid
HIV	Human immunodeficiency virus
IFN	Interferon
ISC	Iron sulfur cluster
IMAC	Immobilized metal affinity chromatography
IPTG	Isopropyl-β-D-thiogalactopyranoside
kb	Kilo base
k_{cat}	Catalytic constant
K_d	Dissociation constant
K_M	Michaelis-Menten constant
l	Liter
LB	Luria broth
LUCA	Last Universal Common Ancestor
m	Meter
M	mol/liter
MALDI	Matrix-assisted laser desorption/ionization
Met-$tRNA_i^{Met}$	Initiator methionyl transfer ribonucleic acid
Mg	Magnesium

min	Minute
mRNA	Messenger ribonucleic acid
MS	Mass spectrometry
MSD	Membrane spanning domain
MutS	DNA mismatch repair enzyme
NAD	Nicotineamide adenine dinucleotide hydrate
NBD	Nucleotide binding domain
NC	Nucleocapsid
NIF	Nitrogen fixation
nm	Nanometer
nt	Nucleotides RNA
OD	Optical density
ON	Overnight
ORF	Open reading frame
PAGE	Polyacrylamide gel electrophoresis
PCR	Polymerase chain reaction
pH	Potentia hydrogenii
P_i	Inorganic phosphate
PIS	Pre-immune serum
PMSF	Phenylmethanesulfonyl fluoride
Rad50	DNA double-strand break repair ATPase
RLI	RNase L inhibitor
RNA	Ribonucleic acid
RNAi	RNA interference
rNTP	Ribonucleoside triphosphate
ROS	Reactive oxygen species
rpm	Rounds per minute
rRNA	Ribosomal ribonucleic acid
RT	Room temperature
S	Svedberg
s	Second
SMC	Structural maintenance of chromosomes
snoRNA	Small nucleolar RNA
SDS	Sodium dodecyl sulfate
SSV	*Sulfolobus shibatae virus*
SUF	Operon for mobilization of sulfur
TAP	Transporter associated with antigen processing
TBST	Tris buffered saline tween
TCA	Trichloroacetic acid
TEMED	N,N,N’,N’-Tetramethylethylenediamine
TOF	Time of flight
Tris	Tris-(hydroxymethyl)-aminomethane
Tween-20	Polyoxyethylenesorbitan monolaureate
TXRF	Total x-ray reflection fluorescence
u	Unit
UTR	Untranslated region
UV	Ultraviolet
UvrA9	Nucleotide excision repair enzyme
V	Volt
Vif	Virion infectivity factor
Vis	Visible

v_{max}	Maximum reaction velocity
wt	Wild-type
2-5A	2’-5’ oligoadenylate

References

Ackrell, B.A., Kearney, E.B., Mims, W.B., Peisach, J. and Beinert, H. (1984) Iron-sulfur cluster 3 of beef heart succinate-ubiquinone oxidoreductase is a 3-iron cluster. *J Biol Chem*, **259**, 4015-4018.

Albers, S.V., Jonuscheit, M., Dinkelaker, S., Urich, T., Kletzin, A., Tampé, R., Driessen, A.J. and Schleper, C. (2006) Production of recombinant and tagged proteins in the hyperthermophilic archaeon Sulfolobus solfataricus. *Appl Environ Microbiol*, **72**, 102-111.

Albers, S.V., Szabo, Z. and Driessen, A.J. (2003) Archaeal homolog of bacterial type IV prepilin signal peptidases with broad substrate specificity. *J Bacteriol*, **185**, 3918-3925.

Aleksandrov, L., Aleksandrov, A.A., Chang, X.B. and Riordan, J.R. (2002) The first nucleotide binding domain of cystic fibrosis transmembrane conductance regulator is a site of stable nucleotide interaction, whereas the second is a site of rapid turnover. *J Biol Chem*, **277**, 15419-15425.

Algire, M.A., Maag, D., Savio, P., Acker, M.G., Tarun, S.Z., Jr., Sachs, A.B., Asano, K., Nielsen, K.H., Olsen, D.S., Phan, L., Hinnebusch, A.G. and Lorsch, J.R. (2002) Development and characterization of a reconstituted yeast translation initiation system. *RNA*, **8**, 382-397.

Ali, V., Shigeta, Y., Tokumoto, U., Takahashi, Y. and Nozaki, T. (2004) An intestinal parasitic protist, Entamoeba histolytica, possesses a non-redundant nitrogen fixation-like system for iron-sulfur cluster assembly under anaerobic conditions. *J Biol Chem*, **279**, 16863-16874.

Andersen, D.S. and Leevers, S.J. (2007) The essential Drosophila ATP-binding cassette domain protein, pixie, binds the 40 S ribosome in an ATP-dependent manner and is required for translation initiation. *J Biol Chem*, **282**, 14752-14760.

Annereau, J.P., Ko, Y.H. and Pedersen, P.L. (2003) Cystic fibrosis transmembrane conductance regulator: the NBF1+R (nucleotide-binding fold 1 and regulatory domain) segment acting alone catalyses a Co^{2+}/Mn^{2+}/Mg^{2+}-ATPase activity markedly inhibited by both Cd^{2+} and the transition-state analogue orthovanadate. *Biochem J*, **371**, 451-462.

Aravin, A., Gaidatzis, D., Pfeffer, S., Lagos-Quintana, M., Landgraf, P., Iovino, N., Morris, P., Brownstein, M.J., Kuramochi-Miyagawa, S., Nakano, T., Chien, M., Russo, J.J., Ju, J., Sheridan, R., Sander, C., Zavolan, M. and Tuschl, T. (2006) A novel class of small RNAs bind to MILI protein in mouse testes. *Nature*, **442**, 203-207.

Aravind, L., Walker, D.R. and Koonin, E.V. (1999) Conserved domains in DNA repair proteins and evolution of repair systems. *Nucleic Acids Res*, **27**, 1223-1242.

Balk, J., Pierik, A.J., Netz, D.J., Mühlenhoff, U. and Lill, R. (2004) The hydrogenase-like Nar1p is essential for maturation of cytosolic and nuclear iron-sulphur proteins. *EMBO J*, **23**, 2105-2115.

Barthelme, D., Scheele, U., Dinkelaker, S., Janoschka, A., Macmillan, F., Albers, S.V., Driessen, A.J., Stagni, M.S., Bill, E., Meyer-Klaucke, W., Schünemann, V. and Tampé,

R. (2007) Structural organization of essential iron-sulfur clusters in the evolutionarily highly conserved ATP-binding cassette protein ABCE1. *J Biol Chem*, **282**, 14598-14607.

Bauer, B.E., Wolfger, H. and Kuchler, K. (1999) Inventory and function of yeast ABC proteins: about sex, stress, pleiotropic drug and heavy metal resistance. *Biochim Biophys Acta*, **1461**, 217-236.

Baykov, A.A., Evtushenko, O.A. and Avaeva, S.M. (1988) A malachite green procedure for orthophosphate determination and its use in alkaline phosphatase-based enzyme immunoassay. *Anal Biochem*, **171**, 266-270.

Beinert, H., Holm, R.H. and Munck, E. (1997) Iron-sulfur clusters: nature's modular, multipurpose structures. *Science*, **277**, 653-659.

Beinert, H. and Kennedy, M.C. (1993) Aconitase, a two-faced protein: enzyme and iron regulatory factor. *FASEB J*, **7**, 1442-1449.

Bell, S.D. and Jackson, S.P. (1998) Transcription and translation in Archaea: a mosaic of eukaryal and bacterial features. *Trends Microbiol*, **6**, 222-228.

Berger, A.L., Ikuma, M., Hunt, J.F., Thomas, P.J. and Welsh, M.J. (2002) Mutations that change the position of the putative gamma-phosphate linker in the nucleotide binding domains of CFTR alter channel gating. *J Biol Chem*, **277**, 2125-2131.

Bhaskara, V., Dupre, A., Lengsfeld, B., Hopkins, B.B., Chan, A., Lee, J.H., Zhang, X., Gautier, J., Zakian, V. and Paull, T.T. (2007) Rad50 adenylate kinase activity regulates DNA tethering by Mre11/Rad50 complexes. *Mol Cell*, **25**, 647-661.

Bisbal, C., Martinand, C., Silhol, M., Lebleu, B. and Salehzada, T. (1995) Cloning and characterization of a RNAse L inhibitor. A new component of the interferon-regulated 2-5A pathway. *J Biol Chem*, **270**, 13308-13317.

Braz, A.S., Finnegan, J., Waterhouse, P. and Margis, R. (2004) A plant orthologue of RNase L inhibitor (RLI) is induced in plants showing RNA interference. *J Mol Evol*, **59**, 20-30.

Busch, J.L., Breton, J.L., Bartlett, B.M., Armstrong, F.A., James, R. and Thomson, A.J. (1997) [3Fe-4S] <--> [4Fe-4S] cluster interconversion in Desulfovibrio africanus ferredoxin III: properties of an Asp14 --> Cys mutant. *Biochem J*, **323**, 95-102.

Callaghan, R. and Riordan, J.R. (1993) Synthetic and natural opiates interact with P-glycoprotein in multidrug-resistant cells. *J Biol Chem*, **268**, 16059-16064.

Chen, C.A. and Cowan, J.A. (2003) Characterization of the soluble domain of the ABC7 type transporter Atm1. *J Biol Chem*, **278**, 52681-52688.

Chen, Z.Q., Dong, J., Ishimura, A., Daar, I., Hinnebusch, A.G. and Dean, M. (2006) The essential vertebrate ABCE1 protein interacts with eukaryotic initiation factors. *J Biol Chem*, **281**, 7452-7457.

Coelho, C.M., Kolevski, B., Bunn, C., Walker, C., Dahanukar, A. and Leevers, S.J. (2005) Growth and cell survival are unevenly impaired in pixie mutant wing discs. *Development*, **132**, 5411-5424.

Coleman, J.E. (1992) Zinc proteins: enzymes, storage proteins, transcription factors, and replication proteins. *Annu Rev Biochem*, **61**, 897-946.

Dean, M., Rzhetsky, A. and Allikmets, R. (2001) The human ATP-binding cassette (ABC) transporter superfamily. *Genome Res*, **11**, 1156-1166.

Dennis, P.P. (1997) Ancient ciphers: translation in Archaea. *Cell*, **89**, 1007-1010.

Dez, C., Froment, C., Noaillac-Depeyre, J., Monsarrat, B., Caizergues-Ferrer, M. and Henry, Y. (2004) Npa1p, a component of very early pre-60S ribosomal particles, associates with a subset of small nucleolar RNPs required for peptidyl transferase center modification. *Mol Cell Biol*, **24**, 6324-6337.

Dong, J., Lai, R., Jennings, J.L., Link, A.J. and Hinnebusch, A.G. (2005) The novel ATP-binding cassette protein ARB1 is a shuttling factor that stimulates 40S and 60S ribosome biogenesis. *Mol Cell Biol*, **25**, 9859-9873.

Dong, J., Lai, R., Nielsen, K., Fekete, C.A., Qiu, H. and Hinnebusch, A.G. (2004) The essential ATP-binding cassette protein RLI1 functions in translation by promoting preinitiation complex assembly. *J Biol Chem*, **279**, 42157-42168.

Dooher, J.E. and Lingappa, J.R. (2004) Conservation of a stepwise, energy-sensitive pathway involving HP68 for assembly of primate lentivirus capsids in cells. *J Virol*, **78**, 1645-1656.

Dooher, J.E., Schneider, B.L., Reed, J.C. and Lingappa, J.R. (2007) Host ABCE1 is at plasma membrane HIV assembly sites and its dissociation from Gag is linked to subsequent events of virus production. *Traffic*, **8**, 195-211.

Douglas, S., Zauner, S., Fraunholz, M., Beaton, M., Penny, S., Deng, L.T., Wu, X., Reith, M., Cavalier-Smith, T. and Maier, U.G. (2001) The highly reduced genome of an enslaved algal nucleus. *Nature*, **410**, 1091-1096.

Elsasser, C., Brecht, M. and Bittl, R. (2002) Pulsed electron-electron double resonance on multinuclear metal clusters: assignment of spin projection factors based on the dipolar interaction. *J Am Chem Soc*, **124**, 12606-12611.

Estevez, A.M., Haile, S., Steinbuchel, M., Quijada, L. and Clayton, C. (2004) Effects of depletion and overexpression of the Trypanosoma brucei ribonuclease L inhibitor homologue. *Mol Biochem Parasitol*, **133**, 137-141.

Floyd-Smith, G., Slattery, E. and Lengyel, P. (1981) Interferon action: RNA cleavage pattern of a (2'-5')oligoadenylate--dependent endonuclease. *Science*, **212**, 1030-1032.

Gorbulev, S., Abele, R. and Tampé, R. (2001) Allosteric crosstalk between peptide-binding, transport, and ATP hydrolysis of the ABC transporter TAP. *Proc Natl Acad Sci U S A*, **98**, 3732-3737.

Haile, D.J., Rouault, T.A., Tang, C.K., Chin, J., Harford, J.B. and Klausner, R.D. (1992) Reciprocal control of RNA-binding and aconitase activity in the regulation of the iron-responsive element binding protein: role of the iron-sulfur cluster. *Proc Natl Acad Sci U S A*, **89**, 7536-7540.

Harnpicharnchai, P., Jakovljevic, J., Horsey, E., Miles, T., Roman, J., Rout, M., Meagher, D., Imai, B., Guo, Y., Brame, C.J., Shabanowitz, J., Hunt, D.F. and Woolford, J.L., Jr. (2001) Composition and functional characterization of yeast 66S ribosome assembly intermediates. *Mol Cell*, **8**, 505-515.

Hausmann, A., Aguilar Netz, D.J., Balk, J., Pierik, A.J., Mühlenhoff, U. and Lill, R. (2005) The eukaryotic P loop NTPase Nbp35: an essential component of the cytosolic and nuclear iron-sulfur protein assembly machinery. *Proc Natl Acad Sci USA*, **102**, 3266-3271.

Hopfner, K.P., Karcher, A., Shin, D.S., Craig, L., Arthur, L.M., Carney, J.P. and Tainer, J.A. (2000) Structural biology of Rad50 ATPase: ATP-driven conformational control in DNA double-strand break repair and the ABC-ATPase superfamily. *Cell*, **101**, 789-800.

Howard, J.B. and Rees, D.C. (2006) How many metals does it take to fix N2? A mechanistic overview of biological nitrogen fixation. *Proc Natl Acad Sci U S A*, **103**, 17088-17093.

Hung, L.W., Wang, I.X., Nikaido, K., Liu, P.Q., Ames, G.F. and Kim, S.H. (1998) Crystal structure of the ATP-binding subunit of an ABC transporter. *Nature*, **396**, 703-707.

Janas, E., Hofacker, M., Chen, M., Gompf, S., van der Does, C. and Tampé, R. (2003) The ATP hydrolysis cycle of the nucleotide-binding domain of the mitochondrial ATP-binding cassette transporter Mdl1p. *J Biol Chem*, **278**, 26862-26869.

Johnson, M.K. (1998) Iron-sulfur proteins: new roles for old clusters. *Curr Opin Chem Biol*, **2**, 173-181.

Jonuscheit, M., Martusewitsch, E., Stedman, K.M. and Schleper, C. (2003) A reporter gene system for the hyperthermophilic archaeon Sulfolobus solfataricus based on a selectable and integrative shuttle vector. *Mol Microbiol*, **48**, 1241-1252.

Karcher, A., Bu Ttner, K., Martens, B., Jansen, R.P. and Hopfner, K.P. (2005) X-Ray Structure of RLI, an Essential Twin Cassette ABC ATPase Involved in Ribosome Biogenesis and HIV Capsid Assembly. *Structure (Camb)*, **13**, 649-659.

Karpowich, N., Martsinkevich, O., Millen, L., Yuan, Y.R., Dai, P.L., MacVey, K., Thomas, P.J. and Hunt, J.F. (2001) Crystal structures of the MJ1267 ATP binding cassette reveal an induced-fit effect at the ATPase active site of an ABC transporter. *Structure*, **9**, 571-586.

Kerr, I.D. (2004) Sequence analysis of twin ATP binding cassette proteins involved in translational control, antibiotic resistance, and ribonuclease L inhibition. *Biochem Biophys Res Commun*, **315**, 166-173.

Kerr, I.M. and Brown, R.E. (1978) pppA2'p5'A2'p5'A: an inhibitor of protein synthesis synthesized with an enzyme fraction from interferon-treated cells. *Proc Natl Acad Sci U S A*, **75**, 256-260.

Khoroshilova, N., Beinert, H. and Kiley, P.J. (1995) Association of a polynuclear iron-sulfur center with a mutant FNR protein enhances DNA binding. *Proc Natl Acad Sci U S A*, **92**, 2499-2503.

Kispal, G., Csere, P., Prohl, C. and Lill, R. (1999) The mitochondrial proteins Atm1p and Nfs1p are essential for biogenesis of cytosolic Fe/S proteins. *EMBO J*, **18**, 3981-3989.

Kispal, G., Sipos, K., Lange, H., Fekete, Z., Bedekovics, T., Janaky, T., Bassler, J., Aguilar Netz, D.J., Balk, J., Rotte, C. and Lill, R. (2005) Biogenesis of cytosolic ribosomes requires the essential iron-sulphur protein Rli1p and mitochondria. *EMBO J.*, **24**, 589-598.

Kriek, M., Peters, L., Takahashi, Y. and Roach, P.L. (2003) Effect of iron-sulfur cluster assembly proteins on the expression of Escherichia coli lipoic acid synthase. *Protein Expr Purif*, **28**, 241-245.

Kuo, C.F., McRee, D.E., Cunningham, R.P. and Tainer, J.A. (1992a) Crystallization and crystallographic characterization of the iron-sulfur-containing DNA-repair enzyme endonuclease III from Escherichia coli. *J. Mol. Biol.*, **227**, 347-351.

Kuo, C.F., McRee, D.E., Fisher, C.L., O'Handley, S.F., Cunningham, R.P. and Tainer, J.A. (1992b) Atomic structure of the DNA repair [4Fe-4S] enzyme endonuclease III. *Science*, **258**, 434-440.

Le Roy, F., Bisbal, C., Silhol, M., Martinand, C., Lebleu, B. and Salehzada, T. (2001) The 2-5A/RNase L/RNase L inhibitor (RLI) [correction of (RNI)] pathway regulates mitochondrial mRNAs stability in interferon alpha-treated H9 cells. *J Biol Chem*, **276**, 48473-48482.

Lee, T.T., Agarwalla, S. and Stroud, R.M. (2004) Crystal structure of RumA, an iron-sulfur cluster containing E. coli ribosomal RNA 5-methyluridine methyltransferase. *Structure*, **12**, 397-407.

Lill, R., Fekete, Z., Sipos, K. and Rotte, C. (2005) Is there an answer? Why are mitochondria essential for life? *IUBMB Life*, **57**, 701-703.

Lill, R. and Mühlenhoff, U. (2006) Iron-sulfur protein biogenesis in eukaryotes: components and mechanisms. *Annu Rev Cell Dev Biol*, **22**, 457-486.

Lingappa, J.R., Dooher, J.E., Newman, M.A., Kiser, P.K. and Klein, K.C. (2006) Basic residues in the nucleocapsid domain of Gag are required for interaction of HIV-1 gag with ABCE1 (HP68), a cellular protein important for HIV-1 capsid assembly. *J Biol Chem*, **281**, 3773-3784.

Locher, K.P., Lee, A.T. and Rees, D.C. (2002) The E. coli BtuCD structure: a framework for ABC transporter architecture and mechanism. *Science*, **296**, 1091-1098.

Londei, P. (2005) Evolution of translational initiation: new insights from the archaea. *FEMS Microbiol Rev*, **29**, 185-200.

Lorentzen, E., Walter, P., Fribourg, S., Evguenieva-Hackenberg, E., Klug, G. and Conti, E. (2005) The archaeal exosome core is a hexameric ring structure with three catalytic subunits. *Nat Struct Mol Biol*, **12**, 575-581.

Majumdar, R., Bandyopadhyay, A. and Maitra, U. (2003) Mammalian translation initiation factor eIF1 functions with eIF1A and eIF3 in the formation of a stable 40 S preinitiation complex. *J Biol Chem*, **278**, 6580-6587.

Martin, A., Yeats, S., Janekovic, D., Reiter, W.D., Aicher, W. and Zillig, W. (1984) SAV 1, a temperate u.v.-inducible DNA virus-like particle from the archaebacterium Sulfolobus acidocaldarius isolate B12. *EMBO J*, **3**, 2165-2168.

Martinand, C., Montavon, C., Salehzada, T., Silhol, M., Lebleu, B. and Bisbal, C. (1999) RNase L inhibitor is induced during human immunodeficiency virus type 1 infection and down regulates the 2-5A/RNase L pathway in human T cells. *J Virol*, **73**, 290-296.

Martusewitsch, E., Sensen, C.W. and Schleper, C. (2000) High spontaneous mutation rate in the hyperthermophilic archaeon Sulfolobus solfataricus is mediated by transposable elements. *J Bacteriol*, **182**, 2574-2581.

Messias, A.C. and Sattler, M. (2004) Structural basis of single-stranded RNA recognition. *Acc Chem Res*, **37**, 279-287.

Moody, J.E., Millen, L., Binns, D., Hunt, J.F. and Thomas, P.J. (2002) Cooperative, ATP-dependent association of the nucleotide binding cassettes during the catalytic cycle of ATP-binding cassette transporters. *J Biol Chem*, **277**, 21111-21114.

Moura, J.J., Moura, I., Kent, T.A., Lipscomb, J.D., Huynh, B.H., LeGall, J., Xavier, A.V. and Munck, E. (1982) Interconversions of [3Fe-3S] and [4Fe-4S] clusters. Mössbauer and electron paramagnetic resonance studies of Desulfovibrio gigas ferredoxin II. *J Biol Chem*, **257**, 6259-6267.

Nilsen, T.W., Maroney, P.A. and Baglioni, C. (1982) Synthesis of (2'-5')oligoadenylate and activation of an endoribonuclease in interferon-treated HeLa cells infected with reovirus. *J Virol*, **42**, 1039-1045.

Nissan, T.A., Bassler, J., Petfalski, E., Tollervey, D. and Hurt, E. (2002) 60S pre-ribosome formation viewed from assembly in the nucleolus until export to the cytoplasm. *EMBO J*, **21**, 5539-5547.

Obmolova, G., Ban, C., Hsieh, P. and Yang, W. (2000) Crystal structures of mismatch repair protein MutS and its complex with a substrate DNA. *Nature*, **407**, 703-710.

Pedulla, N., Palermo, R., Hasenohrl, D., Blasi, U., Cammarano, P. and Londei, P. (2005) The archaeal eIF2 homologue: functional properties of an ancient translation initiation factor. *Nucleic Acids Res*, **33**, 1804-1812.

Pestka, S., Langer, J.A., Zoon, K.C. and Samuel, C.E. (1987) Interferons and their actions. *Annu Rev Biochem*, **56**, 727-777.

Porello, S.L., Cannon, M.J. and David, S.S. (1998) A substrate recognition role for the [4Fe-4S]$^{2+}$ cluster of the DNA repair glycosylase MutY. *Biochemistry*, **37**, 6465-6475.

Randak, C., Neth, P., Auerswald, E.A., Eckerskorn, C., Assfalg-Machleidt, I. and Machleidt, W. (1997) A recombinant polypeptide model of the second nucleotide-binding fold of the cystic fibrosis transmembrane conductance regulator functions as an active ATPase, GTPase and adenylate kinase. *FEBS Lett*, **410**, 180-186.

Randak, C. and Welsh, M.J. (2003) An intrinsic adenylate kinase activity regulates gating of the ABC transporter CFTR. *Cell*, **115**, 837-850.

Reiter, W.D., Zillig, W. and Palm, P. (1988) Archaebacterial viruses. *Adv Virus Res*, **34**, 143-188.

Rice, A.P., Roberts, W.K. and Kerr, I.M. (1984) 2-5A accumulates to high levels in interferon-treated, vaccinia virus-infected cells in the absence of any inhibition of virus replication. *J Virol*, **50**, 220-228.

Sarmiento, C., Nigul, L., Kazantseva, J., Buschmann, M. and Truve, E. (2006) AtRLI2 is an endogenous suppressor of RNA silencing. *Plant Mol Biol*, **61**, 153-163.

Schleper, C., Kubo, K. and Zillig, W. (1992) The particle SSV1 from the extremely thermophilic archaeon Sulfolobus is a virus: demonstration of infectivity and of transfection with viral DNA. *Proc Natl Acad Sci U S A*, **89**, 7645-7649.

Schmitt, L., Benabdelhak, H., Blight, M.A., Holland, I.B. and Stubbs, M.T. (2003) Crystal structure of the nucleotide-binding domain of the ABC-transporter haemolysin B: identification of a variable region within ABC helical domains. *J Mol Biol*, **330**, 333-342.

Schmitt, L. and Tampé, R. (2002) Structure and mechanism of ABC transporters. *Curr Opin Struct Biol*, **12**, 754-760.

She, Q., Brugger, K. and Chen, L. (2002) Archaeal integrative genetic elements and their impact on genome evolution. *Res Microbiol*, **153**, 325-332.

Singleton, M.R., Sawaya, M.R., Ellenberger, T. and Wigley, D.B. (2000) Crystal structure of T7 gene 4 ring helicase indicates a mechanism for sequential hydrolysis of nucleotides. *Cell*, **101**, 589-600.

Skordalakes, E. and Berger, J.M. (2003) Structure of the Rho transcription terminator: mechanism of mRNA recognition and helicase loading. *Cell*, **114**, 135-146.

Smith, P.C., Karpowich, N., Millen, L., Moody, J.E., Rosen, J., Thomas, P.J. and Hunt, J.F. (2002) ATP binding to the motor domain from an ABC transporter drives formation of a nucleotide sandwich dimer. *Mol Cell*, **10**, 139-149.

Tahara, M., Ohsawa, A., Saito, S. and Kimura, M. (2004) In vitro phosphorylation of initiation factor 2 alpha (aIF2 alpha) from hyperthermophilic archaeon Pyrococcus horikoshii OT3. *J Biochem (Tokyo)*, **135**, 479-485.

Takahashi, Y. and Tokumoto, U. (2002) A third bacterial system for the assembly of iron-sulfur clusters with homologs in archaea and plastids. *J Biol Chem*, **277**, 28380-28383.

Tatusov, R.L., Koonin, E.V. and Lipman, D.J. (1997) A genomic perspective on protein families. *Science*, **278**, 631-637.

Thayer, M.M., Ahern, H., Xing, D., Cunningham, R.P. and Tainer, J.A. (1995) Novel DNA binding motifs in the DNA repair enzyme endonuclease III crystal structure. *EMBO J*, **14**, 4108-4120.

Tilley, G.J., Camba, R., Burgess, B.K. and Armstrong, F.A. (2001) Influence of electrochemical properties in determining the sensitivity of [4Fe-4S] clusters in proteins to oxidative damage. *Biochem J*, **360**, 717-726.

Tschochner, H. and Hurt, E. (2003) Pre-ribosomes on the road from the nucleolus to the cytoplasm. *Trends Cell Biol*, **13**, 255-263.

Tyzack, J.K., Wang, X., Belsham, G.J. and Proud, C.G. (2000) ABC50 interacts with eukaryotic initiation factor 2 and associates with the ribosome in an ATP-dependent manner. *J Biol Chem*, **275**, 34131-34139.

van der Does, C., Presenti, C., Schulze, K., Dinkelaker, S. and Tampé, R. (2006) Kinetics of the ATP hydrolysis cycle of the nucleotide-binding domain of Mdl1 studied by a novel site-specific labeling technique. *J Biol Chem*, **281**, 5694-5701.

van der Does, C. and Tampé, R. (2004) How do ABC transporters drive transport? *Biol Chem*, **385**, 927-933.

Venema, J. and Tollervey, D. (1999) Ribosome synthesis in Saccharomyces cerevisiae. *Annu Rev Genet*, **33**, 261-311.

Verdon, G., Albers, S.V., Dijkstra, B.W., Driessen, A.J. and Thunnissen, A.M. (2003a) Crystal structures of the ATPase subunit of the glucose ABC transporter from Sulfolobus solfataricus: nucleotide-free and nucleotide-bound conformations. *J Mol Biol*, **330**, 343-358.

Verdon, G., Albers, S.V., van Oosterwijk, N., Dijkstra, B.W., Driessen, A.J. and Thunnissen, A.M. (2003b) Formation of the productive ATP-Mg^{2+}-bound dimer of GlcV, an ABC-ATPase from Sulfolobus solfataricus. *J Mol Biol*, **334**, 255-267.

Vojdani, A., Choppa, P.C. and Lapp, C.W. (1998) Downregulation of RNase L inhibitor correlates with upregulation of interferon-induced proteins (2-5A synthetase and

RNase L) in patients with chronic fatigue immune dysfunction syndrome. *J Clin Lab Immunol*, **50**, 1-16.

Williams, B.R., Golgher, R.R., Brown, R.E., Gilbert, C.S. and Kerr, I.M. (1979) Natural occurrence of 2-5A in interferon-treated EMC virus-infected L cells. *Nature*, **282**, 582-586.

Yarunin, A., Panse, V.G., Petfalski, E., Dez, C., Tollervey, D. and Hurt, E. (2005) Functional link between ribosome formation and biogenesis of iron-sulfur proteins. *EMBO J.*, **24**, 580-588.

Ye, J., Osborne, A.R., Groll, M. and Rapoport, T.A. (2004) RecA-like motor ATPases-lessons from structures. *Biochim Biophys Acta*, **1659**, 1-18.

Zago, M.A., Dennis, P.P. and Omer, A.D. (2005) The expanding world of small RNAs in the hyperthermophilic archaeon Sulfolobus solfataricus. *Mol Microbiol*, **55**, 1812-1828.

Zhao, Z., Fang, L.L., Johnsen, R. and Baillie, D.L. (2004) ATP-binding cassette protein E is involved in gene transcription and translation in Caenorhabditis elegans. *Biochem Biophys Res Commun*, **323**, 104-111.

Zheng, L. and Dean, D.R. (1994) Catalytic formation of a nitrogenase iron-sulfur cluster. *J Biol Chem*, **269**, 18723-18726.

Zheng, M., Wang, X., Templeton, L.J., Smulski, D.R., LaRossa, R.A. and Storz, G. (2001) DNA microarray-mediated transcriptional profiling of the Escherichia coli response to hydrogen peroxide. *J Bacteriol*, **183**, 4562-4570.

Zhou, A., Hassel, B.A. and Silverman, R.H. (1993) Expression cloning of 2-5A-dependent RNAase: a uniquely regulated mediator of interferon action. *Cell*, **72**, 753-765.

Zimmerman, C., Klein, K.C., Kiser, P.K., Singh, A.R., Firestein, B.L., Riba, S.C. and Lingappa, J.R. (2002) Identification of a host protein essential for assembly of immature HIV-1 capsids. *Nature*, **415**, 88-92.

Publications

Albers, S.-V., Jonuscheit, M., **Dinkelaker, S.**, Urich, T., Kletzin, A., Tampé, R., Driessen, A.J. and Schleper, C. (2006) Production of recombinant and tagged proteins in the hyperthermophilic archaeon Sulfolobus solfataricus. *Appl Environ Microbiol*, 72, 102-111.

Barthelme, D., Scheele, U., **Dinkelaker, S**., Janoschka, A., Macmillan, F., Albers, S.V., Driessen, A.J., Salamone-Stagni, M., Bill, E., Meyer-Klaucke, W., Schünemann, V. and Tampé, R. (2007) Structural organization of essential iron-sulfur clusters in the evolutionarily highly conserved ATP-binding cassette protein ABCE1. *J Biol Chem*, 282, 14598-14607.

van der Does, C., Presenti, C., Schulze, K., **Dinkelaker, S.** and Tampé, R. (2006) Kinetics of the ATP hydrolysis cycle of the nucleotide-binding domain of Mdl1 studied by a novel site-specific labeling technique. *J Biol Chem*, **281**, 5694-5701.

Danksagung

Vor allem möchte ich mich bei Prof. Dr. Robert Tampé für die Förderung während meiner Zeit am Institut für Biochemie bedanken, und besonders für das Ermöglichen von zwei Auslandsaufenthalten. Lieber Robert, ich danke Dir, dass Du meine Vorhaben immer unterstützt hast.

Prof. Dr. Bernd Ludwig danke ich für die Übernahme des Zweitgutachtens.

Ganz besonders möchte ich mich bei Prof. Dr. Paola Londei für die außerordentlich freundliche Aufnahme in ihrem Labor in Rom bedanken.

Ganz herzlicher Dank geht an Prof. Dr. Joachim Kirsch, der mich als Mentor immer sehr unterstützt hat.

Ein großer Dank gilt Prof. Dr. Anna Starzinski-Powitz für das Initiieren des Mentoring-Programms SciMento, im Rahmen dessen auch sie mich persönlich unterstützt hat.

Besonders danke ich Dr. Sonja Albers, in deren Labor in Groningen ich eine sehr produktive Zeit verbringen konnte, für die Zusammenarbeit und Unterstützung.

Bei Prof. Dr. Volker Müller und dem ganzen Arbeitskreis am Institut für Mikrobiologie in Frankfurt möchte ich mich für die Möglichkeit der Anzucht von *Sulfolobus*-Zellen in ihrem Institut bedanken, ins Besondere sei Michael Fritz für seine Hilfe gedankt.

Bei Dr. Claudia Rittmeyer möchte ich mich für ihre Hilfe bei den TXRF-Messungen bedanken.

Dr. Fraser MacMillen sei für die Durchführung der EPR-Messungen gedankt.

Dr. Dario Benelli danke ich für die Kollaboration in Rom.

Besonderer Dank gilt Dominik Barthelme und Dr. Urte Scheele für die erfolgreiche Zusammenarbeit und Hilfe auf dem ABCE1-Projekt.

Ganz herzlich möchte ich mich bei Dr. Chris van der Does und Chiara Presenti bedanken, die mir bei den ersten Schritten auf dem ABCE1-Projekt sehr geholfen haben.

Der gesamten Arbeitsgruppe Tampé möchte ich für die Hilfsbereitschaft und die vielen gemeinsam erlebten Stunden danken. Insbesondere danke ich Matthias Hofacker, Simone Gompf, Ariane Zutz, Meike Herget und Gabriele Plewnia, sowie Markus Endress, Annika Heil und Malin Gustafsson. Außerdem danke ich Dr. Rupert Abele, Dr. Alexander Gottschalk, Dr. Ricarda Jahnel, Dr. Joachim Koch und Dr. Jacob Piehler für die zahlreichen Diskussionen.

Ganz herzlich danke ich Dr. Eva Janas, Dr. Sonja Albers, Dr. Susanne Schrodt und Dominik Barthelme dafür, dass sie sich Zeit genommen haben diese Arbeit Korrektur zu lesen.

Tanja Babuke und Dr. Susanne Schrodt aus meiner Mentoringgruppe danke ich für ihre Unterstützung und Freundschaft in den letzten Jahren.

Bei Daniela Maneg, Stefan Jenewein und Steffen Grimm möchte ich mich für ihre Freundschaft während des Studiums und der Zeit meiner Doktorarbeit bedanken.

Schließlich möchte ich mich bei meiner ganzen Familie unendlich bedanken. Ohne Euer offenes Ohr, Eure Liebe und Unterstützung wäre meine Arbeit nicht möglich gewesen. Besonders danke ich meinem Mann Peter, der mich immer unterstützt hat. An dieser Stelle möchte ich auch meiner Mutter danken, die viele Stunden auf meine Tochter Anna aufgepasst hat, so dass ich genügend Zeit zum Schreiben dieser Arbeit gefunden habe.

Lebenslauf

Name: Stephanie Karola Dinkelaker geb. Becker

Geburtsdatum: 07.04.1979, Frankfurt am Main

Nationalität: Deutsch

Akademische Ausbildung

01/04-11/07	Promotion am Institut für Biochemie an der Johann Wolfgang Goethe-Universität Frankfurt am Main (Arbeitsgruppe Prof. Dr. Robert Tampé). Thema: Functional analysis of the ABC protein ABCE1 from the archaeon *Sulfolobus solfataricus*.
10/05-12/05	Forschungsaufenthalt an der Universität Rom „La Sapienza“ (Italien) am Institut für Biotechnologie und Hämatologie bei Prof. Dr. Paola Londei finanziert durch ein EMBO short term fellowship.
08/04-09/04	Forschungsaufenthalt an der Universität Groningen (Niederlande) am Institut für Mikrobiologie bei Prof. Dr. Arnold Driessen in der Gruppe von Dr. Sonja-Verena Albers.
10/03-11/03	Praktikum bei Sanofi-Aventis Pharma Deutschland GmbH in Frankfurt im Bereich „Functional Genomics“.
12/02-07/03	Diplomarbeit am Institut für Biochemie an der Johann Wolfgang Goethe-Universität Frankfurt am Main (Arbeitsgruppe Prof. Dr. Robert Tampé). Thema: Charakterisierung des ATP-Hydrolyse-Zyklus des mitochondrialen ABC-Peptidtransporters Mdl1p.
11/02	Diplomprüfungen in Biochemie mit der Note sehr gut.
06/02-07/02	Praktikum am Georg Speyer-Haus in Frankfurt in der Brustkrebsforschung.
09/01	Praktikum am Deutschen Krebsforschungszentrum in Heidelberg.
10/98-07/03	Studium der Biochemie an der Johann Wolfgang Goethe-Universität in Frankfurt am Main.
07/98	Abitur am Goethe-Gymnasium in Frankfurt am Main mit der Note 1,6.